Targeting neuronal populations by AAV-mediated gene transfer for studying the endocannabinoid system

Dissertation

zur Erlangung des Grades

“Doktor der Naturwissenschaften”

am Fachbereich Biologie

der Johannes Gutenberg-Universität

in Mainz

Stephan Guggenhuber

geboren am 22.10.1980 in München

Mainz, 2013

Dekan:

1. Berichterstattung:

2. Berichterstattung:

Tag der mündlichen Prüfung: 18.06.2013

Table of contents

1 Summary / Zusammenfassung

1.1 Summary

The cannabinoid type 1 (CB1) receptor is involved in a plethora of physiological functions and heterogeneously expressed on different neuronal populations. Several conditional loss-of-function studies revealed distinct effects of CB1 receptor signaling on glutamatergic and GABAergic neurons, respectively. To gain a comprehensive picture of CB1 receptor-mediated effects, the present study aimed at developing a gain-of-function approach, which complements conditional loss-of-function studies. Therefore, adeno-associated virus (AAV)-mediated gene delivery and Cre-mediated recombination were combined to recreate an innovative method, which ensures region- and cell type-specific transgene expression in the brain.

This method was used to overexpress the CB1 receptor in glutamatergic pyramidal neurons of the mouse hippocampus. Enhanced CB1 receptor activity at glutamatergic terminals caused impairment in hippocampus-dependent memory performance. On the other hand, elevated CB1 receptor levels provoked an increased protection against kainic acid-induced seizures and against excitotoxic neuronal cell death. This finding indicates the protective role of CB1 receptor on hippocampal glutamatergic terminals as a molecular stout guard in controlling excessive neuronal network activity. Hence, CB1 receptor on glutamatergic hippocampal neurons may represent a target for novel agents to restrain excitotoxic events and to treat neurodegenerative diseases.

Endocannabinoid synthesizing and degrading enzymes tightly regulate endocannabinoid signaling, and thus, represent a promising therapeutic target. To further elucidate the precise function of the 2-AG degrading enzyme monoacylglycerol lipase (MAGL), MAGL was overexpressed specifically in hippocampal pyramidal neurons. This genetic modification resulted in highly increased MAGL activity accompanied by a 50 % decrease in 2-AG levels without affecting the content of arachidonic acid and anandamide. Elevated MAGL protein levels at glutamatergic terminals eliminated depolarization-induced suppression of excitation (DSE), while depolarization-induced suppression of inhibition (DSI) was unchanged. This result indicates that the on-demand availability of the endocannabinoid 2-AG is crucial for short-term plasticity at glutamatergic synapses in the hippocampus. Mice overexpressing MAGL exhibited elevated corticosterone levels under basal conditions and an increase in anxiety-like behavior, but surprisingly, showed no

changes in aversive memory formation and in seizure susceptibility. This finding suggests that 2-AG-mediated hippocampal DSE is essential for adapting to aversive situations, but is not required to form aversive memory and to protect against kainic acid-induced seizures. Thus, specific inhibition of MAGL expressed in hippocampal pyramidal neurons may represent a potential treatment strategy for anxiety and stress disorders.

Finally, the method of AAV-mediated cell type-specific transgene expression was advanced to allow drug-inducible and reversible transgene expression. Therefore, elements of the tetracycline-controlled gene expression system were incorporated in our “conditional” AAV vector. This approach showed that transgene expression is switched on after drug application and that background activity in the uninduced state was only detectable in scattered cells of the hippocampus. Thus, this AAV vector will proof useful for future research applications and gene therapy approaches.

1.2 Zusammenfassung

Der Cannabinoid Typ 1 (CB1) Rezeptor ist an einer Vielzahl physiologischer Funktionen beteiligt und heterogen in verschiedenen neuronalen Populationen exprimiert. Die unterschiedlichen Auswirkungen der CB1 Rezeptoraktivierung in glutamatergen bzw. GABAergen Neuronen wurden in verschiedenen Studien an Zelltyp-spezifischen CB1 Rezeptor-Knockout-Mäusen gezeigt. Um ein umfassendes Bild der CB1 Rezeptor-vermittelten Effekte zu gewinnen, wurde in dieser Studie ein Mausmodell entwickelt, das eine Zelltyp-spezifische Erhöhung der CB1 Rezeptorexpression aufweist und Zelltyp-spezifische CB1 Rezeptor-Knockout-Modelle komplementieren soll. Hierfür wurde eine innovative Methode durch Kombination von Adeno-assoziierten Virus (AAV)-vermitteltem Gentransfer und Cre-vermittelter Rekombination entwickelt, die Hirnregion- und Zelltyp-spezifische Transgenexpression gewährleistet.

Mithilfe dieser Methode konnte eine Überexpression des CB1 Rezeptors in glutamatergen Pyramidenneuronen des Hippocampus der Maus erzeugt werden. Es wurde gezeigt, dass eine Steigerung der CB1 Rezeptoraktivität in glutamatergen Neuronen zu einer Beeinträchtigung der Hippocampus-abhängigen Gedächtnisleistung führte. Andererseits schützten erhöhte CB1 Rezeptormengen vor Kainat-induzierten epileptischen Krampfanfällen und vor excitotoxischem Zelltod. Diese Erkenntnis deutet an, dass der CB1 Rezeptor in glutamatergen Neuronen eine protektive Funktion vor übermäßiger Netzwerkaktivität einnimmt und somit einen Ansatzpunkt für die Therapie von neurodegenerativen Erkrankungen darstellt.

Endocannabinoid-synthetisierende und -degradierende Enzyme regulieren das Ausmaß der Endocannabinoid-vermittelten Rezeptoraktivierung und stellen dadurch einen vielversprechenden therapeutischen Ansatzpunkt dar. Um die exakte Funktion des 2-AG-degradierenden Enzyms Monoacylglycerol-Lipase (MAGL) weiter aufzuklären, wurde MAGL spezifisch in hippocampalen Pyramidenneuronen überexprimiert. Diese genetische Modifikation führte zu einer gesteigerten MAGL-Aktivität und zu einer Reduzierung von 2-AG um 50 % ohne den Gehalt an Arachidonsäure und Anandamid zu beeinflussen. Erhöhte MAGL Mengen in glutamatergen Neuronen unterbanden die synaptische Depression der Glutamatausschüttung, genannt „depolarization-induced suppression of excitation" (DSE), während die synaptische Depression der GABA-Ausschüttung, genannt „depolarization-induced suppression of inhibition" (DSI), unverändert war. Dieses Ergebnis deutet an, dass die Verfügbarkeit des Endocannabinoids 2-AG entscheidend für die Kurzzeitdepression an glutamatergen Synapsen im Hippocampus ist. MAGL-überexprimierende Mäuse wiesen erhöhte Werte des Stresshormons Corticosteron unter Basalbedingungen auf und zeigten erhöhtes Angstverhalten. Überraschenderweise hatte die MAGL-Überexpression keinen Einfluss auf die Bildung eines aversiven Gedächtnisses und auf die Anfälligkeit für Krampfanfälle. Die gewonnen Erkenntnisse weisen darauf hin, dass 2-AG-vermitteltes hippocampales DSE für eine Adaptierung auf eine aversive Situation erforderlich ist, aber nicht für die Bildung eines aversiven Gedächtnisses und die Protektion vor Kainat-induzierten Krampfanfällen benötigt wird. Folglich könnte eine spezifische Inhibition von MAGL in hippocampalen Pyramidenneuronen eine potentielle Behandlungsstrategie für Angst- und Belastungsstörungen darstellen.

Schließlich wurde die Methode der AAV-vermittelten Zelltyp-spezifischen Transgenexpression weiterentwickelt, um eine Pharmakon-induzierbare und reversible Transgenexpression zu ermöglichen. Hierfür wurden Elemente des Tetracyclin-induzierbaren Genexpressionssystems in unseren „konditionalen" AAV Vektor integriert. Dieser Ansatz zeigte, dass die Transgenexpression nach Gabe des Tetracyclin-Analogons Doxycyclin angeschaltet werden kann, und dass unspezifische Hintergrundexpression in Abwesenheit von Doxycyclin nur in vereinzelten Zellen des Hippocampus nachgewiesen werden konnte. Dieser AAV Vektor wird sich für künftige Forschungsansätze und Gentherapiestudien als nützlich erweisen.

2 Introduction

According to the World Health Organization (WHO), up to one billion people worldwide suffer from neurological disorders, which include epilepsy, stroke, Parkinson's disease, multiple sclerosis, Alzheimer's disease and other dementia. Neurological disorders affect people in all countries, irrespective of age, sex, education or income, and an estimated 6.8 million people die every year as a result of these diseases (World Health Organization, 2006). Moreover, over a third of people in industrialized countries exhibit mental distress once in their lifetime that meet the criteria for diagnosis of a mental disorder, comprising depression, schizophrenia, fear and anxiety disorders (World Health Organization, 2000). To treat these diseases, neuroscientists aim at understanding the fundamental molecular changes in brain functionality which arise with progression of the disorder.

Molecular neuroscience investigates the impact of specific genes and gene products on the regulation of brain function, control of synaptic plasticity and operation within neuronal circuits. For this purpose, genetic engineering has been used for many decades to systematically modify the genetic specification by artificial means for the functional analysis of a distinct gene. In this context, the mouse represents an exceptional animal model because it is prone to targeted gene modifications, shares the complex genome and neuroanatomical organization of mammals and can be studied in paradigms which model the wide array of human neurological and psychiatric diseases (Gaveriaux-Ruff and Kieffer, 2007). Manipulations of the mouse genome generally involve gain-of-function or loss-of-function approaches. The latter comprise the generation of a null allele using embryonic stem cell technology, resulting in a transgenic mouse line, in which the gene of interest is deleted. But these knockout animal models may show several disadvantages because gene ablation may lead to an embryonic lethality and possible compensatory effects may arise during development. The complementary gain-of-function approach involves the analysis of reinforced gene function and requires the introduction of additional DNA copies of the gene of interest into host cells. This manipulation can either be accomplished by pronuclear microinjection of the DNA sequence of interest, which is then randomly integrated into the host genome, or by integrating the DNA sequence at a specific site of the mouse genome using embryonic stem cell technology. Both approaches are time- and cost-intensive and the previously mentioned drawbacks may still arise. Moreover, germ line transgenics would require highly specific promoter elements to restrict transgene expression to a particular time point and to a particular

brain region. An alternative approach to somatic gene transfer is the utilization of viral vectors, which enable very specific spatiotemporal control of transgene expression by stereotaxic injection.

Animal viruses have evolved over millions of years in order to optimize the delivery of genetic material into host cells and are considered the most effective and promising vectors for *in vivo* gene delivery (Nonnenmacher and Weber, 2012). Viral vectors were applied for the first time in the 1970s, when Berg and colleagues used a SV40 virus to transduce kidney cells *in vitro* (Goff and Berg, 1976). Originally developed as an alternative method to transfect cells *in vitro*, this methodology soon showed great promise for both basic research and therapeutic applications. The most commonly applied viral vectors used recently in laboratory and clinics were mainly derived from murine and human RNA and DNA viruses comprising lentivirus, adenovirus, herpes simplex virus and adeno-associated virus (Walther and Stein, 2000). Simple viruses, such as adenovirus and adeno-associated virus, consist of genetic material encased within a protective protein coat called a capsid. In contrast, enveloped virions, including lentivirus and herpes simplex virus, bear capsids surrounded by a lipid bilayer envelope. They all differ with regard to their genetic material, size, and natural tropism (target cell specificity).

According to Somia and Verma, an ideal viral vector for gene delivery to the central nervous system (CNS) should comprehend (a) infection of non-dividing cells because neurons are post-mitotic, (b) large packaging capacity to be able to transfer large cDNAs, (c) non-immunogenicity against capsid proteins to avoid a neutralizing immune response that would result in reduced transgene expression or in the elimination of transduced cells, (d) tissue specificity to minimize side effects due to off-target transduction, (e) sustained and stable transgene expression, (f) simple production for generation of high titer vector stocks and (g) episomal nuclear localization to avoid random mutagenesis or position effects due to vector genome integration into the host genome (Somia and Verma, 2000). There is currently no vector that meets all these criteria, but the adeno-associated virus (AAV) comes closest.

2.1 Adeno-associated virus

AAVs are small non-enveloped DNA viruses first discovered as contaminants of adenovirus preparations (Hoggan et al., 1966). They belong to the family *Parvoviridae* (lat. *parvus*: small) and the genus *Dependovirus.* This classification is based on the fact that AAV replication and initiation of a productive infection cycle is depending on the co-infection with helper DNA viruses such as adenovirus, herpes simplex virus or papilloma virus (Afione et al., 1996). Although the majority of the human population is seropositive for AAV, no pathology has been observed with AAV infection (Blacklow et al., 1968; Chimurle et al., 1999).

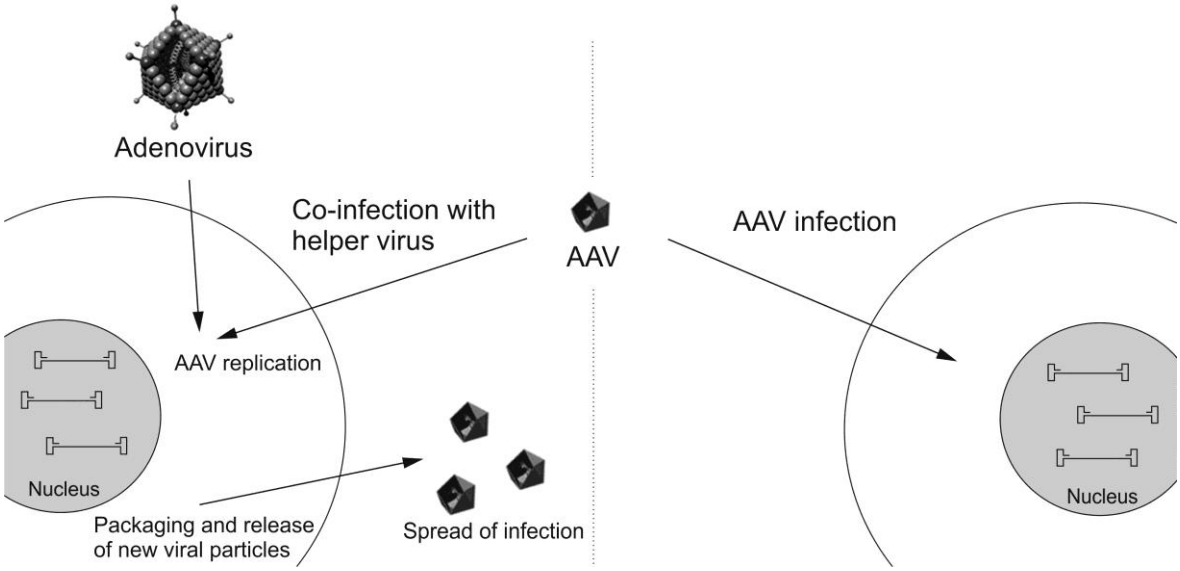

Figure 1.1. Life cycle of wild-type AAV. AAV undergoes productive infection in case of a co-infection with a helper virus (here adenovirus). This is characterized by genome replication, viral gene expression, and production of new viral particles (left). The absence of a helper virus induces the latent cycle, in which the AAV genome remains as circular episome in the nucleus (right).

The AAV virion is an icosahedral particle of about 25 nm in diameter and contains a single-stranded DNA genome of approximately 5 kb (Dong et al., 1996). The genome is encased by a capsid and can be divided into three functional regions: the inverted terminal repeats (ITRs) flanking two open reading frames for *rep* and *cap* genes, which are required for viral replication and for the synthesis of capsid proteins, respectively. The ITRs are t-shaped hairpin palindromic sequences which play a key role in virus life cycle. Thus, they are the origin of DNA replication and serve as primer for second strand synthesis (Ortolano et al., 2012). Due to an efficient combination of differential splicing and alternative start codon usage, the small genome is able to express four replication and three capsid proteins (Büning et al., 2008). If the host cell is co-infected with a helper

virus, the expression of *rep* and *cap* genes induces the lytic cycle, which results in the production and release of new viral particles (Fig. 1.1) (Daya and Berns, 2008). Cell infection in the absence of a helper virus results in the onset of the latent cycle, in which the AAV genome persists mostly in episomal form in the nucleus (Chen et al. 2005; Schnepp et al. 2005).

AAVs are formally grouped into serotypes within the genus *Dependovirus*. By definition, AAV serotypes are variations in the viral capsid protein motifs that do not cross-react with neutralizing antibodies specific for all other existing and characterized serotypes (Wu et al., 2006a). There are approximately 14 known AAV serotypes isolated from human or non-human primate tissue (Ortolano et al., 2012), and new AAV genomes have also been identified in a number of species including birds and reptiles (Wu et al. 2006a). AAV serotypes differ in their natural tropism to specific tissues by attaching to distinct cell surface receptors. Among all known serotypes, AAV serotype 2 was used in the vast majority of studies, as it was the first infectious clone established in a laboratory (Samulski et al., 1982). A recombinant AAV2 was generated by removing 95 % of the viral genome (AAV-encoded ORFs *rep* and *cap*) and replacing them with a transgene expression cassette formed by the gene of interest and a promoter sequence, which regulates its expression (Fig. 1.2). By ablating *rep* and *cap* genes from the viral genome and replacing them with a gene of interest, recombinant AAVs are not able to reproduce and infect a host cell but for a single round of replication. Concomitantly, the transgene is deposited within the target cell. The ITRs, which flank the wild-type AAV genome, need to be present in the recombinant AAV expression cassette because they are critical for the AAV production process in the presence of a helper virus.

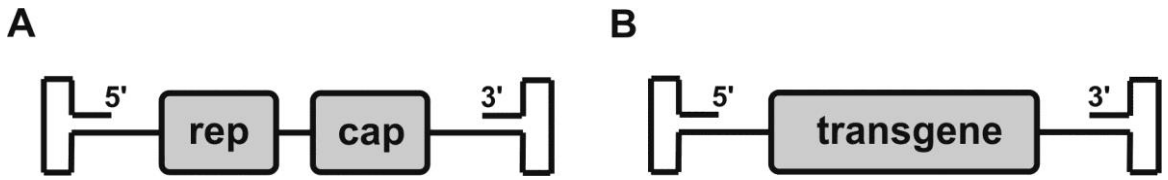

Figure 1.2. Illustration of the genome structure of wild-type (A) and recombinant (B) adeno-associated virus. ITRs form T-structure at both 5' and 3' ends. rep, genes required for viral replication; cap, genes of viral capsid proteins.

Subsequent studies using recombinant AAV2 demonstrated effective gene transfer and long-term, non-toxic gene expression in the CNS (Kaplitt et al., 1994; McCown et al., 1996). However, other recently discovered serotypes, such as AAV1, AAV5, AAV8, AAV9 and AAVrh10 showed increased transduction efficiency and vector spread in the CNS, and thus, superseded AAV2 (Burger et al., 2005; Cearley and Wolfe, 2006; Klein et al., 2008; McFarland et al., 2009; Hu et al., 2010). To further improve the application

spectrum of AAVs, mosaic vectors were generated whose capsid structure is composed of a mixture of capsid subunits from different serotypes (Rabinowitz et al., 2004; Wu et al., 2006a; Büning et al., 2008). Thus, selective features from different sources are combined that synergistically enhance transgene expression. For instance, a mosaic vector composed of the capsid subunits from AAV1 and AAV2 (AAV1/2) occupies the beneficial properties from both parental serotypes, which afford a rigorous vector purification using heparin affinity chromatography as used for AAV2 purification (Hauck et al., 2003) and a far more widespread transgene expression in the hippocampus than AAV2, as observed for AAV1 (Richichi et al., 2004).

In order to infect a host cell, AAV virions need to cross multiple biologic barriers, which include receptor binding, cell entry, intracellular trafficking, endosomal release, viral uncoating and nuclear entry. Cell entry of all serotypes seems to occur via receptor-mediated endocytosis. Typically, non-enveloped (capsid only) viruses bind cell surface glycosaminoglycan receptors. Subsequent secondary interactions of viral capsid proteins with co-receptors appear to be essential for internalization. It is this stage of the infectious pathway which determines the transduction efficiency and which can be significantly influenced by the choice of the AAV serotype. As AAV2 was predominantly used as a model to study AAV biology, the mechanism of viral infection has been extensively described for this serotype. AAV2 capsids interact with heparan sulfate proteoglycan (HSPG) (Summerford and Samulski, 1998), which is present throughout the brain on the surface of neurons and astroglia (Fuxe et al., 1994). After binding to HSPG, AAV2 capsids undergo a structural rearrangement required for a second step in viral entry, which is dependent on co-receptors (Asokan et al., 2006). As such, fibroblast growth factor receptor 1, hepatocyte growth factor receptor and laminin receptor are implicated in cell contact, whereas $\alpha_v\beta_5$ and $\alpha_5\beta_1$ integrins facilitate endocytosis (Summerford et al., 1999; Qing et al., 1999; Sanlioglu et al., 2000). Because the different AAV serotypes enter cells via distinct cell surface receptors, they can target various tissues. For instance, the primary receptor for AAV1, AAV5 and AAV6 is N-linked sialic acid (Kaludov et al., 2001; Wu et al., 2006b). Following attachment to surface receptors (Fig. 1.3), AAV2 particles are internalized presumably via clathrin-mediated endocytosis, although other mechanisms have been suggested (for review, see Nonnenmacher and Weber, 2012). Vector particles escape endosomal compartments due to an inherent phospholipase A2 activity of the N-terminal domain of the viral capsid protein 1, which is triggered by a conformational change of the capsid (Sonntag et al., 2006; Kronenberg et al., 2005). However, a significant portion of input vector may be degraded by the proteasome or lysosomal proteases. Viral particles, which were released from the endosome, are then translocated to the nucleus. Recent studies suggested that intact vector particles are translocated into

the nucleus before DNA release (Sonntag et al., 2006; Johnson and Samulski, 2009). Upon uncoating of the viral genome in the nucleus, second-strand synthesis provides a transcriptionally active template leading to expression of the delivered transgene.

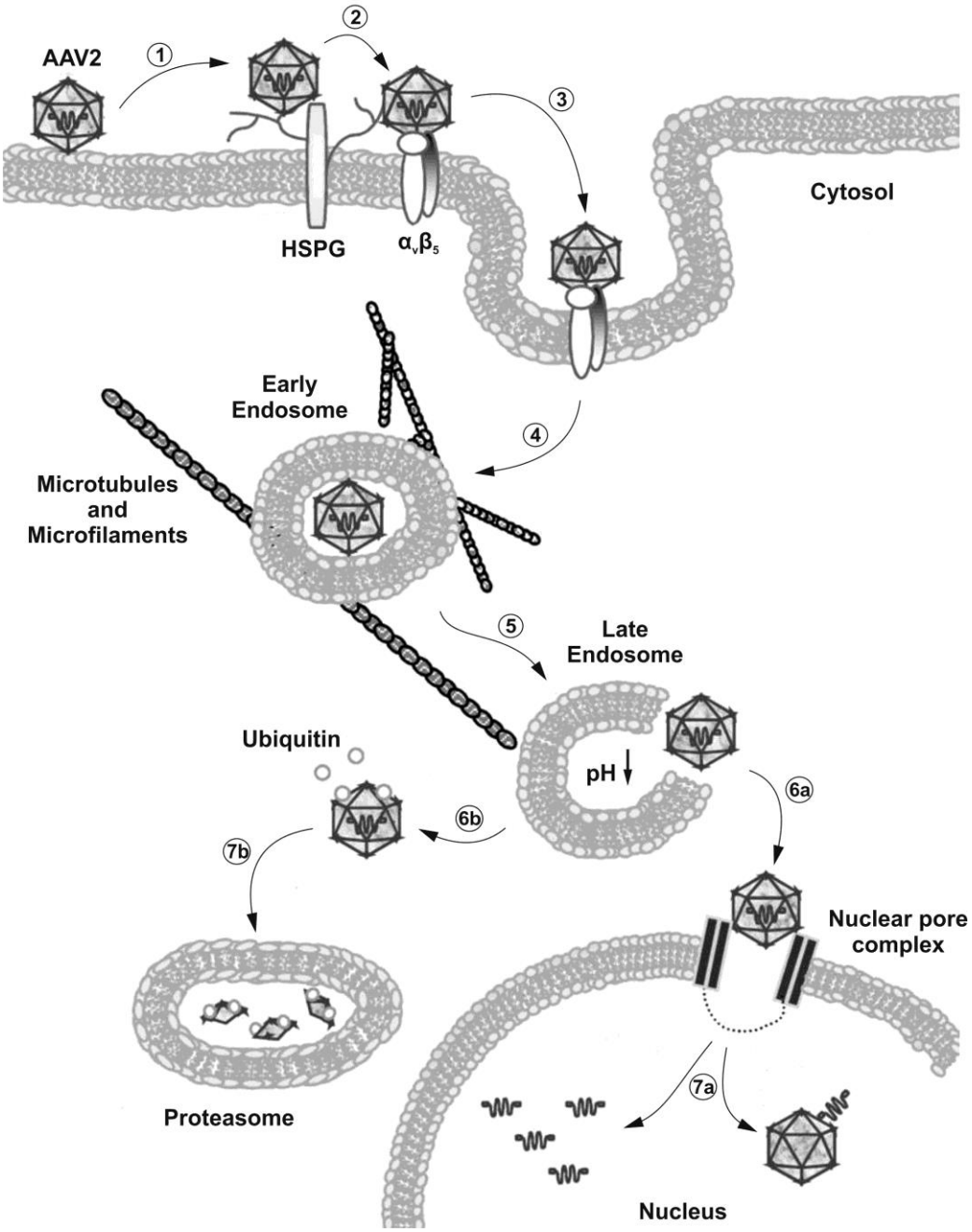

Figure 1.3. Schematic representation of AAV2 cell entry. AAV2 contacts the extracellular side of the plasma membrane multiple times, until it binds to heparan sulfate proteoglycan (HSPG) (1). Then, the viral particle interacts with integrins ($\alpha_v\beta_5$ and $\alpha_5\beta_1$) and other co-receptors, such as fibroblast growth factor receptor 1, hepatocyte growth factor receptor and laminin receptor (2), to enter the cell via endocytosis (3). The early endosome traffics towards the nucleus along the cytoskeleton (4). A pH decrease inside the endosome initiates phospholipase A2 activity of the viral capsid protein 1, which results in the release of the virus (5). Viral particles can get ubiquitinated (6b) and degraded in the proteasome (7b), or are translocated to the nucleus (6a). It is still unclear whether the capsid is eliminated before or after entrance into the nucleus (7a). In the nucleus, AAV2 can start replication if helper genes are available or enter the latent phase (modified from Ortolano et al., 2012).

Previous studies showed that AAV vectors facilitate transgene expression for up to 19 months in the rat brain (Peel and Klein, 2000) and more than eight years in the non-human primate brain (Hadaczek et al., 2010). Hence, it can be assumed that AAV presumably supports permanent transgene expression in the brain (Mandel et al., 2006).

Despite the limited capacity to package DNA genome, AAV vectors have become increasingly popular in CNS gene delivery applications due to their neurotropism, lack of pathogenicity, low immunogenicity and ability to establish sustained transgene expression. Hence, the therapeutic potential of AAVs as a gene therapy vector has been exploited in clinical trials to treat neurological disorders, such as Parkinson's disease and Canavan disease (LeWitt et al., 2011; reviewed in Ortolano et al., 2012; Weinberg et al., 2012).

Efficient gene transfer to neurons in the adult rodent hippocampus has been reported using mosaic AAV1/2 (Richichi et al., 2004; Klugmann et al., 2005). Therefore, we used mosaic AAV1/2 vectors in this study to target hippocampal neurons and to elicit an overexpression of constituents of the endocannabinoid system, a neuromodulatory system implicated in several physiological functions.

2.2 The endocannabinoid system

The endocannabinoid system is named according to its sensitivity to the main psychoactive compound of *Cannabis sativa,* Δ^9-tetrahydrocannabinol (THC). The isolation of the terpenoid THC led to the identification of its chemical structure (Gaoni and Mechoulam, 1964) and initiated the development of potent and selective THC analogs. Using the potent radioactively labeled synthetic cannabinoid agonist [^{3}H]CP-55,940, Howlett and colleagues described the presence of a specific G protein-coupled cannabinoid receptor in the rat brain (Devane et al., 1988), which was cloned in 1990 (Matsuda et al., 1990). The cannabinoid type 1 (CB1) receptor turned out to be a $G_{i/o}$ protein-coupled seven-transmembrane receptor located at the presynaptic terminal and shows a notably similar amino acid sequence (97-99 % identity) across mammalian species, supporting a phylogenetically conserved function for the CB1 receptor (Katona and Freund, 2012). Moreover, a second cannabinoid receptor (CB2 receptor) was discovered (Munro et al., 1993), which owes 44 % amino acid homology to CB1 receptor.

The discovery of cannabinoid receptors in the brain initiated a quest for their endogenous brain-derived ligands, called endocannabinoids. Finally, two lipophilic molecules were identified: the partial CB1 receptor agonist N-arachidonoylethanolamide (anandamide, AEA) (Devane et al., 1992) and the full CB1 receptor agonist 2-arachidonoylglycerol (2-AG) (Mechoulam et al., 1995; Sugiura et al., 1995). AEA is synthesized by N-acyl phosphatidylethanolamine phospholipase D (NAPE-PLD) and degraded by fatty acid amide hydrolase (FAAH). In turn, 2-AG is produced by diacylglycerol lipase (DAGL) α and β and is primarily degraded by monoacylglycerol lipase (MAGL) (Piomelli, 2003). The endocannabinoid ligands, together with their receptors and specific processes of synthesis, transport and degradation, constitute the endocannabinoid system (Fig. 1.4).

The endocannabinoid system is involved in a plethora of physiological functions including locomotion, pain perception, thermoregulation, energy balance, appetite, stress, anxiety, depression, memory, seizure severity and excitotoxicity (Marsicano et al., 2003; Monory et al., 2006; Monory et al., 2007; Marsicano and Lafenetre, 2009; Bellocchio et al., 2010; Hill et al., 2010; Ruehle et al., 2012).

Unlike traditional neurotransmitters such as amino acids, amines, or neuropeptides, which are stored in synaptic vesicles, endocannabinoids are produced on-demand from lipid precursor molecules at the postsynaptic membrane (Kano et al., 2009). Endocannabinoid biosynthesis is triggered by a depolarization-induced rise in intracellular calcium concentrations (Kim et al., 2002; Di et al., 2005) and/or by stimulation of metabotropic glutamate receptors (Maejima et al., 2001; Varma et al., 2001). Released endocannabinoids travel retrogradely by a still unknown mechanism to activate presynaptic CB1 receptor. Both release and reuptake of endocannabinoids is supposed to be mediated by a membrane transport process (Fowler and Jacobsson, 2002). A recent study identified a putative AEA transporter, which is a catalytically silent variant of FAAH (Fu et al., 2012). CB1 receptor activation leads to the inhibition of voltage-gated, inwardly rectified Ca^{2+} channels and stimulation of K^{+} currents, which results in blunted membrane depolarization and concomitantly in suppressed neurotransmitter release (Kano et al., 2009). This characteristic feature of endocannabinoid signaling is called depolarization-induced suppression of excitation (DSE) for the suppression of glutamate release or depolarization-induced suppression of inhibition (DSI) for the suppression of γ-aminobutyric acid (GABA) release.

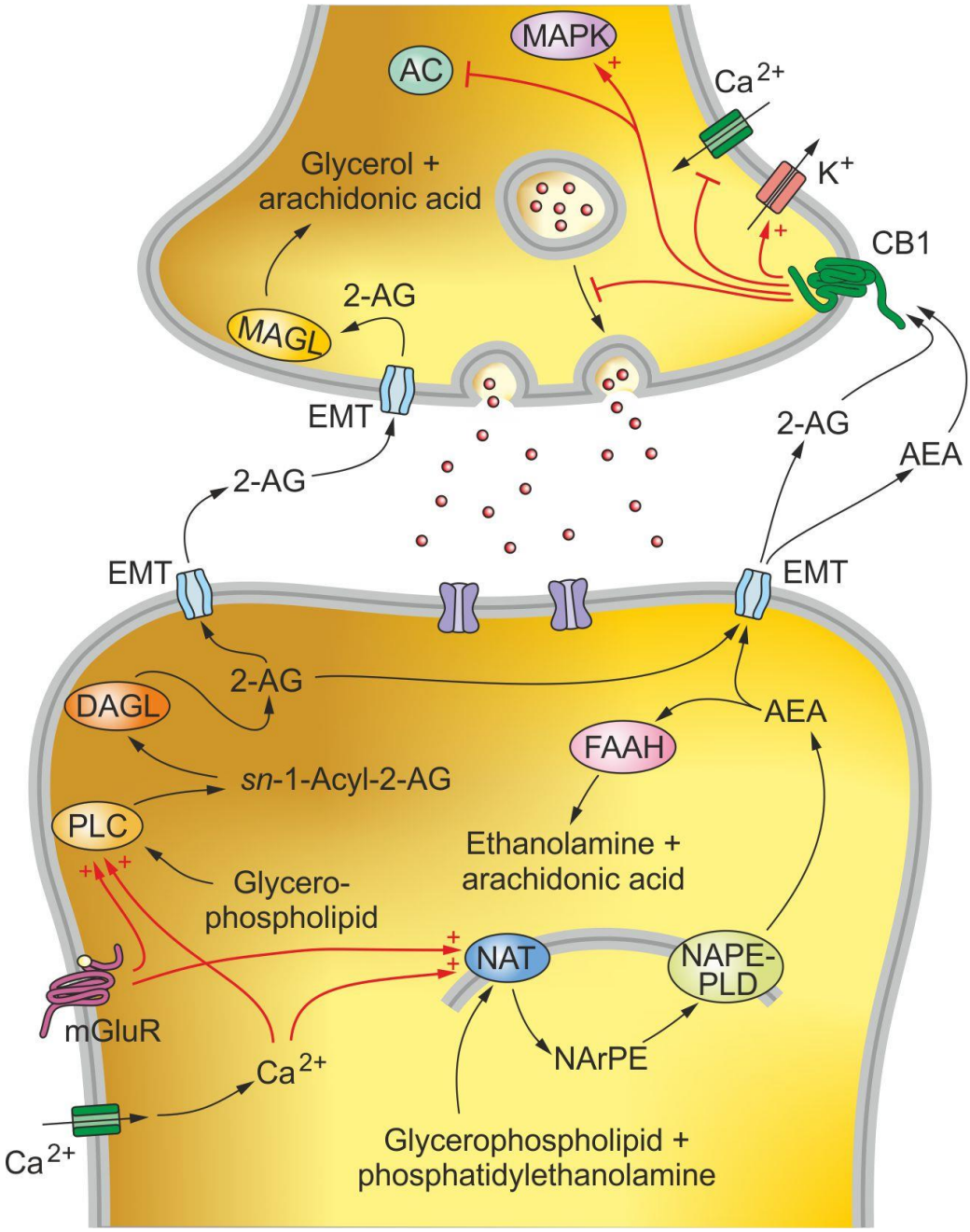

Figure 1.4. Synthesizing and degrading pathways of endocannabinoids, their subcellular localization and endocannabinoid signaling. Presynaptic neurotransmitter release induces postsynaptic activity, resulting in calcium influx and/or activation of metabotropic glutamate receptors (mGluR). These stimuli lead to the synthesis of endocannabinoids in postsynaptic neurons. The enzymes for 2-arachidonoylglycerol (2-AG) biosynthesis, phospholipase C (PLC) and diacylglycerol lipase (DAGL) seem to be mostly localized on the plasma membrane. The anandamide (AEA) biosynthetic enzymes *N*-acyltransferase (NAT) and *N*-acyl phosphatidyl-ethanolamine phospholipase D (NAPE-PLD) are located on intracellular membranes. The AEA-degrading enzyme fatty acid amide hydrolase (FAAH) is most abundant on neurons postsynaptically located to the CB1 receptor, indicating that anandamide acts principally on these neurons. Endocannabinoids are thought to be transported via an endocannabinoid membrane transporter (EMT) localized on both pre- and postsynaptic terminals, but might also be directly released into the synaptic cleft after their synthesis. 2-AG is inactivated by monoacylglycerol lipase (MAGL) localized in presynaptic neurons, which supports a role as retrograde messenger at presynaptic CB1 receptor for 2-AG. 2-AG and AEA activate presynaptic CB1 receptor which induces the inhibition of calcium channels and adenylyl cyclase (AC) and the activation of potassium channels and mitogen-activated protein kinase (MAPK). Red arrows indicate activating (+) and inhibiting (I) processes, respectively. NArPE, *N*-arachidonoyl phosphatidylethanolamine.

Furthermore, CB1 receptor stimulation inhibits adenylyl cyclase (AC) and activates downstream targets, such as mitogen-activated protein kinase (MAPK) (Howlett et al., 2010). CB1 receptor signaling is terminated by hydrolytic inactivation of the endocannabinoids. 85 % of the brain's 2-AG hydrolysis activity is accounted for MAGL located on the presynaptic site, although other enzymes, such as cyclooxygenase 2 (COX-2) and the serine hydrolases α-β-hydrolase domain 6 (ABHD6) and 12 (ABHD12) contribute to this process (Kozak et al., 2004; Blankman et al., 2007; Marrs et al., 2010). Interestingly, the AEA-degrading enzyme FAAH is found in the postsynaptic fraction suggesting different signaling properties for AEA and 2-AG (Cristino et al., 2008).

To date, there is clear evidence for other receptors in the CNS that are modulated by endocannabinoids, such as G protein-coupled receptor 55 (GPR55) (Nevalainen and Irving, 2010), transient receptor potential cation channel subfamily V1 (TRPV1) (De Petrocellis and Di Marzo, 2010), peroxisome proliferator-activated receptor (PPAR) family of nuclear receptors (O'Sullivan and Kendall, 2010), and $GABA_A$ receptor (Sigel et al., 2011), which further impedes understanding the functions of the endocannabinoid system.

The CB1 receptor is one of the most abundant G protein-coupled receptors in the mammalian brain (Mechoulam and Parker, 2013). Highest densities of the CB1 receptor are found in the basal ganglia, cerebellum, hippocampus and cerebral cortex, whereas thalamic, hypothalamic and brainstem regions show moderate to low CB1 receptor levels (Marsicano and Lutz, 1999; Howlett et al., 2002; Mackie, 2005). Moreover, CB1 receptor is expressed in distinct neuronal populations with very high levels in GABAergic interneurons belonging mainly to the cholecystokinin-positive and parvalbumin-negative type and moderate to low levels in glutamatergic, cholinergic, noradrenergic and serotonergic neurons (Marsicano and Lutz, 1999; Degroot et al., 2006; Monory et al., 2006; Oropeza et al., 2007; Häring et al., 2007; Morozov et al., 2009). Recent studies showed that CB1 receptor is also expressed on astroglial cells and oligodendrocytes (Benito et al., 2007; Navarrete and Araque, 2010). This divergent CB1 receptor expression in multiple brain regions, which differentially respond to extraneous stimulatory influences, and on distinct neuronal populations, which may have opposing functions (e.g. GABA and glutamate), may contribute to the biphasic effect of CB1 receptor agonist treatment (Moreira and Lutz, 2008; Rey et al., 2012). The generation of conditional knockout mice, which lack the CB1 receptor only in a specific cell-type, enabled to dissect CB1 receptor functions. For instance, previous studies revealed that mice lacking CB1 receptor in principal forebrain neurons showed less protection against excitotoxicity (Marsicano et al., 2003) and an impairment in working memory (Han et al., 2012) and were more vulnerable to acute epileptiform seizures (Monory et al., 2006). In contrast,

CB1 receptor deletion from GABAergic neurons had no effect on seizure severity (Monory et al., 2006), but induced age-dependent neurodegeneration (Albayram et al., 2011) and hyperphagia (Bellocchio et al., 2010) and abolished THC-mediated memory deficits (Puighermanal et al., 2009). Taken together, CB1 receptor expressed on a particular neuronal population exhibits diverse functions. Thus, the dissection of CB1 receptor function in a specific cell-type is of great importance to gain a comprehensive picture of the endocannabinoid system and to exploit its therapeutic potential.

2.3 Aim of the thesis

In the hippocampus, cannabinoid type 1 (CB1) receptor modulates glutamatergic and GABAergic neurotransmission, two neurotransmitter systems with opposing functions. Several studies revealed distinct effects of CB1 receptor in either of the two cell populations by using conditional knockout mice, which lack CB1 receptor in a particular neuronal population. However, these conditional loss-of-function studies have not yet been complemented by the corresponding gain-of-function approach entailing CB1 receptor overexpression, thus preventing a comprehensive picture of CB1 receptor-mediated effects. The present study aimed at developing a genetic approach which allows targeting specific neuronal populations in a particular brain region by using adeno-associated virus (AAV)-mediated gene transfer. To this end, the Cre/loxP system was incorporated into the AAV platform to enable tight surveillance over transgene expression in subsets of neurons under very precise spatiotemporal control *in vivo*. This efficient system was implemented to overexpress the CB1 receptor in glutamatergic pyramidal neurons of the mouse hippocampus and concomitant effects were analyzed at the cellular and behavioral level (Chapter 4).

Endocannabinoid signaling is tightly regulated by endocannabinoid synthesizing and degrading enzymes. Monoacylglycerol lipase (MAGL) is the primary degrading enzyme of the major endocannabinoid 2-arachidonoylglycerol (2-AG) and abundantly expressed in the hippocampus. Recent studies used MAGL knockout mice to investigate the consequences of MAGL ablation, which was however accompanied with a reduction in the content of arachidonic acid, a substrate for a number of enzymes to generate other lipid signaling molecules, including prostaglandins. These compensatory effects limit the usefulness of this mouse line as a model to define the functions of 2-AG in the brain. Thus, the goal of this study was to overexpress MAGL specifically in hippocampal pyramidal neurons by AAV-mediated gene transfer and to assess affiliated changes in endocannabinoid signaling and mouse behavior (Chapter 5).

To further extend the application spectrum of AAVs, we aimed at generating an AAV system which enables conditional, inducible and reversible transgene expression. To this end, we combined the Cre/loxP system and the tetracycline-controlled gene expression system to develop an autoregulatory AAV which contains all components in a single vector. This vector should repress transgene expression in the uninduced state and allow switching on transgene expression by drug application (Chapter 6).

3 Material and Methods

3.1 DNA constructs

All constructs used in this study are based on an AAV2 expression cassette (pAAV) generally containing the woodchuck hepatitis virus posttranscriptional regulatory element (WPRE) and the bovine growth hormone polyadenylation sequence (bGHpA) flanked by AAV2 inverted terminal repeats (ITRs). All PCR products created in this study were cloned and sequenced in pCR™2.1-TOPO® TA cloning vector (Invitrogen, Carlsbad, CA, USA). DNA construct design was performed using Vector NTI software (Invitrogen, Carlsbad, CA, USA).

To drive transgene expression, the ubiquitous 1.1 kb cytomegalovirus immediate early enhancer/chicken β-actin hybrid promoter (CAG) was incorporated in pAAV. The 340 bp transcriptional Stop cassette was designed to entail a herpes simplex virus thymidin kinase polyadenylation signal and a polyadenylation terminator from pGL3 (Promega, Madison, WI, USA) flanked by loxP sites, and was synthesized by a commercial provider (Epochbiolabs, Missouri City, TX, USA). The Stop cassette was transferred into the BamHI-site downstream of the promoter to receive pAAV-CAG-Stop. Proximal to the Stop element, the open reading frame of the transgene was integrated in the pAAV-CAG-Stop backbone: humanized renilla green fluorescent protein (hrGFP) to obtain pAAV-CAG-Stop-GFP for the proof-of-principle approach; rat CB1 receptor fused downstream of the coding region of the human influenza hemagglutinin epitope (HA) tag (generous gift from Ken Mackie) to receive pAAV-CAG-Stop-CB1 for the CB1 receptor gain-of-function approach; mouse MAGL fused downstream of the HA tag to receive pAAV-CAG-Stop-MAGL for the MAGL gain-of-function approach. For N-terminal HA tagging of the mouse MAGL cDNA (generous gift from Giovanni Marsicano), HpaI-linkers were introduced by PCR (MAGL fw, 5'-TCTAGTTAACATGCCTGAGGCAAGTT-3'; MAGL rev, 5'-CATTGTTAACTCAGGGTAGACACCTAGCT-3') using proof-reading KOD hot-start DNA polymerase (EMC Chemicals, San Diego, CA, USA). The PCR product was subcloned in frame of the HA tag into the pAAV backbone. In addition, the pAAV backbone containing the CAG promoter and no cDNA (pAAV-empty) or the sequence encoding Cre recombinase fused to the HA tag and a nuclear localization signal (pAAV-Cre) were used for *in vitro* experiments.

For the tetracycline-inducible AAV approach, an AAV2 expression cassette was used that contains a short form of the woodchuck hepatitis virus posttranscriptional regulatory element (WPRE2) and a short bovine growth hormone polyadenylation sequence (spA) flanked by AAV2 inverted terminal repeats. A 480 bp fragment of the neuron-specific human synapsin 1 promoter (Syn) (Kugler et al., 2003) drives transgene expression in this construct. To integrate a tetracycline-responsive element (TRE) upstream of the synapsin promoter, PstI-linkers were introduced by PCR (TRE fw, 5'-CATCCTGCAGTAAAACGACGGCCAGTGAAT-3'; TRE rev, 5'-TTTTCTGCAGGGGTACCGAGCTCTGCTTAT-3'). A construct, which entails the sequences of the reporter gene hrGFP, the peptide linker 2A and the tetracycline-regulatable transcriptional silencer (tTS) in frame, was generated by overlap extension PCR (OE-PCR) comprising two PCR steps (Warrens et al., 1997; see results section). SpeI-linkers were introduced to enable incorporation of the construct in the pAAV backbone at the appropriate position.

3.2 Animals

Adult (2-6 months old) male mice were used in all experiments of this study. Animals were housed in groups of maximum five individuals per cage in a temperature- and humidity-controlled room (22°C ±1; 50 % ±1) with a 12 h light-dark cycle (lights on 7:00-19:00) and had access to food and water *ad libitum*. All experiments were carried out in accordance with the European Communities Council Directive of 24 November 1986 (86/609/EEC) and were approved by the local animal care committee (Landesuntersuchungsamt Koblenz, permit numbers 23177-07/051-47V1 and 23177/G10-1-037). Transgenic mouse lines used in this study were bred for >10 generations on the background of C57BL/6-N mice (Charles River, Sulzfeld, Germany). The NEX-Cre mouse line drives Cre expression in forebrain glutamatergic neurons (Goebbels et al., 2006). Dlx-Cre mice express Cre recombinase in GABAergic interneurons (Monory et al., 2006). Wild-type littermates of Cre driver mouse lines do not carry the respective Cre recombinase transgenic allele. Generation, breeding and genotyping of these mouse lines were performed as described (Monory et al., 2006)

3.3 Production of recombinant AAVs

The generation of pseudotyped AAV vectors was performed using a cross-packaging strategy which is based on the observation that coexpression of AAV2 *rep* proteins and *cap* proteins of a different serotype results in the packaging of AAV2 genomes (Rabinowitz et al., 2002). In the present study mosaic virions AAV1/2 were produced using a helper virus-free standard method as described (During et al., 2003; Hauck et al., 2003). Briefly, human embryonic kidney 293 (HEK) cells were transfected with the AAV *cis* plasmid, the AAV1 (pH21, containing *cap* genes of AAV1) and AAV2 (pRV1, containing *rep* and *cap* genes of AAV2) helper plasmids, and the adenovirus helper plasmid (pFD6) providing adenoviral helper functions (E2A, E4 and VA, with E1 encoded in the HEK cell genome) by standard calcium phosphate transfection methods. 60 hours after plasmid transfections, cells were harvested and the vector was purified using heparin affinity columns (Sigma Aldrich, St. Louis, MO, USA). AAV vectors were subjected to quality controls comprising the analysis of vector purity on a Coomassie gel and the determination of genomic vector titers by quantitative PCR using the ABI 7700 real time PCR cycler (Applied Biosystems, Foster City, CA, USA) with primers designed to WPRE (WPRE fw, 5'-GGCTGTTGGGCACTGACAAT-3'; WPRE rev, 5'-CCGAAGGGACGTAGCAGAAG-3').

3.4 AAV vector administration

Adult mice (8-9 weeks of age) were anesthetized by intraperitoneal injection of fentanyl (0.05 mg/kg), midazolam (5 mg/kg) and medetomidin (0.5 mg/kg). Fentanyl is an opioid agonist and has analgesic properties commonly applied in surgery. Midazolam, a benzodiazepine, is used for sedation and muscle relaxation, while the α2-adrenoceptor agonist medetomidin exhibits analgesic and sedative properties. Anesthetized mice were fixed in a small animal stereotaxic frame (Kopf instruments, Tujunga, CA, USA) and the scalp was removed by cutting in rostrocaudal direction. Afterwards bregma was identified and assessed as zero point. For bilateral hippocampus injection, the microsyringe was positioned at the following coordinates: anterior-posterior -2.0 mm, mediolateral ±2.0 mm, dorsoventral -2.0 mm. Vector delivery was performed at a rate of 150 nl/min using a microprocessor controlled mini-pump with 34G beveled needles (World Precision Instruments, Sarasota, FA, USA). After injecting 1 µl of vector solution, the microsyringe was held in place for approximately 5 min before retracting the needle from the target site. Finally, the scalp was sewed and anesthesia was antagonized by subcutaneous injection of flumazenil (benzodiazepine antagonist, 0.5 mg/kg), naloxon (opioid antagonist, 1.2 mg/kg) and atipamezol (α2-adrenoceptor antagonist, 2.5 mg/kg). Furthermore, mice

received subcutaneous injection of buprenorphine (0.05 mg/kg), a long-lasting analgesic, and saline to compensate fluid loss during surgery. Mice were monitored and kept under an infrared heat lamp until anesthesia disappeared and they fully recovered.

3.5 Immunohistochemistry

The rostral-caudal extent of transgene expression of all animals used in this study was assessed by immunohistochemistry. Animals that were subjected to behavioral experiments and did not show a robust pattern of transgene expression in the major hippocampal fields were excluded from the study. Mice were deeply anesthetized (pentobarbital; 160 mg/kg) and transcardially perfused with phosphate buffered saline (PBS) containing 4 % paraformaldehyde. Brains were removed from the skull and cut (40 µm) in the coronal plane on a cryostat after postfixation overnight in 4 % paraformaldehyde and subsequent cryoprotection in 30 % sucrose. Free-floating brain sections were rinsed with PBS containing 0.2 % Triton X-100 (PBS-Triton) to rupture cell membranes, then blocked in immunobuffer (4 % donkey serum in PBS-Triton) for 30 min at room temperature, and incubated overnight at 4°C with the following primary antibodies: rabbit anti-hrGFP (Stratagene, LaJolla, CA, USA; 1:1000), rabbit anti-HA (Santa Cruz Biotechnology, Santa Cruz, CA, USA; 1:1000), mouse anti-GFAP (Sigma-Aldrich, St. Louis, MO, USA; 1:1000), guinea pig anti-VGlut1 (Chemicon, Temecula, CA, USA; 1:5000). Sections were washed with PBS-Triton and then incubated for 1 h with the appropriate Alexa488- or Alexa546-conjugated goat IgG (Invitrogen, Carlsbad, CA, USA; 1:1000). Prior to the third wash in PBS, sections were counterstained with the nuclear dye 4’,6-diamidino-2-phenylindole (DAPI) for 5 min. Sections were then transferred onto glass slides and coverslipped with Mowiol mounting medium. Immunostaining was visualized using a Leica DM5500 fluorescence microscope (Leica microsystems, Wetzlar, Germany) or a Zeiss Axiovert LSM 710 laser scanning confocal microscope (Carl Zeiss, Oberkochen, Germany). Fluorescence intensities were quantified throughout the hippocampus using a 5x objective on the Leica DM5500 microscope and Leica Application Suite software (Leica microsystems, Wetzlar, Germany). Digitalized images were processed with Adobe Photoshop CS5.

3.6 Fluoro-Jade staining

For detection and quantification of neuronal degeneration evoked by kainic acid injection, Fluoro-Jade C (Millipore, Schwalbach, Germany) staining was performed as described previously (Klugmann et al., 2006). Briefly, sections were mounted on slides and rinsed in

1 % sodium hydroxide in 80 % ethanol for 3 min. After washing steps in 70 % ethanol and dH_2O, sections were incubated for 8 min in 0.06 % potassium permanganate. Then sections were rinsed two times in dH_2O followed by 10 min incubation in 0.0002 % Fluoro-Jade C diluted in 0.1 % acetic acid. Following several washing steps, nuclei were stained with DAPI and sections were fixed with Histokit (Carl Roth, Karlsruhe, Germany). Sections were collected every 120 µm for analysis of neuronal degeneration of hippocampal neurons in each mouse (10 sections per animal). Fluoro-Jade C staining was visualized under a FITC filter and quantified by two independent observers unaware of the genotype.

3.7 Western blot

Protein content of hippocampal homogenates or of transfected HEK cell lysates was determined by using the BCA™ protein assay kit (Pierce, Rockford, IL, USA) according to the manufacturer's protocol. Protein samples were separated on a 10 % SDS-PAGE and electroblotted onto nitrocellulose membrane. After blocking in 5 % nonfat dry milk, the membrane was incubated overnight at 4°C with the respective primary antibodies: rabbit anti-hrGFP (Stratagene, LaJolla, CA, USA; 1:10,000), rabbit anti-CB1 (Frontier Sciences, Hokkaido, Japan; 1:500), rabbit anti-HA (Santa Cruz Biotechnology, Santa Cruz, CA, USA; 1:1000), rabbit anti-MAGL (generous gift from Ken Mackie; 1:2000). α-tubulin (Sigma-Aldrich, St. Louis, MO, USA; 1:400,000), actin (Merck Millipore, Billerica, MA, USA; 1:2000) or GAPDH (Abcam, Cambridge, UK; 1:5000) were used as loading control. Secondary antibodies were horseradish peroxidase-conjugated anti-rabbit or anti-mouse IgG (Dianova, Hamburg, Germany; 1:1000). Bound antibodies were detected using a chemiluminescent substrate followed by digitalization using the FUSION-SL chemiluminescence imaging system (Peqlab, Erlangen, Germany).

.

3.8 Agonist stimulated [^{35}S]GTPγS binding

As the CB1 receptor is a G protein-coupled receptor, the level of activated G proteins following CB1 receptor agonist stimulation is a significant indicator of CB1 receptor activity. Activated G proteins bind GTP and stimulate downstream targets followed by hydrolyzation of GTP to GDP. This results in the inactivation of the G protein. In the binding assay, GTP is displaced by [^{35}S]GTPγS, which cannot be hydrolyzed to GDP by the intrinsic GTPase activity. Hence, activated G proteins are labeled by radioactive [^{35}S]GTPγS, and thus, the amount of radioactivity indicates the amount of activated G proteins.

Agonist-stimulated [^{35}S]GTPγS binding was performed as described (Breivogel, 2006). Briefly, mouse hippocampi were isolated and homogenized in 1 ml of ice-cold membrane buffer (50 mM Tris-HCl, pH 7.4, 3 mM $MgCl_2$, 0.2 mM EGTA, complete protease inhibitor). Protein content was determined using the BCA™ protein assay kit (Pierce, Rockford, IL, USA) according to the manufacturer's protocol. Hippocampus homogenates (10 µg) were preincubated for 10 min at 30°C in 0.004 U/ml adenosine deaminase (240 U/mg of protein; Sigma-Aldrich, St. Louis, MO, USA) to remove endogenous adenosine. Samples were incubated with 0.05 nM [^{35}S]GTPγS (Perkin Elmer, Waltham, MA, USA) and appropriate concentrations of the CB1 receptor agonist (6aR)-trans-3-(1,1-Dimethylheptyl)-6a,7,10,10a-tetrahydro-1-hydroxy-6,6-dimethyl-6H-dibenzo[b,d]pyran-9-methanol (HU-210) (Tocris Bioscience, Bristol, UK) in assay buffer (50 mM Tris-HCl, pH 7.4, 3 mM $MgCl_2$; 0.2 mM EGTA, 100 mM NaCl) containing 30 µM GDP and 0.1 % BSA in a final volume of 0.5 ml for 60 min at 30°C. Nonspecific binding was determined in the presence of 30 µM unlabeled GTPγS. Basal binding was measured in the absence of receptor agonist and defined as 0 % in each experiment. Bound [^{35}S]GTPγS was harvested by vacuum filtration through Whatman GF/B filters with a Brandel Cell Harvester (Brandel, Gaithersburg, MD, USA) and washed three times with 3 ml of ice-cold 50 mM Tris-HCl buffer, pH 7.4. Whatman filters were incubated for 2 h in 2.5 ml of scintillation mixture Aquasafe 300 plus (Zinsser Analytic, Frankfurt a.M., Germany) and radioactivity was determined by liquid scintillation counting. All data are expressed as percentage stimulation above basal [^{35}S]GTPγS binding.

3.9 MAGL activity assay

The monoacylglycerol lipase (MAGL) activity assay is based on the hydrolysis of 4-nitrophenyl acetate (4-NPA) by MAGL resulting in the product 4-nitrophenol, a chromogenic molecule with absorbance at 405-412 nm. Isolated dorsal mouse hippocampi were homogenized in 400 µl ice-cold assay buffer (100 mM Tris-HCl, pH 7.4) and sonicated (Brandelin, Berlin, Germany). Protein content of the samples was determined by using the BCA™ protein assay kit (Pierce, Rockford, USA) according to the manufacturer's protocol. Lysates were stored frozen in aliquots at -80°C until use. For the standard curve, 4-nitrophenol (Sigma Aldrich, St. Louis, MO, USA) was dissolved in 70 % ethanol and diluted with assay buffer to obtain the following final concentrations: 15.625 µM, 31.25 µM, 62.5 µM, 125 µM, 250 µM, 500 µM. Accordingly, 4-NPA (Sigma Aldrich, St. Louis, MO, USA) was dissolved in 70 % ethanol and diluted with assay buffer to obtain the following final concentrations: 62.5 µM, 125 µM, 250 µM, 500 µM, 1000 µM, 2000 µM. All standard and sample measurements were performed in duplicates in a 96-well plate in a

total volume of 200 µl. 4 µg of sample protein were incubated with the appropriate substrate concentration at 37°C and the absorbance at 405 nm was measured in the FLUOstar apparatus (BMG Labtech, Ortenberg, Germany) at the beginning (baseline values) and after 20 min incubation. Because 4-NPA underlies chemical hydrolysis, wells containing buffer and 4-NPA only were used as controls and this value was systematically subtracted from the sample values. The amount of produced 4-nitrophenol was calculated according to the standard curve and baseline values were subtracted to obtain exclusively metabolized 4-nitrophenol within the 20 min incubation step. Values were analyzed by Michaelis-Menten-kinetics with GraphPad Prism 4.0 (GraphPad Software, La Jolla, CA, USA) and non-linear regression curve fitting revealed maximum turnover rates of the samples.

3.10 Lipid analysis

The levels of AEA, 2-AG, arachidonic acid, oleoyl ethanolamide and palmitoyl ethanolamide were quantified as previously described (Schulte et al., 2012). Isolated hippocampi were stored at -80°C until extraction. Samples were weighed into 2 mL centrifuge tubes, spiked with 50 µL acetonitrile containing the internal standards and homogenized in 500 µL ice-cold 0.1 M formic acid with a 5-mm-steel ball using the TissueLyser II (Qiagen, Hilden, Germany) for 1 cycle of 30 s at 30 Hz. Ethylacetate/hexane (500 µL; 9:1, v/v) were added to extract the homogenate (for 10 s at 30 Hz), then the tubes were centrifuged for 10 min at 10,000×g and 4°C, the upper (organic) phase was removed, evaporated to dryness under a gentle stream of nitrogen at 37°C and re-dissolved in 50 µL acetonitrile. Analyses were performed on a LC-MS/MS system consisting of a 5500 QTrap triple-quadrupole linear ion trap mass spectrometer equipped with a Turbo V Ion Source (AB SCIEX, Darmstadt, Germany), an Agilent 1200 series LC system (degasser, pump and thermostatted column compartment; Agilent, Waldbronn, Germany) and a CTC HTC PAL autosampler (CTC Analytics AG, Zwingen, Switzerland).

Endocannabinoids were separated with a Phenomenex Luna 2.5 µm C18(2)-HST column, 100 × 2 mm, combined with a SecurityGuard pre-column (C18, 4 × 2 mm; Phenomenex, Aschaffenburg, Germany) with solvents A (0.1% formic acid in 20:80 acetonitrile/water, v/v) and B (0.1% formic acid in acetonitrile), using the following gradient: 55–90% B (0–2 min), then held at 90% B (2–7.5 min) and re-equilibrated at 55% B (7.5–10 min). The column temperature was 25°C, the flow rate was 0.3 mL/min, and the injection volume was 10 µL. Positive and negative ions were analyzed simultaneously by combining two experiments in “positive-negative-switching” mode. The Turbo V Ion Source was operated

with the electrospray (“TurboIon”) probe with nitrogen as curtain and nebulizer gas and using the following settings: temperature 550°C, curtain gas 40 psi, GS1 50 psi, GS2 50 psi, and capillary voltage −4,500 V (negative) and +4800 V (positive). The following precursor-to-product ion transitions were used for multiple-reaction monitoring (MRM): Experiment 1 (positive)—AEA m/z 348.3 → 62.1, AEA-d4 m/z 352.3 → 66.1, 2-AG m/z 379.1 → 287.2, 2-AG-d5 m/z 384.2 → 287.2; Experiment 2 (negative)—AA m/z 303.1 → 259.1, AA-d8 311.0 → 267.0. Dwell times were 20 ms in Experiment 1 and 50 ms in Experiment 2; pause between MRM transitions was 5 ms and settling time between Experiments 1 and 2 was 50 ms. Data acquisition and analysis were performed using Analyst software (version 1.5.1; AB SCIEX). Endocannabinoid levels were normalized to the weight of tissue samples.

3.11 Electrophysiological recordings

As previously described (Monory et al., 2006; Lourenco et al., 2010), mice (P8-10 weeks old) were anesthetized with isoflurane (5 %) and decapitated, their brains were rapidly removed and put into oxygenated (95 % O_2, 5 % CO_2) ice-cold artificial cerebrospinal fluid (ACSF) containing: 120 mM NaCl, 2.5 mM KCl, 1.25 mM NaH_2PO_4, 22 mM $NaHCO_3$, 2 mM $MgSO_4$, 2 mM $CaCl_2$ and 15 mM glucose; pH 7.4. Parasagittal hippocampal slices (300 µm thick) were cut on a vibratome (Leica Microsystems, Wetzlar, Germany) at 4°C. Slices were incubated at 34°C for 20min, then allowed to equilibrate for at least 1h at room temperature (RT) and finally transferred to a recording chamber continuously superfused with ACSF (approx. 2 ml/min).

Whole-cell voltage-clamp recordings were made at RT from pyramidal cells in CA1, visualized by infrared video microscopy (S/W-camera CF8/1, Kappa, Gleichen, Germany). Patch pipettes (3-4 MΩ) were filled with an intracellular solution containing: 100 mM K-Gluconic acid, 50 mM KCl, 10 mM CsCl, 1 mM HEPES, 0.2 mM EGTA, 1 mM $MgCl_2$, 1 mM Mg-ATP, 0.3 mM Na-GTP, pH 7.3 adjusted with 1M KOH. EGTA-concentration was kept low because of the Ca^{2+}-dependence of DSE or DSI (Lenz and Alger, 1999). Neurons were voltage-clamped at -70 mV. Access resistance was continuously evaluated during recordings upon a 3 mV, 10 ms pulse applied 2 s after each evoked response and cells were discarded from analysis if the access resistance changed by >20% over the course of the experiment. Correction for liquid junction potential changes (10 mV) was applied. Switching frequency was 30 kHz, gain 1.0-1.2. Records were filtered at 3 kHz (eight-pole Bessel filter), sampled at 10 kHz using Patchmaster (HEKA Elektronik, Ludwigshafen, Germany) software and analyzed off-line using the programs MiniAnalysis

(Synaptosoft, Decatur, GA, USA), Clampfit 10.0 (Molecular Devices Corporation, Sunnyvale, CA, USA) and GraphPad Prism 5 (GraphPad Software, La Jolla, CA, USA).

After reaching a stable baseline (approx. 10 min after establishing the whole cell configuration for infusion of intracellular solution), extracellular stimuli (100 µs, 50-600 µA) were delivered through a bipolar stainless-steel electrode. The stimulation electrode was placed in the stratum radiatum for stimulation of the Schaffer collaterals (approx. 100 µm from the recorded neuron). Glutamatergic (eEPSCs) and GABAergic (eIPSCs) components of synaptic responses were isolated by addition of gabazine (1 µM) and CGP55845 (50 µM), or DNQX (10 µM) and AP-5 (50 µM), respectively.

DSE/DSI tests consisted of 60 evoked postsynaptic currents (ePSCs), evoked every 3 s, before the depolarization step (from −70 to 0 mV, 3 s) and 90-100 responses thereafter. At least three DSE/DSI tests were applied to each cell (Lourenco et al., 2010). Amplitudes of three consecutive eEPSCs/eIPSCs were averaged and normalized against mean amplitude in control (2 min previous to the depolarization step). These normalized values were then averaged for all neurons recorded under a given condition, and presented as mean ± SEM. Data were plotted against time. Effect of postsynaptic depolarization was presented as “suppression to (%)”, where 100 % refers to no suppression. For comparative data analysis (shown in bar graphs), DSE/DSI magnitude was calculated as follows (modified from Wilson and Nicoll, 2001): Δ of ePSCs = [(x2 – x1)/x1] * 100, where x1 = mean of last 5 ePSC amplitudes before the depolarization, and x2 = mean of first three ePSCs amplitudes immediately after the depolarization. Calculated magnitudes were statistically tested, and significant deviation from zero was considered as DSE/DSI.

3.12 Behavioral analysis

Two weeks prior to behavioral phenotyping, animals were separated and single-housed to prevent abnormal behavior caused by fighting or suppression by the alpha male. All experiments were performed in the animal’s light phase (between 9:00-17:00) in this order: elevated plus maze, light/dark avoidance test, open field test, Morris water maze, passive avoidance, kainic acid-induced seizures. Mouse behavior was recorded when feasible by an overhead video camera and a computer equipped with Noldus Ethovision XT software (Noldus, Wageningen, Netherlands).

3.12.1 Elevated plus maze

In order to analyze anxiety behavior, we used the elevated plus maze (Fig. 2.1), which is a cross-shaped structure elevated 100 cm above the floor consisting of two opposite open and two opposite closed arms interconnected by a central platform (central platform, 6 × 6 cm^2; open arms, 35 × 6 cm^2; closed arms, 35 × 6 × 15 cm^3; illumination 40 lux). This test is based on an innate aversion of small rodents to well-lit, open spaces, which is presumably derived from selective pressure on defense against predation. As mice are also a naturally foraging, exploratory species, this model exploits the conflict of approaching versus avoiding a potentially dangerous area (Cryan and Holmes, 2005). This conflict is also utilized in other paradigms such as the light/dark avoidance task and the passive avoidance task. Mice were placed in the central platform, facing a closed arm and allowed to freely explore the plus maze for 5 min. Mouse behavior was recorded to calculate the time spent in open or closed arms, number of arm visits and distance traveled. The proportion of time spent in open arms was used to estimate open arm aversion (anxiety equivalent).

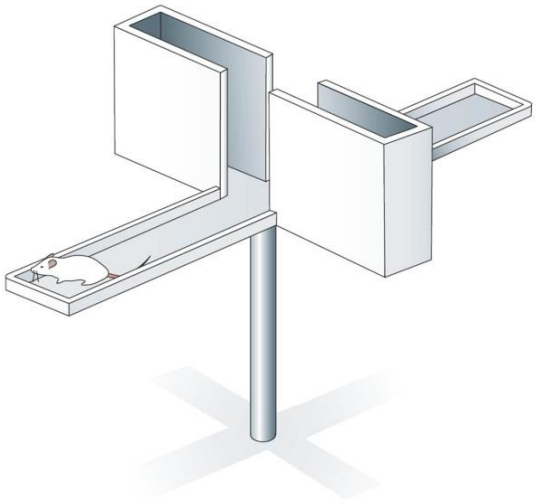

Figure 2.1. Elevated plus maze setup. (from Cryan and Holmes, 2005).

3.12.2 Light/dark avoidance test

The light/dark avoidance task is a test to analyze basic anxiety behavior and is also based on the rodent's conflict to approach versus avoid a potentially dangerous area. The experimental setup (Fig. 2.2) comprises an open, white, brightly-illuminated (100 lux at entry site) compartment (40 x 27 x 40 cm^3) and a closed, black, dark compartment (40 x 13 x 40 cm^3). Mice are able to enter and leave compartments via an entry site, which is closed before the start of the experiment. Animals were placed in the dark compartment and allowed to habituate for 1 min. Then, the entry site was opened and mice were allowed to freely explore both compartments for 5 min. The entries and the time spent in the lit compartment were used as parameters to assess aversive behavior.

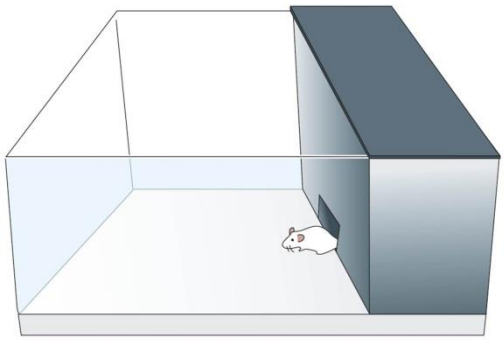

Figure 2.2. Light/dark avoidance setup. (from Cryan and Holmes, 2005).

3.12.3 Open field

The open field is an illuminated (100 lux) white box (40 x 40 x 40 cm^3) used to evaluate locomotor activity (Fig. 2.3). However, this test may also indicate anxiety-like behavior by estimating the time spent in the center compartment, which is the most illuminated and most unsheltered area in an open field box. The center of the open field box was defined as a square comprising 13 x 13 cm^2. Mice were placed in one of the corners of the open field and allowed to freely explore it for 10 min. Mouse behavior was recorded to calculate the distance traveled and the time spent in the center.

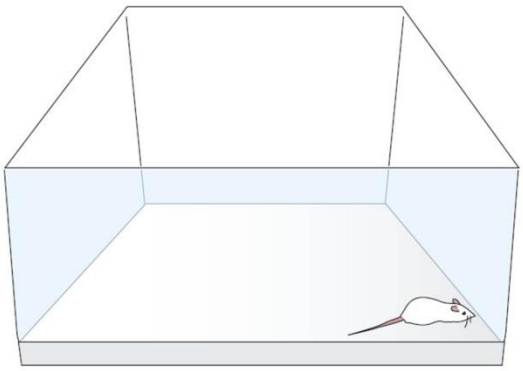

Figure 2.3. Open field setup. (from Cryan and Holmes, 2005).

3.12.4 Morris water maze

The Morris water maze is a spatial learning task originally developed for rats (Morris et al., 1982). A large circular tank (diameter 1.5 m) was filled with opaque water (25 ± 1°C). The escape platform (diameter 10 cm) was submerged 1 cm below the surface (Fig. 2.4). On the first day, mice were allowed to habituate to the task by swimming in a restrained area (50 x 30 cm^2) around the platform until they found it. To reduce the number of mice floating during the task, mice were subjected to the habituation protocol three times without any cues present. The next following seven days, mice were trained to find a hidden platform which was located at the center of one of the four quadrants of the pool. The location of the platform was fixed throughout testing. Mice had to navigate using extra-maze cues which were placed on the walls of the testing room. Every day, mice went through four trials with an intertrial interval of 10 min. Mice were placed into the pool facing the side wall randomly at one of four start locations and allowed to swim until they find the platform, or for a maximum of 90 sec. Any mouse that failed to find the platform within 90 sec was guided to the platform. The animal then remained on the platform for 20 sec before being removed from the pool. The latency and the path length to find the hidden platform were recorded for each mouse.

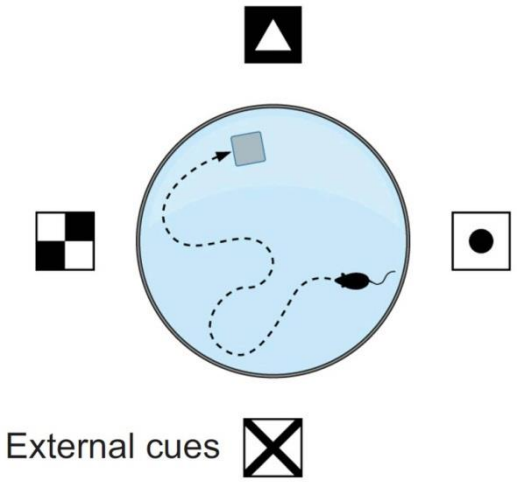

Figure 2.4. Morris water maze setup. (from Karlen et al., 2009).

3.12.5 Passive avoidance

The passive avoidance task is a fear-aggravated test used to evaluate learning and memory in rodents. In this test, subjects learn to avoid an environment in which an aversive stimulus (such as a foot-shock) was previously delivered. The passive avoidance test comprises a highly-illuminated, white compartment and a dark, black compartment that are connected by a door (Fig. 2.5) (Ugo Basile, Comerio, Italy). On the training day, mice were placed in the lit compartment and allowed to habituate for 30 sec. Then, the door was automatically opened and mice were allowed to enter the dark compartment. As mice exhibit an innate aversion to well-lit areas and a preference to dark, sheltered spaces, animals entered the dark compartment rather quickly in the training session. Having arrived in the dark compartment, the door was automatically closed and a mild foot shock (0.3 mA, 2 sec) was delivered to the animal. Mice eventually learn to associate the dark compartment with the foot shock. 24 hours later in the retention test, mice were subjected to the same procedure and the latency to enter the dark compartment is used as an indicator of learning and memory.

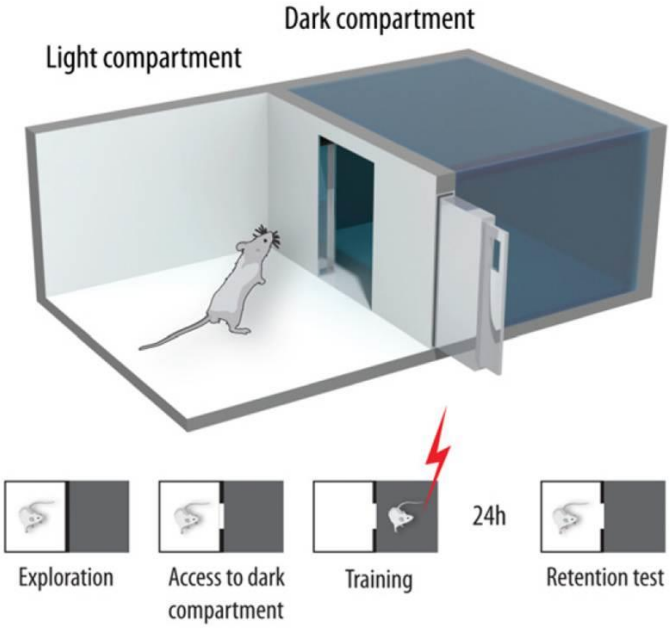

Figure 2.5. Passive avoidance setup. (from Karlen et al., 2009).

3.12.6 Kainic-acid induced seizures

Kainic acid (Sigma Aldrich, St. Louis, MO, USA) was dissolved in 0.9 % saline and administered intraperitoneally in a volume of 10 ml/kg body weight to induce epileptiform seizures. Two trained observers blind to the genotype of the mice monitored the severity of seizures for 2 hours and scored every 15 min according to the following scale (Monory et al., 2006): 0 - no response; 1 - immobility and staring; 2 - forelimb and/or tail extension, rigid posture; 3 - repetitive movements, head bobbing; 4 - rearing and falling; 5 - continuous rearing and falling: 6 - severe clonic-tonic seizures; 7 - death.

3.13 Data analysis

Data are presented as means ± standard error of mean (SEM). Normally distributed variables were analyzed using unpaired, two-tailed student's t-test, one-way analysis of variance (ANOVA) or two-way ANOVA for repeated measures followed by Bonferronni's post-hoc test to evaluate statistical significance with $p < 0.05$. Non-normally distributed seizure scores were analyzed using the two-sided Mann-Whitney U test with $p < 0.05$ as level of statistical significance. The Kaplan-Meier method was used to evaluate survival, followed by the log rank test to identify significant differences. Densitometric measurement of immunoblot signals was performed using NIH ImageJ software (Image Processing and Analysis in Java) or Bio1D software (Vilber Lourmat, Eberhardzell, Germany). All immunoblot signals were standardized to α-tubulin. For agonist-stimulated [^{35}S]GTPγS binding, data were analyzed using non-linear regression and sigmoidal curve fitting to obtain potency (EC_{50}) and efficacy (E_{max}) values. For the assessment of MAGL activity, data were analyzed using Michaelis-Menten-kinetics and non-linear curve fitting to receive the maximum turnover rate of the samples. Graphs and statistics were generated with GraphPad Prism 4.0 (GraphPad Software, La Jolla, CA, USA).

4 AAV vector-mediated overexpression of CB1 receptor in pyramidal neurons of the hippocampus protects against seizure-induced excitotoxicity

4.1 Introduction

Maintaining an optimal balance between excitatory and inhibitory activity of central nervous system (CNS) neurons is essential for proper physiological network activities, since either excessive glutamatergic transmission or insufficient GABAergic transmission can lead to excitotoxicity and epileptiform seizures in rodents and man (Ben-Ari and Cossart, 2000). The endocannabinoid system represents a molecular safeguard for efficient control of dangerous neuronal overexcitation (Mechoulam and Lichtman, 2003; Lutz, 2004; Katona and Freund, 2008). Endocannabinoids are produced on-demand from endogenous lipid precursors, and act as retrograde messengers that transiently inhibit the release of neurotransmitters by activation of the presynaptic cannabinoid type 1 (CB1) receptor. This phenomenon was termed depolarization-induced suppression of inhibition (DSI) for the suppression of presynaptic GABA release and depolarization-induced suppression of excitation (DSE) for the suppression of presynaptic glutamate release, respectively (Kano et al., 2009).

CB1 receptor activation has anticonvulsant and neuroprotective effects in acute and chronic seizure models (Marsicano et al., 2003; Wallace et al., 2003) and extracts of the plant *Cannabis sativa* have been used as epilepsy medication for thousands of years (Mechoulam and Lichtman, 2003). CB1 receptor is expressed on both GABAergic interneurons and glutamatergic principal neurons in the hippocampus (Marsicano and Lutz, 1999; Katona et al., 1999; Domenici et al., 2006; Monory et al., 2006; Katona and Freund, 2008), a brain region strongly implicated in the development of epilepsy. The endocannabinoid system has been implicated as a therapeutical target in epilepsy (van der Stelt et al., 2002) and as such, effective treatment strategies utilizing CB1 receptor regulation require a detailed understanding of CB1 receptor effects in neuronal subtypes. To this end, the analysis of conditional mouse mutants lacking the CB1 receptor on different subtypes of neurons subjected to kainic acid (KA)-induced seizures revealed that the CB1 receptor on hippocampal glutamatergic but not GABAergic neurons is required for protection against excitotoxic seizures (Monory et al., 2006). In line with this preclinical

data, specific downregulation of CB1 receptor protein and mRNA on glutamatergic, but not on GABAergic axon terminals was reported in epileptic human hippocampal tissue (Ludanyi et al., 2008). However, these conditional loss-of-function studies have not yet been complemented by the corresponding gain-of-function approach entailing CB1 receptor overexpression, preventing a comprehensive picture of CB1 receptor-mediated control of overexcitation.

Here, the effects of increased CB1 receptor gene dosage in the hippocampus were investigated on basic behavior performance, such as locomotion, anxiety and memory, and on the development of epileptiform seizures and neuronal damage in the KA model. To this end, adeno-associated virus (AAV) vectors were used for the delivery of the CB1 receptor to the hippocampus of adult mice. Because of its inherent neurotropism, stereotaxic delivery of AAV has been used widely for gene transfer to the rodent hippocampus in the context of animal models of excitotoxic seizures (Klugmann et al., 2005; Monory et al., 2006). However, conventional AAV vectors transduce all types of hippocampal neurons (Richichi et al., 2004), which might result in confounding results. To avoid this confounding factor, transgene expression is restricted exclusively to principal neurons expressing Cre recombinase, using an AAV expression cassette with a transcriptional Stop cassette flanked by loxP sites, preceding the transgene. This study shows that somatic transfer of the CB1 receptor gene to glutamatergic hippocampal neurons is sufficient to provide protection against acute seizures and neuronal damage.

4.2 Results

4.2.1 AAV-Stop-mediated transgene expression requires Cre-induced recombination

The neurotropic mosaic AAV1/2 has previously been shown to efficiently deliver genes to all neuronal subtypes of the rodent hippocampus (Richichi et al., 2004; Monory et al., 2006). To restrict virus-mediated transduction to glutamatergic hippocampal neurons, our approach was to excise a transcriptional termination element preceding the cDNA in the AAV-expression cassette by providing Cre recombinase in *trans* (Fig. 3.1A). The packaging limit of AAV is 5 kb (Dong et al., 1996), and accommodation of large transgenes requires minimizing the size of *cis* elements in the expression cassette. To adhere to this concept, a transcriptional termination ("Stop") element was designed entailing two loxP sites (34 bp) flanking a herpes simplex virus thymidin kinase polyadenylation site (70 bp) and a polyadenylation terminator (154 bp).

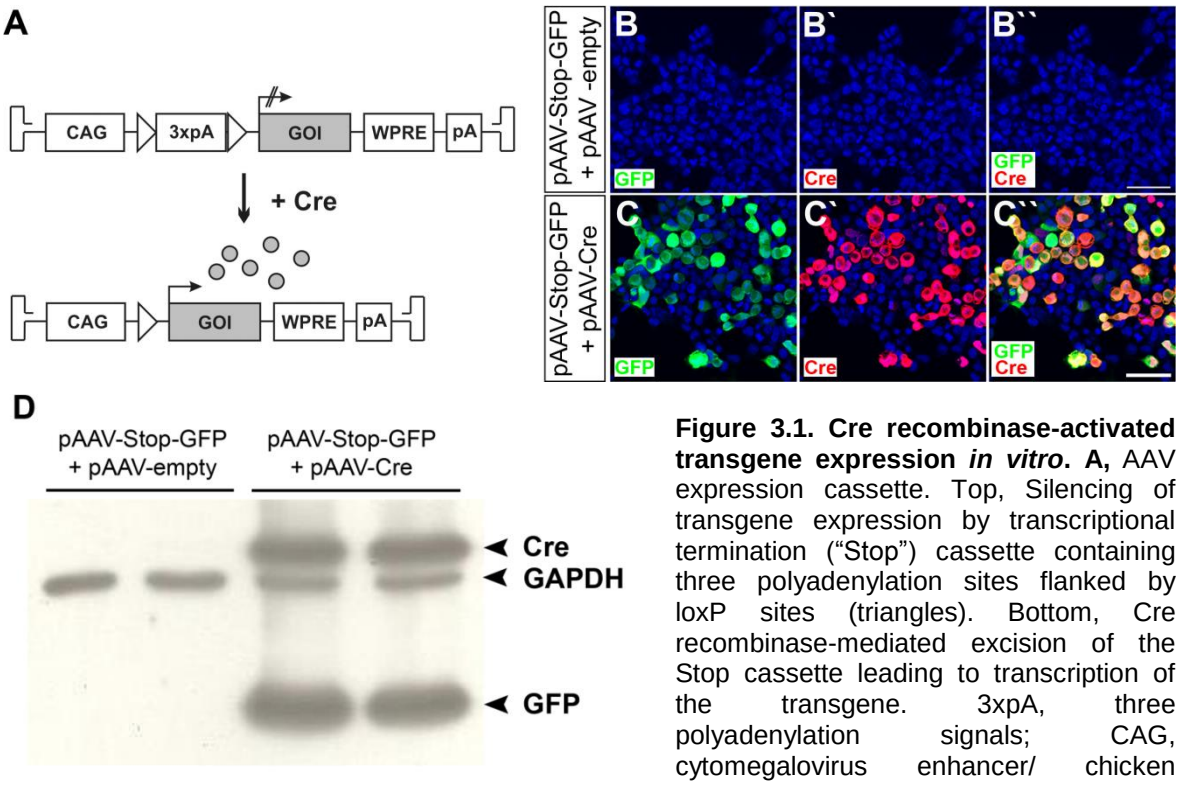

Figure 3.1. Cre recombinase-activated transgene expression *in vitro*. A, AAV expression cassette. Top, Silencing of transgene expression by transcriptional termination ("Stop") cassette containing three polyadenylation sites flanked by loxP sites (triangles). Bottom, Cre recombinase-mediated excision of the Stop cassette leading to transcription of the transgene. 3xpA, three polyadenylation signals; CAG, cytomegalovirus enhancer/ chicken β-actin promoter; GOI, gene of interest; pA, polyadenylation signal; WPRE, woodchuck hepatitis virus post-transcriptional regulatory element. **B and C,** HEK cells were co-transfected with pAAV-Stop-GFP and pAAV-empty (B) or pAAV-Cre (C) revealing that GFP immunofluorescence is strictly limited to Cre transfectants. Transgene expression is tightly inhibited when pAAV-Stop-GFP is co-transfected with pAAV-empty. Blue: cell nucleus staining with DAPI. Bar in C``, 50 µm. **D,** Western blot analysis of HEK cell lysates confirms that Cre-mediated excision of the Stop cassette causes expression of GFP. In absence of Cre recombinase, the expression of GFP was efficiently inhibited. GAPDH was used as loading control. Cre recombinase: 38 kD, GAPDH: 36 kD, GFP: 27 kD.

The Stop cassette was cloned into our latest generation AAV expression cassette (Klugmann et al., 2005) between the cytomegalovirus enhancer/chicken β-actin (CAG) promoter and the cDNA of humanized renilla green fluorescent protein (hrGFP) to obtain pAAV-Stop-GFP. Human embryonic kidney 293 (HEK) cells were transfected with this reporter construct to assess the efficacy of the Cre-induced AAV system *in vitro*. Immunocytochemical analysis showed that the absence of Cre recombinase prevented transcription of the reporter (Fig. 3.1B), whereas co-transfection with a Cre plasmid caused efficient activation of GFP expression (Fig. 3.1C). This finding was confirmed by western blot analysis further revealing no leakiness of the system (Fig. 3.1D).

For *in vivo* analysis, either generic AAV-GFP or conditional AAV-Stop-GFP were injected into the hippocampus of adult (>2 months) wild-type mice (C57BL/6-N) and Cre driver mice (NEX-Cre and dlx-Cre). NEX-Cre mice express Cre recombinase specifically in glutamatergic forebrain neurons under the control of regulatory sequences of the NEX gene. The NEX gene is active in pyramidal neurons and dentate gyrus mossy cells, but not in interneurons, oligodendrocytes and astrocytes, nor in granule cells of the dentate gyrus after P10 (Goebbels et al., 2006). In dlx-Cre mice, Cre recombinase is expressed under control of the regulatory sequences of the Dlx5/6 genes (Monory et al., 2006). These homeobox genes are transcription factors that are required for the proper differentiation and migration of inhibitory interneurons (Batista-Brito et al., 2008).

Mice were sacrificed four weeks post-injection when AAV-mediated transgene expression had peaked to remain at stable levels. Vector spread was determined by immunohistochemistry disclosing that GFP immunoreactivity was observed throughout the dorsal hippocampus of AAV-GFP-injected mice. As expected, transduction of all types of neurons occurred in the hippocampal formation, CA1 to CA3, hilar region and the dentate gyrus (Fig. 3.2A). The abundant reporter protein expression in processes of principal neurons generally prevented visualization of transduced interneurons. However, assessment of sections showing moderate GFP levels in stratum radiatum and stratum lacunosum unmasked the presence of GFP immunoreactivity also in interneurons (arrowheads in Fig. 3.2A). In contrast, no GFP expression was detected after delivery of AAV-Stop-GFP into wild-type mice (Fig. 3.2B), even after prolonged exposure times (not shown), validating the effective inhibition of transcription by the Stop cassette *in vivo*. In AAV-Stop-GFP injected NEX-Cre mice, pyramidal neurons in CA1 and CA3 showed robust GFP expression (Fig. 3.2C). As expected, dentate granule cells were unlabeled, indicating the lack of Cre expression in these neurons at adult stages when AAV-delivery was performed (Goebbels et al., 2006). In contrast, an insular GFP immunoreactivity was detected when AAV-Stop-GFP was injected into the hippocampus of dlx-Cre mice

(Fig. 3.2D). This scattered pattern indicates a successful targeting of GABAergic interneurons whose spreading neurites represent a typical morphological feature (inset in Fig. 3.2D). In summary, these findings demonstrate that the presence of a small Stop element confers tight spatiotemporal control over transgene expression after AAV delivery to Cre driver mouse lines.

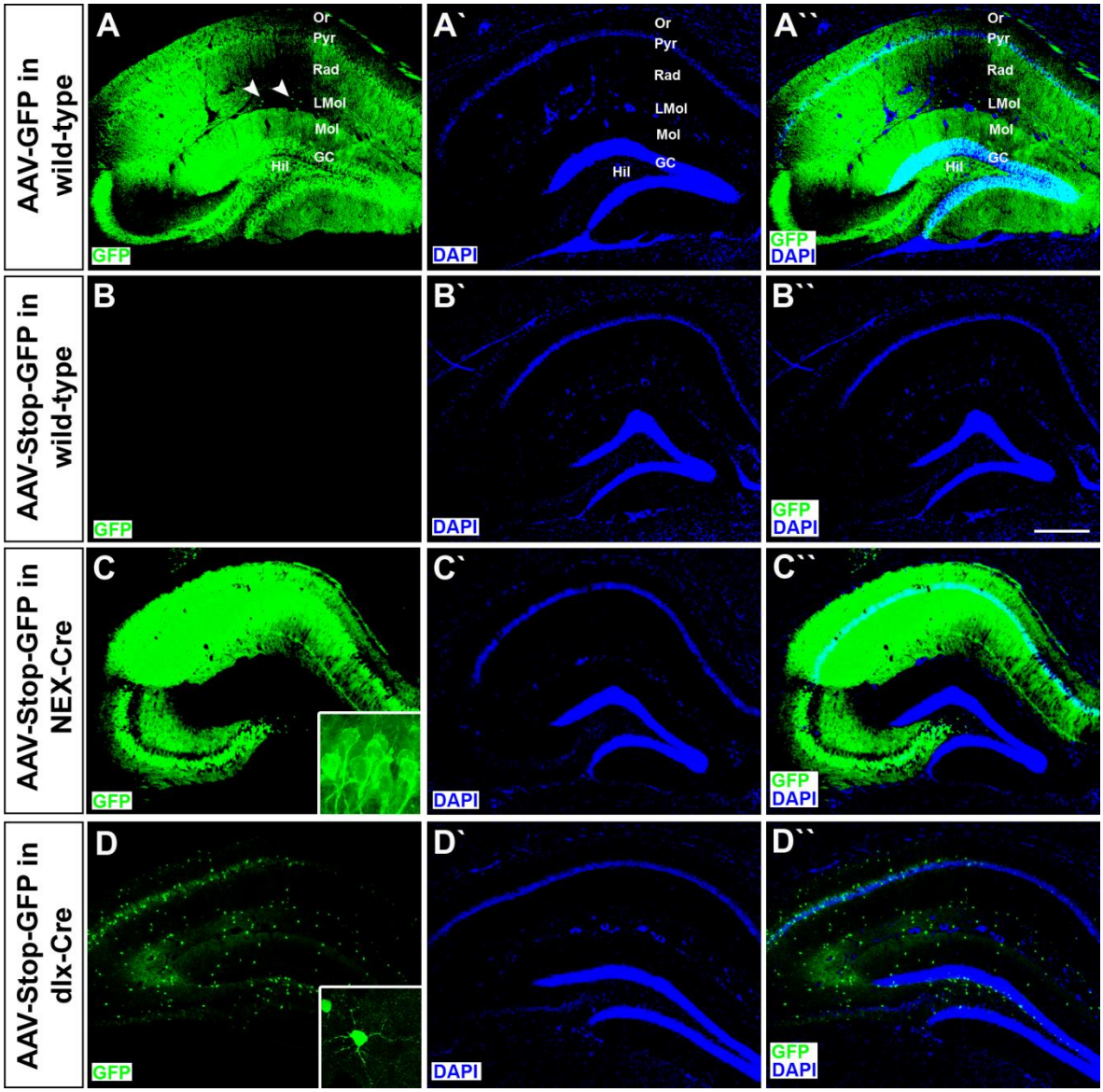

Figure 3.2. Cre recombinase-activated transgene expression *in vivo*. Two months after stereotaxic vector delivery (AAV-GFP or AAV-Stop-GFP) to the dorsal hippocampus of adult wild-type, NEX-Cre or dlx-Cre mice, GFP expression was assessed in brain sections by immunohistochemistry. **A,** AAV-GFP efficiently transduces all types of neurons of the hippocampal formation, in particular in CA1, CA3, the hilar region and the dentate gyrus. Note that transduced interneurons (arrowheads in A) can be visualized in areas of low GFP abundance. **B,** After AAV-Stop-GFP injection, GFP expression was not detectable in wild-type mice. **C,** In NEX-Cre mice, neurons of the pyramidal cell layer express the reporter gene, while granule cells of the dentate gyrus are spared. Note that in this mouse line, Cre recombinase is not expressed in the adult dentate gyrus (Goebbels et al., 2006). The inset depicts pyramidal cells in CA1 under high magnification. **D,** Reporter expression is exclusive to GABAergic interneurons after injection of AAV-Stop-GFP into the hippocampus of dlx-Cre mice. The inset illustrates a GABAergic cell with spreading neurites under high magnification. GC, granule cell layer; Hil, hilar region; LMol, stratum lacunosum-moleculare; Mol, stratum moleculare; Or, stratum oriens; Pyr, CA1/CA3 pyramidal cell layer; Rad, stratum radiatum. Bar in B``, 250 µm.

4.2.2 CB1 receptor overexpression in hippocampal pyramidal neurons

4.2.2.1 Conditionally expressed CB1 receptor in hippocampal pyramidal cells is functional

CB1 receptor is known to be expressed in distinct neuronal subpopulations in the hippocampus (Marsicano and Lutz, 1999; Monory et al., 2006; Kano et al., 2009) with very high levels in GABAergic interneurons which belong mainly to the cholecystokinin-positive and parvalbumin-negative type (Marsicano and Lutz, 1999; Morozov et al., 2009), and 10-20 times less CB1 receptor protein in glutamatergic pyramidal terminals (Kawamura et al., 2006; Kano et al., 2009; Steindel et al., 2013). For a cell type-specific CB1 receptor overexpression, the reporter gene in pAAV-Stop-GFP was replaced with the coding region of the HA-tagged rat CB1 receptor cDNA to receive pAAV-Stop-CB1 (Fig. 3.3). The presence of the HA-epitope tag facilitates immunological detection of the transgene and allows specific assessment of ectopic versus endogenous CB1 receptor protein. After confirming the functionality of pAAV-Stop-CB1 by HEK cell transfection and immunocytochemistry (data not shown), a viral vector was produced (named as AAV-Stop-CB1) and subjected to standard quality controls, such as Coomassie gel staining and qPCR analysis to quantify the vector titer.

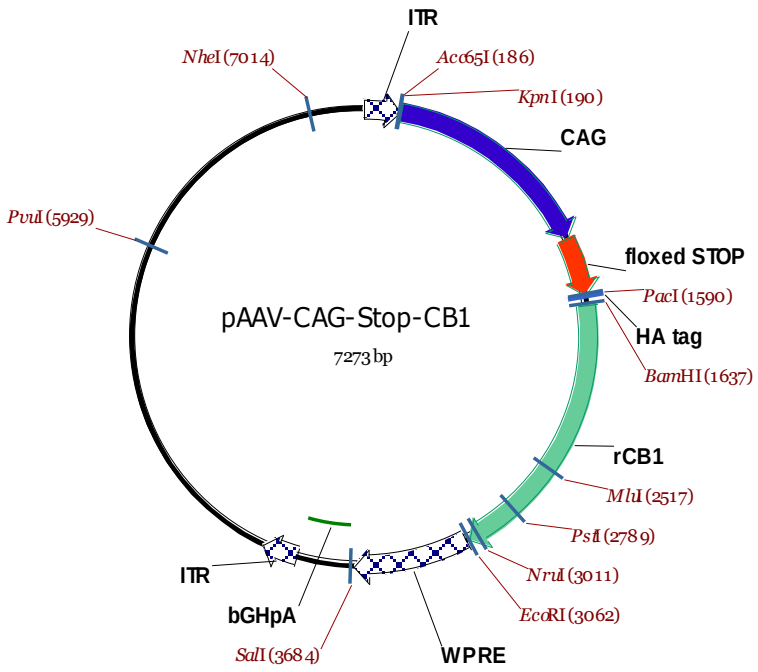

Figure 3.3. Plasmid map of pAAV-Stop-CB1. bGHpA, bovine growth hormone polyadenylation signal; CAG, cytomegalovirus enhancer/ chicken β-actin promoter; floxed Stop, transcriptional terminator flanked by loxP sites; ITR, inverted terminal repeat; rCB1, rat cannabinoid type 1 receptor; WPRE, woodchuck hepatitis virus post-transcriptional regulatory element.

The AAV-Stop-CB1 vector (3.0E+08 vector copies) was injected into the hippocampus of adult NEX-Cre mice to achieve conditional CB1 receptor overexpression in hippocampal glutamatergic cells (AAV-Glu-CB1 mice). Wild-type littermates of NEX-Cre mice, which do not express Cre recombinase, were also injected with the AAV-Stop-CB1 vector and served as control group (AAV-WT mice). Immunohistochemical detection of the HA tag revealed Cre-activated CB1 receptor expression in hippocampal pyramidal neurons (Fig. 3.4A) in a similar pattern as compared to AAV-Stop-GFP-injected animals, confirming the integrity of the conditional AAV system. Co-localization of ectopic CB1 receptor and vesicular glutamate transporter 1 (VGluT1), a marker for glutamatergic presynaptic sites, in the inner third of the molecular layer of the dentate gyrus, where the mossy cells are synapsing on granule cell dendrites, demonstrated presynaptic location of ectopic CB1 receptor protein (Fig. 3.4B). Thus, the subcellular localization in glutamatergic cells of exogenous CB1 receptor protein matches that of the endogenous CB1 receptor (Monory et al., 2006), and the detection of HA-immunoreactivity in somata is likely to reflect accumulated CB1 receptor destined for transport to axonal terminals.

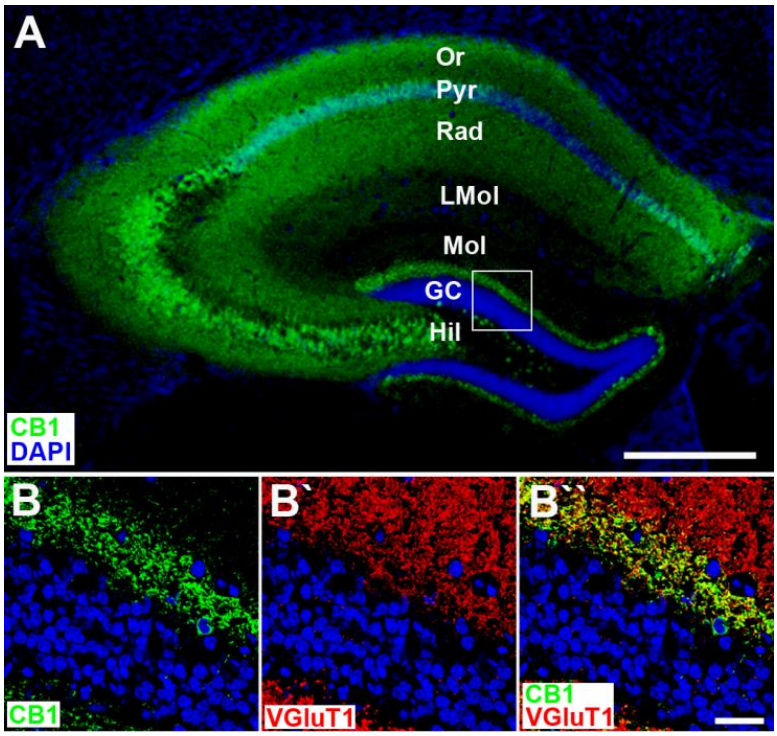

Figure 3.4. Transgenic HA tagged CB1 receptor is expressed in hippocampal pyramidal neurons. AAV-Stop-CB1 was injected bilaterally into the hippocampus of NEX-Cre transgenic mice (AAV-Glu-CB1) and their respective wild-type littermates (AAV-WT). **A,** Cre-activated CB1 receptor expression occurred in pyramidal neurons and appeared in a similar pattern compared to AAV-Stop-GFP confirming the integrity of the system. GC, granule cell layer; Hil, hilar region of dentate gyrus; LMol, stratum lacunosum-moleculare; Mol, stratum moleculare; Or, stratum oriens; Pyr, CA1/CA3 pyramidal cell layer; Rad, stratum radiatum. Bar, 250 µm. **B,** Higher magnification micrographs of dentate granule cells shown in A. Immunohistochemistry for the HA tag reveals coexpression of CB1 receptor and VGluT1 in the inner molecular layer of the dentate gyrus, validating the presynaptic localization of transgenic CB1 receptor. Bar in B``, 25 µm.

Furthermore, CB1 receptor protein levels were examined in hippocampal homogenates of AAV-WT and AAV-Glu-CB1 mice by Western blot analysis (Fig. 3.5A). CB1 receptor protein levels were significantly increased in AAV-Glu-CB1 mice as compared to AAV-WT controls following normalization to α-tubulin (AAV-WT, 72.5 ± 4.87 %, n = 3; AAV-Glu-CB1, 261.4 ± 19.74 %, n = 3; unpaired t test, two-tailed, $p < 0.001$). Quantitative biochemical analyses revealed an overall CB1 receptor upregulation of 3.5-fold as compared to controls. However, this value might underestimate the actual increase of CB1 receptor in AAV-Stop-CB1 treated pyramidal neurons, given the moderate expression levels of endogenous CB1 receptor protein in this neuronal subtype as compared to the high expression levels in GABAergic neurons.

Increased CB1 receptor levels may result in enhanced cannabinoid-induced G protein activation, and thus, enhanced endocannabinoid signaling. To address this, HU-210-stimulated [^{35}S]GTPγS binding was performed with hippocampal homogenates of AAV-WT and AAV-Glu-CB1 mice previously analyzed by immunoblot. AAV-WT mice reached a maximum stimulation of 93.77 ± 4.99 % over baseline, while HU-210-induced G protein activation was significantly increased in AAV-Glu-CB1 mice, reaching a maximum of 224.4 ± 7.39 % (Fig. 3.5B; two-way repeated-measures ANOVA, $p < 0.0001$). This finding demonstrates an enhancement of CB1 receptor signaling in AAV-Glu-CB1 mice.

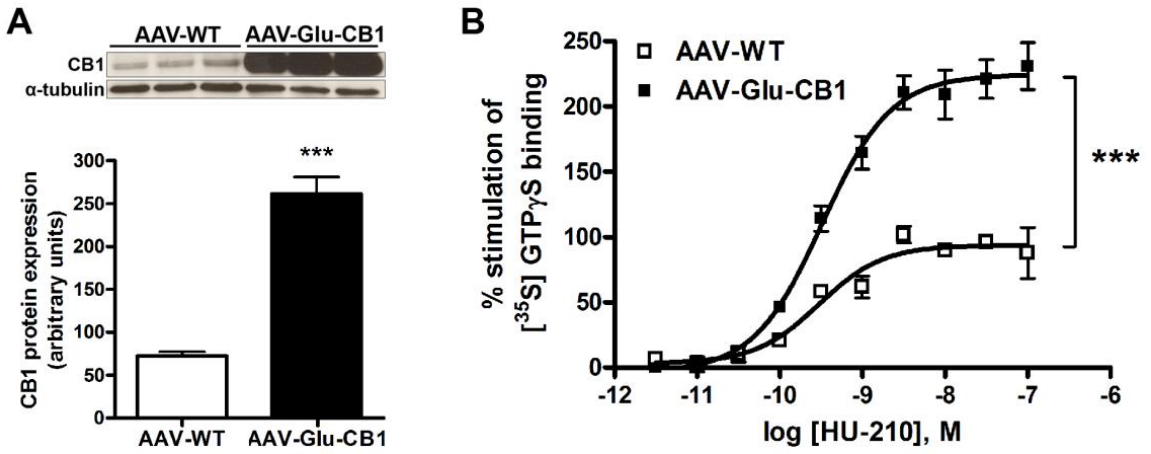

Figure 3.5. AAV-mediated CB1 receptor overexpression enhances cannabinoid-induced G protein activation. AAV-Stop-CB1 was injected bilaterally to the hippocampus of NEX-Cre transgenic mice (AAV-Glu-CB1) and their respective wild-type littermates (AAV-WT). **A,** Western blot analysis of hippocampal homogenates of AAV-WT and AAV-Glu-CB1 mice showed that AAV-Glu-CB1 mice express significantly elevated levels of CB1 receptor protein (unpaired t test, two-tailed, $p < 0.001$). Data are normalized for α-tubulin. **B,** Stimulation of [^{35}S]GTPγS binding in hippocampal homogenates of AAV-WT and AAV-Glu-CB1 mice was determined by various concentrations of the CB1 receptor agonist HU-210. Basal binding was measured in absence of HU-210 and defined as 0 % in each experiment. Data are presented as percentage stimulation above basal [^{35}S]GTPγS binding and are the means ± SEM, all performed in duplicates. The non-linear regression curve illustrates that overexpression of the CB1 receptor in hippocampal pyramidal neurons resulted in significantly enhanced cannabinoid-induced G protein activation (AAV-WT, EC_{50} = 2.97 ± 0.13 nM, n = 3; AAV-Glu-CB1, EC_{50} = 3.26 ± 0.08 nM, n = 6; two-way ANOVA for repeated measures, followed by Bonferronni post-hoc test, genotype x agonist concentration effect, $F(9, 70) = 10.93$, $p < 0.0001$). *** $p < 0.0001$.

Taken together, ectopic CB1 receptor was shown to be robustly expressed cell type-specifically in hippocampal pyramidal neurons, to be located at presynaptic sites and to be coupled to G proteins. Thus, ectopic CB1 receptor showed common characteristics of endogenous CB1 receptor protein.

4.2.2.2 Elevated CB1 receptor at glutamatergic hippocampal terminals affect basal locomotion and hippocampal-dependent memory performance

To analyze behavioral alterations in locomotion, anxiety, memory and seizure susceptibility, AAV-WT and AAV-Glu-CB1 mice were subjected to a battery of behavioral tests including open field, light/dark avoidance test, Morris water maze, passive avoidance task and kainic acid-induced epileptiform seizures.

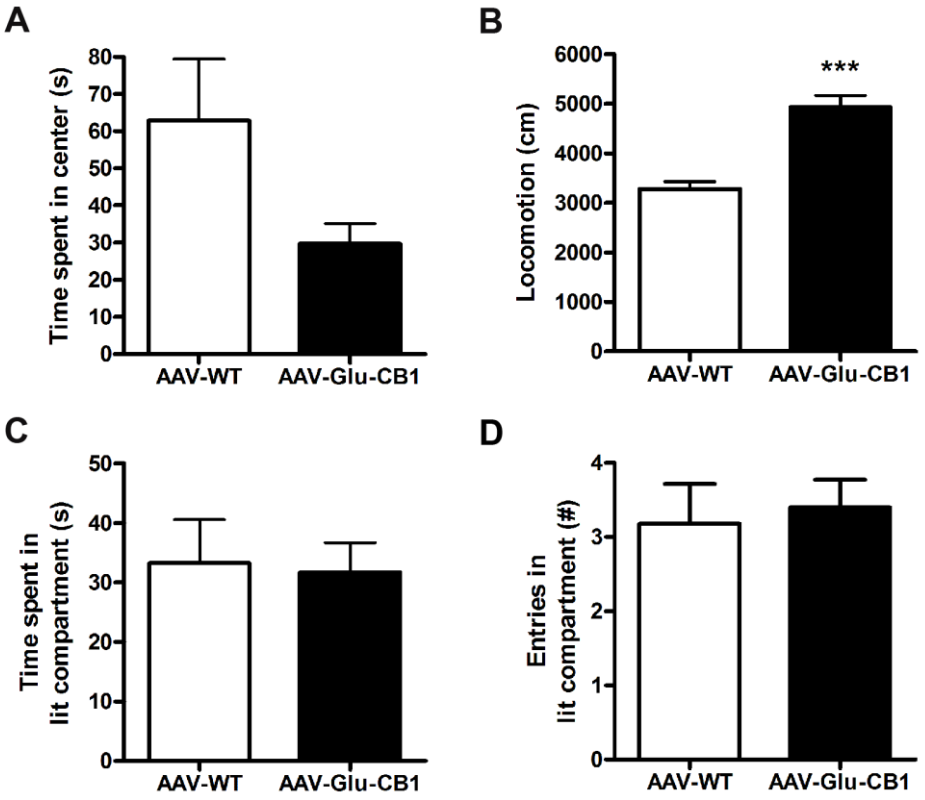

Figure 3.6. AAV-WT and AAV-Glu-CB1 mice tested for locomotion and anxiety. A, In the open field test, AAV-Glu-CB1 mice showed a trend to decreased time spent in the center, which was close to but did not reach statistical significance (unpaired t test, two-tailed, $p = 0.062$). **B,** During the time course of 10 min, AAV-Glu-CB1 mice covered a significantly higher distance than AAV-WT controls (unpaired t test, two-tailed, $p < 0.0001$). **C and D,** Anxiety behavior did not differ between both genotypes as indicated by the time spent in the lit compartment and the entries into the lit compartment in the light/dark avoidance task. Values are expressed as means ± SEM; n = 11 to 14 mice per group. *** $p < 0.0001$.

In the open field, the time spent in the center was attenuated in AAV-Glu-CB1 without reaching significance (Fig. 3.6A), which may indicate changes in anxiety behavior. However, as AAV-Glu-CB1 mice showed a significantly increased locomotor activity relative to AAV-WT controls (Fig. 3.6B; unpaired t test, two-tailed, $p < 0.0001$), the time parameter in this test must be considered negligible. Moreover, the analysis of anxiety behavior in the light/dark avoidance task revealed no alterations between both groups (Fig. 3.6C, D).

Several studies showed that an enhanced CB1 receptor signaling, induced by exposure to cannabis or synthetic cannabinoids, causes cognitive deficits that are primarily associated with the hippocampus (Lichtman et al., 1995; Boucher et al., 2009). As AAV-Glu-CB1 mice showed enhanced cannabinoid-induced G protein activation, we determined whether hippocampus-dependent learning and memory were altered in these mice. Mice were trained in the Morris water maze to find the hidden platform for seven days, four trials per day. Two-way repeated-measures ANOVA revealed that there was a significant effect of CB1 receptor overexpression in hippocampal pyramidal neurons on both the latency (Fig. 3.7A; two-way repeated measures ANOVA, $F(1, 126) = 7.83$, $p < 0.05$) and the distance travelled (Fig. 3.7B; two-way repeated measures ANOVA, $F(1, 126) = 35.7$, $p < 0.0001$) to find the hidden platform. This finding suggests that hippocampus-dependent learning is affected in AAV-Glu-CB1 mice. To corroborate this result, transgenic mice underwent the passive avoidance task. Here, subjects learn to avoid an environment in which an aversive stimulus (foot-shock) was previously delivered. The latency to re-enter this environment 24 hours after memory acquisition is an indicator of learning and memory. During memory acquisition, latencies to enter the dark compartment did not differ between the two groups. In the retention test, latencies of AAV-Glu-CB1 mice were significantly decreased relative to AAV-WT controls (Fig. 3.7C; unpaired t test, two-tailed, $p < 0.01$). This finding further confirms that elevated levels of the CB1 receptor at hippocampal pyramidal terminals impaired hippocampal memory performance.

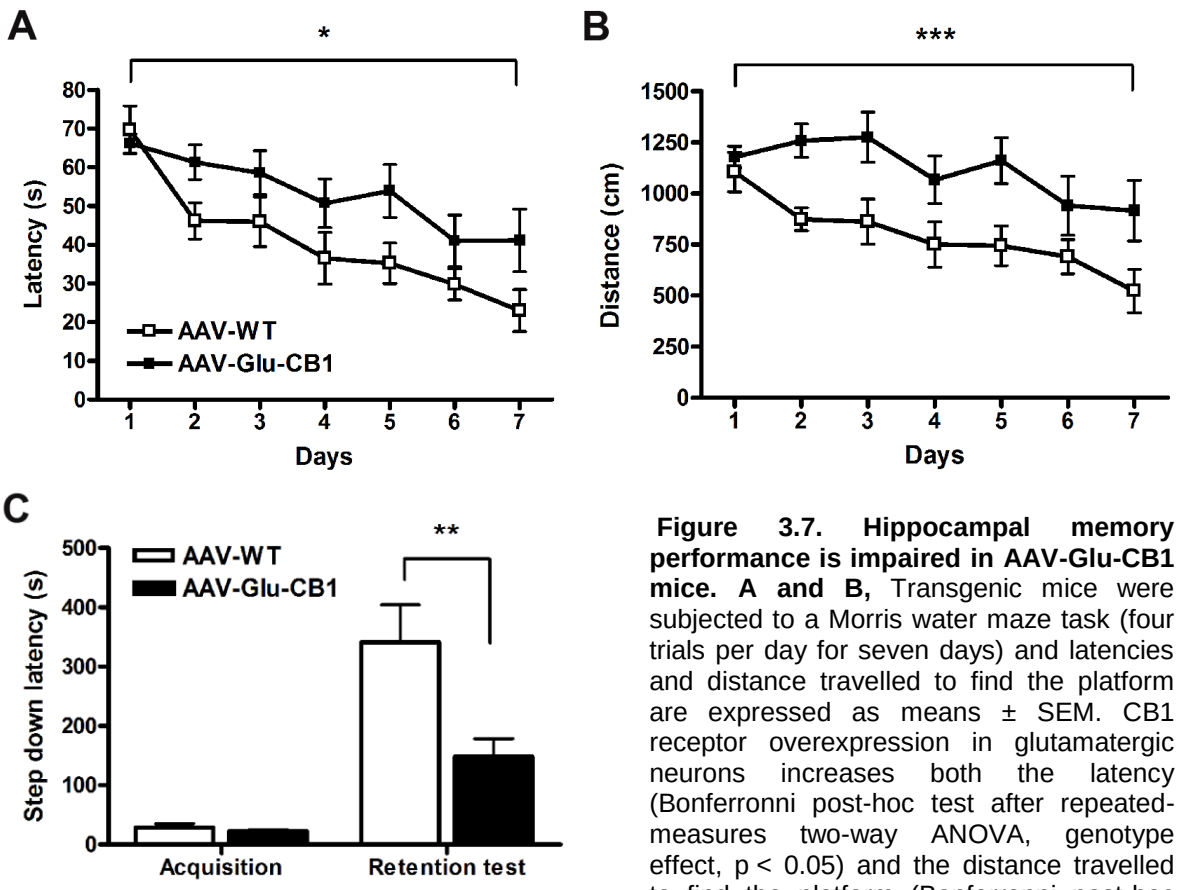

Figure 3.7. Hippocampal memory performance is impaired in AAV-Glu-CB1 mice. A and B, Transgenic mice were subjected to a Morris water maze task (four trials per day for seven days) and latencies and distance travelled to find the platform are expressed as means ± SEM. CB1 receptor overexpression in glutamatergic neurons increases both the latency (Bonferroni post-hoc test after repeated-measures two-way ANOVA, genotype effect, $p < 0.05$) and the distance travelled to find the platform (Bonferroni post-hoc test after repeated-measures two-way ANOVA, genotype effect, $p < 0.0001$). **C,** Hippocampal memory performance was analyzed in the passive avoidance test and data are expressed as mean latency ± SEM to enter the dark compartment. During memory acquisition, latencies of AAV-Glu-CB1 mice did not differ from AAV-WT controls. 24 hours later in the retention test, AAV-Glu-CB1 latencies were significantly reduced compared to AAV-WT (unpaired t test, two-tailed, $p < 0.01$). n = 10 to 13 mice per group. * $p < 0.05$, ** $p < 0.01$, *** $p < 0.0001$.

4.2.2.3 Increased CB1 receptor gene dosage in hippocampal glutamatergic neurons confers protection against epileptiform seizures

CB1 receptor activation on glutamatergic neurons was shown to play an essential role in the protection against excitotoxic seizures (Marsicano et al., 2003; Wallace et al., 2003; Monory et al., 2006; Falenski et al., 2007). This provided the rationale to investigate the therapeutic potential of CB1 receptor overexpression in the context of the pathogenic consequences of experimentally induced overexcitation of glutamatergic circuits in the hippocampus. Kainic acid (KA) was injected (30 mg/kg, i.p.) to AAV-WT and AAV-Glu-CB1 mice to induce robust activation of excitatory pathways resulting in acute epileptiform seizures. At every time point of scoring, seizure severity was moderated in AAV-Glu-CB1 mice compared to AAV-WT controls, which was close to but did not reach statistical significance (Fig. 3.8A; Mann Whitney U test, two-tailed, $p = 0.065$). However, the average behavioral score over a period of 120 min was significantly decreased in

AAV-Glu-CB1 mice (Fig. 3.8B; Mann Whitney U test, two-tailed, $p < 0.001$). Severe KA-induced motor seizures can be fatal. Kaplan-Meier survival analysis demonstrated a significant difference between both genotypes in the course of the KA treatment (Fig. 3.8C, log rank test, $p < 0.05$). 180 min after the start of the experiment, 53 % of AAV-Glu-CB1 mice but only 18 % of AAV-WT mice had survived. No animals died at later stages. Importantly, it was previously shown that expression of Cre recombinase in glutamatergic neurons of the forebrain per se does not alter susceptibility to KA-induced seizures (Marsicano et al., 2003; Monory et al., 2006). These results demonstrate that CB1 receptor overexpression in glutamatergic hippocampal neurons ameliorates the severity of acute epileptiform seizures, indicating an essential role of hippocampal pyramidal neurons and mossy cells in CB1 receptor-dependent on-demand protection against excessive excitatory activity.

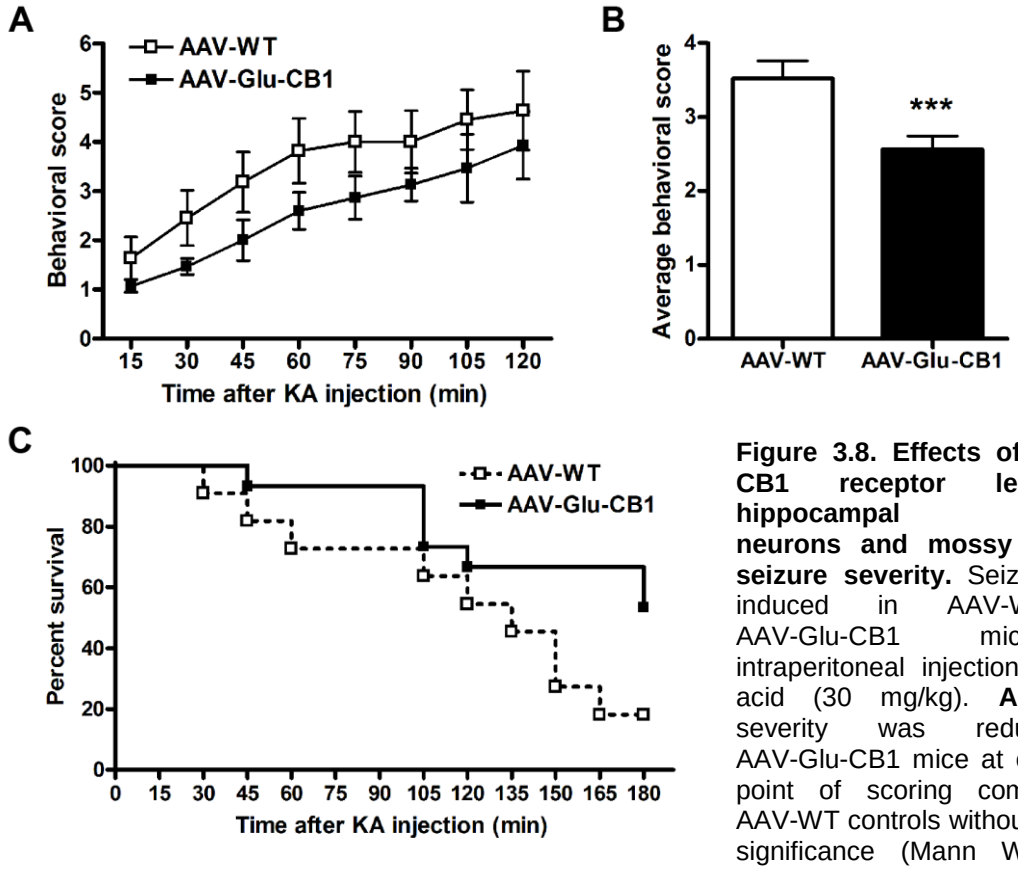

Figure 3.8. Effects of elevated CB1 receptor levels in hippocampal pyramidal neurons and mossy cells on seizure severity. Seizures were induced in AAV-WT and AAV-Glu-CB1 mice by intraperitoneal injection of kainic acid (30 mg/kg). **A,** Seizure severity was reduced in AAV-Glu-CB1 mice at every time point of scoring compared to AAV-WT controls without reaching significance (Mann Whitney U test, two-tailed, $p = 0.065$). **B,** The average behavioral score over a period of 120 min was significantly decreased in AAV-Glu-CB1 mice (Mann Whitney U test, two-tailed, $p < 0.001$), indicating improved protection against KA-induced seizures. **C,** Kaplan–Meier survival curves during KA treatment differ significantly between both genotypes (log rank test, $p < 0.05$). The survival rate at 180 min after KA injection was 18 % of AAV-WT versus 53 % of AAV-Glu-CB1 mice. n = 11 to 15 mice per group. *** $p < 0.001$.

4.2.2.4 CB1 receptor overexpression and excitotoxicity

Systemic KA treatment leads to neuronal degeneration especially in CA3 pyramidal neurons of the hippocampus (Ben-Ari and Cossart, 2000). Five days after KA injections, mice were sacrificed and brain sections were stained with Fluoro-Jade C (FJC), a green fluorescent dye specific for labeling degenerating neurons (Schmued et al., 2005). Representative images of FJC-labeled cells in the cortex (Fig. 3.9A, C) and in the CA3 area (Fig. 3.9B, D) of AAV-WT and AAV-Glu-CB1 mice are shown.

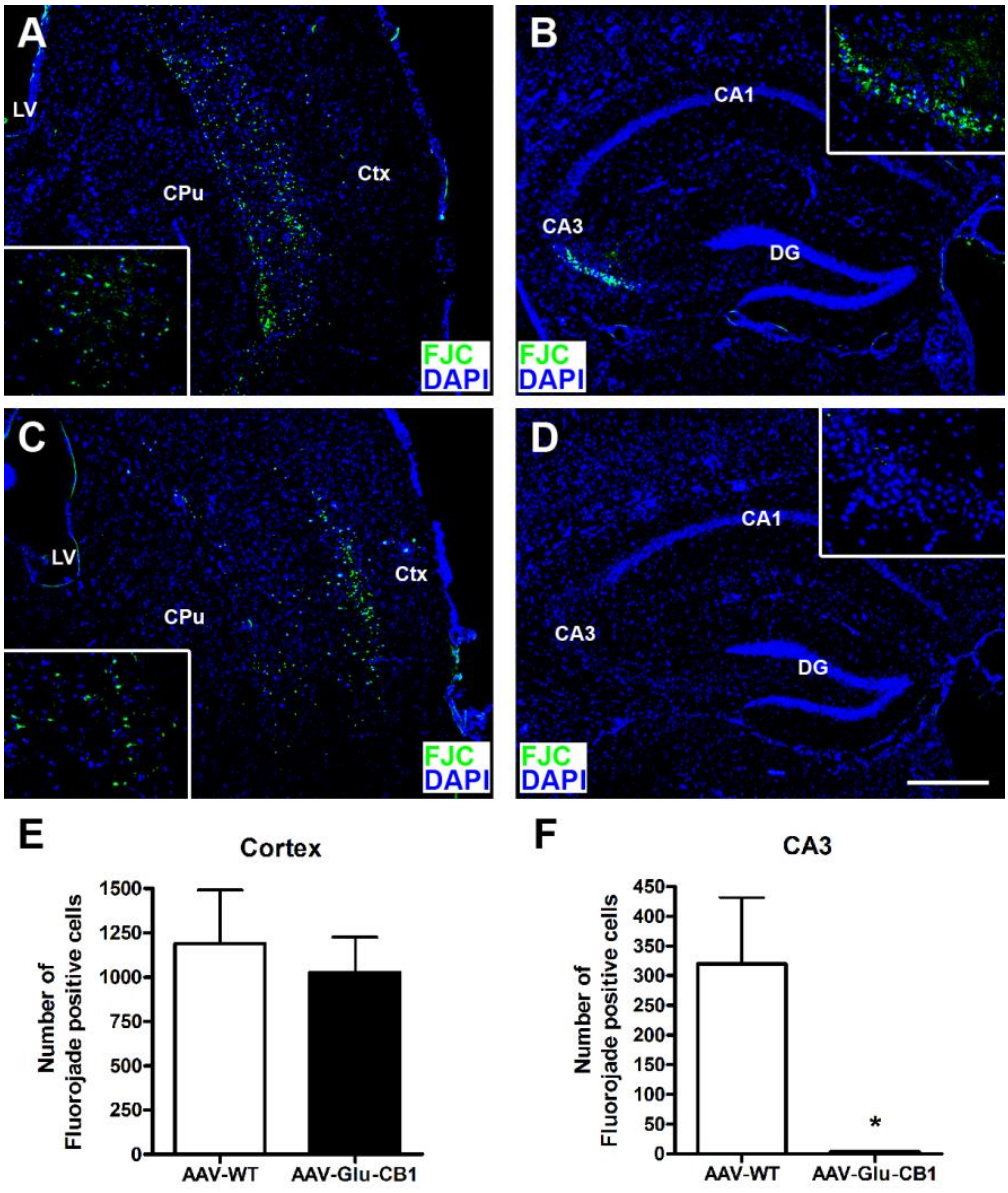

Figure 3.9. Increased CB1 receptor levels prevent degeneration of CA3 pyramidal neurons. Assessment of neurodegeneration by Fluoro-Jade C (FJC) staining five days after exposure to KA. **A-D,** Representative images show FJC staining in the cortex and hippocampus of AAV-WT (A, B) and AAV-Glu-CB1 mice (C, D). Insets show magnifications of FJC-labeled neurons in the cortex (A, C) and the CA3 area (B, D). CPu, caudate putamen; Ctx, cortex; DG, dentate gyrus; LV, lateral ventricle. Bar in D, 250 µm. **E,** Quantification of FJC-labeled neurons demonstrated comparable levels of neurodegeneration in the cortex in both groups. **F,** In contrast, degeneration of CA3 pyramidal neurons was blocked in AAV-Glu-CB1 but not in AAV-WT mice (unpaired t test analysis, two-tailed, $p < 0.05$). n = 5 to 6 mice per group. * $p < 0.05$.

Robust neuronal cell death was evident in subcortical areas of both AAV-WT and AAV-Glu-CB1 mice. FJC-positive cell counts in the cortex revealed a similar extent of neurodegeneration in the two groups (Fig. 3.9E). However, neuronal damage was almost absent in the CA3 area of AAV-Glu-CB1 mice (Fig. 3.9F; unpaired t test, two-tailed, $p < 0.05$). FJC-labeling of degenerating neurons is known to be preserved even two weeks after KA injection (Hopkins et al., 2000), excluding the possibility that CA3 pyramidal cells of AAV-Glu-CB1 mice might have already died five days after KA injection and hence did not display FJC staining. This finding demonstrates that genetically increased CB1 receptor levels in glutamatergic cells of the hippocampus are sufficient to provide protection from excitotoxic cell death after prolonged motor seizures.

4.3 Discussion

The present study shows that incorporation of the highly versatile Cre-loxP system (Branda and Dymecki, 2004) into the AAV platform allows tight control over expression of almost any gene in subsets of neurons under very precise spatiotemporal control *in vivo*. The Cre-activated AAV system affords a broad application spectrum comprising (1) analysis of the Cre expression pattern of newly generated cell type-specific Cre driver mouse lines, (2) intense labeling of neurons to trace long-range axon projections to reveal connectivity of specific regions within the brain, (3) manipulation of neurons by expression of light-activated ion channels to selectively induce network activity (Cardin et al., 2009; Murray et al., 2011) and (4) overexpression of the gene of interest in a neuronal population. Cre-activated transgene expression in a neuronal population is determined by the transgenic mouse line driving Cre recombinase under a cell type-specific promoter. To achieve an overexpression of the gene of interest, Cre expression must resemble the expression pattern of the gene of interest in the particular brain region. Therefore, the choice of the Cre driver line requires serious consideration. In the proof-of-principle approach, analysis of Cre-mediated recombination revealed reporter gene expression in the NEX-Cre line in pyramidal neurons of CA1, CA2 and CA3, and hilar mossy cells, while dentate granule cells were spared (Fig. 3.2C). Hence, Cre expression in the hippocampus of NEX-Cre mice resembles endogenous CB1 receptor expression in hippocampal glutamatergic neurons (Monory et al., 2006).

Elevated CB1 receptor levels at glutamatergic terminals led to an increase in cannabinoid-induced G protein activation in the hippocampus (Fig. 3.5B). This enhancement in CB1 receptor signaling at glutamatergic synapses further manifested in an impairment of hippocampal memory performance (Fig. 3.7). This result is coherent with pharmacological studies showing that CB1 receptor agonists suppress the induction of long-term potentiation (LTP) in the hippocampus (Hill et al., 2004) and produce cognitive deficits (Lichtman et al., 1995; Mishima et al., 2001; Boucher et al., 2009). These deficits rely on the activation of CB1 receptor in the hippocampus because intra-hippocampal infusions of CB1 receptor agonists induce similar effects (Lichtman et al., 1995; Nasehi et al., 2010). Furthermore, an increase in endocannbinoid tone mediated by dual inhibition of the 2-AG-degrading enzyme monoacylglycerol lipase (MAGL) and the AEA-degrading enzyme fatty acid amide hydrolase (FAAH) impairs spatial memory performance in a manner similar to that of cannabinoid agonists (Wise et al., 2012). On the other hand, CB1 receptor antagonists improve memory performance in hippocampal dependent memory tasks (Lichtman, 2000). Moreover, CB1 knockout mice display higher levels of LTP (Jacob et al., 2012) and are able to retain memory for a longer period than wild-type mice in the novel object recognition paradigm (Reibaud et al., 1999). Interestingly, CB1 receptor knockout mice and wild-type controls show identical acquisition rates in the Morris water maze task, though CB1 receptor ablation causes an impairment in the reversal learning phase when the platform was moved to another location of the pool (Varvel and Lichtman, 2002). These studies suggested that the endocannabinoid system is involved in memory processing, particularly in extinction and/or “forgetting” processes. A recently published study further demonstrated that conditional deletion of the CB1 receptor from cortical glutamatergic neurons impairs spatial working memory in the Morris water maze (Han et al., 2012). Hence, both a lack of CB1 receptor in cortical glutamatergic neurons and an increase of CB1 receptor levels in glutamatergic hippocampal neurons impair memory performance, indicating that CB1 receptor expressed in glutamatergic neurons participates in controlling spatial memory.

The present study further revealed that increased CB1 receptor levels in hippocampal glutamatergic neurons protected against excitotoxic seizures. This finding is in agreement with previous conditional knockout studies showing that CB1 receptor activation on glutamatergic terminals, especially of mossy cells projecting to dentate granule cells, plays an essential role in the protection against excitotoxic seizures (Marsicano et al., 2003; Monory et al., 2006), while genetic CB1 receptor ablation from GABAergic interneurons had no effect on seizure severity (Monory et al., 2006). Excessive excitatory neurotransmission causes an increase in Ca^{2+} influx leading to neuronal degeneration, a harmful process known as excitotoxicity (Ben-Ari and Cossart, 2000). The dispersal of

excessive excitatory neurotransmission finally results in behavioral symptoms, such as paroxysmal seizures. It is thought that this procedure participates in the progress of various forms of epilepsy. The endocannabinoid system can dampen glutamatergic transmission via CB1 receptor activation (Lutz, 2004; Kawamura et al., 2006; Takahashi and Castillo, 2006; Katona and Freund, 2008), and therefore, represents a control system to limit the danger of excessive excitatory activity. These genetic data are supported by the findings of several pharmacological studies. Anticonvulsive effects in acute seizure models were demonstrated after increasing endocannabinoid signaling through systemic administration of CB1 receptor agonists (Wallace et al., 2002) or endocannabinoid degradation inhibitors (Marsicano et al., 2003; Coomber et al., 2008; Naderi et al., 2008), while application of the CB1 receptor antagonist SR141716A can block the anticonvulsant effect of cannabinoids (Wallace et al., 2002; Marsicano et al., 2003). Moreover, seizure activity is accompanied by increased synthesis of the endocannabinoids AEA (Marsicano et al., 2003) and 2-AG (Wallace et al., 2003; Wettschureck et al., 2006).

In the hippocampus of patients with temporal lobe epilepsy, CB1 receptor expression is downregulated and the fraction of glutamatergic axon terminals equipped with CB1 receptor is reduced (Ludanyi et al., 2008). As a consequence, negative feedback control at excitatory synapses is impaired in epileptic patients. Interestingly, recent studies demonstrated that CB1 receptor expression undergoes a long-term redistribution in the hippocampus following epileptogenesis in the pilocarpine model of acquired epilepsy (Wallace et al., 2003; Falenski et al., 2007). Falenski and colleagues suggested that the redistribution might serve as a compensatory effect comprising an upregulation of CB1 receptor in glutamatergic and a downregulation in GABAergic neurons (Falenski et al., 2007). Our results support the hypothesis that CB1 receptor in glutamatergic hippocampal neurons is essential to provide endogenous protection against KA-induced seizures. However, recent reports on an anti-convulsive role of CB1 receptor signaling in GABAergic neurons in different seizure models suggest that a potential therapeutic efficacy of cannabinoids might depend on the type of epilepsy (Magloczky et al., 2010; Wyeth et al., 2010). Furthermore, this study demonstrated that elevated CB1 receptor levels safeguard from neuronal cell death caused by excessive excitatory neurotransmission. This result is consistent with previous studies (Marsicano et al., 2003; Monory et al., 2006), showing that genetic deletion of CB1 receptor from principal forebrain neurons results in higher levels of neuronal degeneration in the hippocampus following KA treatment.

As electrophysiological data on depolarization-induced suppression of excitation (DSE) and long-term potentiation (LTP) in AAV-Glu-CB1 mice are missing in this study, we can only speculate about the changes in synaptic signaling mediated by a glutamatergic overexpression of the CB1 receptor in the hippocampus. Given that ectopic CB1 receptor was exclusively expressed in glutamatergic neurons and that cannabinoid-induced G protein activation was enhanced in AAV-Glu-CB1 mice, it can be assumed that DSE is highly increased in AAV-Glu-CB1 mice. Thus, on-demand suppression of glutamate release may be much more pronounced in these mice, which precludes a dispersal of excessive excitatory neurotransmission resulting in an improved protection against paroxysmal seizures.

LTP is a long-lasting enhancement of neurotransmission and thought to represent a putative cellular model of learning and memory. It was shown that blockade of N-methyl-D-aspartate (NMDA) receptors prevents the induction of LTP in the hippocampus and impairs spatial memory (Morris et al., 1986). To induce LTP in hippocampal neurons, the presynaptic terminal needs to provide a sufficient concentration of glutamate to activate adequate quantities of NMDA receptors (Bliss and Collingridge, 1993). This glutamate spillover may be prevented in AAV-Glu-CB1 mice via an enhanced transient suppression of glutamate release by CB1 receptors. Thus, an efficient induction of LTP may be diminished, which results in an impaired hippocampal memory performance.

In conclusion, this study provided strong evidence for the protective role of CB1 receptor on hippocampal glutamatergic terminals as a molecular stout guard in controlling excessive network activity (Mechoulam and Lichtman, 2003). Thus, CB1 receptor expression on hippocampal glutamatergic neurons may represent a target for novel agents to restrain excitotoxic events and to treat neurodegenerative diseases. However, specific activation of glutamatergic CB1 receptor may constitute a double-edged sword as side effects, such as cognitive deficits, may arise.

5 Impaired 2-AG signaling in hippocampal glutamatergic neurons abolishes short-term plasticity at glutamatergic synapses and increases anxiety-like behavior

5.1 Introduction

The endocannabinoid system involves two major signaling molecules, 2-arachidonoyl glycerol (2-AG) and anandamide (AEA), which activate the CB1 receptor. Unlike traditional neurotransmitters such as amino acids, amines, or neuropeptides, which are stored in synaptic vesicles, endocannabinoids are produced and released on-demand (Kano et al., 2009). Hence, their endogenous levels determine the magnitude and duration of CB1 receptor stimulation and are generally regulated by endocannabinoid synthesizing and degrading enzymes. The endocannabinoid 2-AG is produced by diacylglycerol lipase (DAGL) α and β at the postsynaptic membrane (Bisogno et al., 2003). Hydrolysis of 2-AG to glycerol and arachidonic acid is principally mediated by monoacylgycerol lipase (MAGL) at the presynaptic terminal, though other enzymes such as cyclooxygenase 2 (COX-2) and the serine hydrolases α-β-hydrolase domain 6 (ABHD6) and 12 (ABHD12) also contribute to 2-AG degradation (Kozak et al., 2004; Blankman et al., 2007; Marrs et al., 2010). Blankman and colleagues (2007) showed that approximately 85 % of the brain's 2-AG hydrolysis activity is accounted to MAGL.

In the rodent brain, MAGL is heterogeneously distributed with highest levels of expression in brain regions where the CB1 receptor is abundant, such as the hippocampus, cortex, and cerebellum (Dinh et al., 2002). MAGL mRNA is found in regions CA1 to CA3 of the hippocampus and parallels that of CB1 receptor levels (Dinh et al., 2002). In the hippocampus, MAGL protein has a specific laminar distribution with intense immunostaining in the stratum radiatum and stratum oriens of CA1 to CA3, representing excitatory fibers such as Schaffer collaterals and mossy fibers (Suarez et al., 2010). MAGL is also detected in GABAergic basket cell axons (Dinh et al., 2002). In the CA1 and CA3 areas, cell bodies and primary dendrites of the pyramidal cells lack MAGL expression. Thus, as the CB1 receptor, MAGL is expressed at presynaptic terminals, suggesting it contributes to terminating retrograde endocannabinoid signaling (Gulyas et al., 2004; Uchigashima et al., 2011). For this purpose, MAGL protein is associated with the cell membrane via a hydrophobic lid domain (Labar et al., 2010). In contrast to CB1

receptor being localized at perisynaptic sites (Kawamura et al., 2006), MAGL is predominantly found in the central part of axon terminals close to synaptic vesicles and to active zone release sites (Ludanyi et al., 2011). This divergence in the localization of MAGL and CB1 receptor on the presynaptic membrane facilitates a MAGL-dependent regulation of retrograde endocannabinoid signaling (Fig. 4.1). Presynaptic neurotransmitter release induces postsynaptic activation, which results in the production and release of 2-AG from the postsynaptic site. 2-AG molecules migrate retrogradely and activate perisynaptic CB1 receptors or are degraded by MAGL. Thus, the duration of CB1 receptor stimulation can be regulated by modulating the level of MAGL expression.

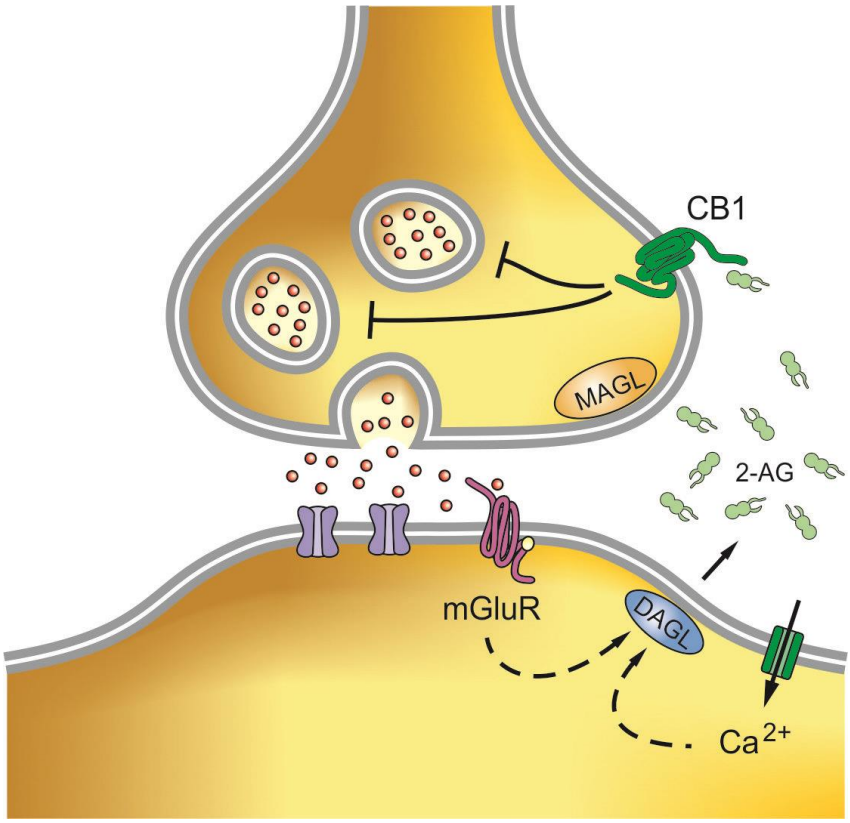

Figure 4.1. MAGL-dependent regulation of endocannabinoid signaling. Neurotransmitter release (here glutamate) induces postsynaptic activity or activation of G protein-coupled metabotropic glutamate receptors (mGluR). Consequentially, 2-AG is produced and travels retrogradely. 2-AG molecules stimulate the cannabinoid receptor (CB1) on presynaptic terminals or are degraded by MAGL. CB1 receptor activation inhibits the release of neurotransmitters. DAGL, diacylglycerol lipase; MAGL, monoacylglycerol lipase.

The reduction of glutamatergic and GABAergic neurotransmitter release is a particular feature of the endocannabinoid system and is known as depolarization-induced suppression of excitation (DSE) and inhibition (DSI), respectively. Recent publications showed that this form of retrograde synaptic depression is mediated by 2-AG-induced activation of CB1 receptor, because DSE and DSI are abolished in mice lacking the 2-AG biosynthetic enzyme DAGLα (Gao et al., 2010; Tanimura et al., 2010). Moreover,

enhanced DSE and DSI are found in MAGL knockout animals (Zhong et al., 2011; Pan et al., 2011) and after application of MAGL inhibitors (Hashimotodani et al., 2007; Pan et al., 2009).

As the endocannabinoid system is involved in a plethora of physiological functions, several studies investigated the therapeutic potential of elevated 2-AG levels by pharmacological MAGL inhibition. For instance, MAGL blockade exerts CB1 receptor-dependent antinociceptive effects in mouse pain models (Kinsey et al., 2009; Long et al., 2009; Guindon et al., 2011). By hydrolyzing and degrading 2-AG to glycerol and arachidonic acid, MAGL increases the major precursor pool for the synthesis of pro-inflammatory eicosanoids, such as prostaglandins (Fig. 4.2) (Nomura et al., 2011b). Thus, MAGL inhibitors exhibit anti-inflammatory and neuroprotective effects by lowering the arachidonic acid precursor pool and accordingly pro-inflammatory eicosanoid levels (Mulvihill and Nomura, 2012).

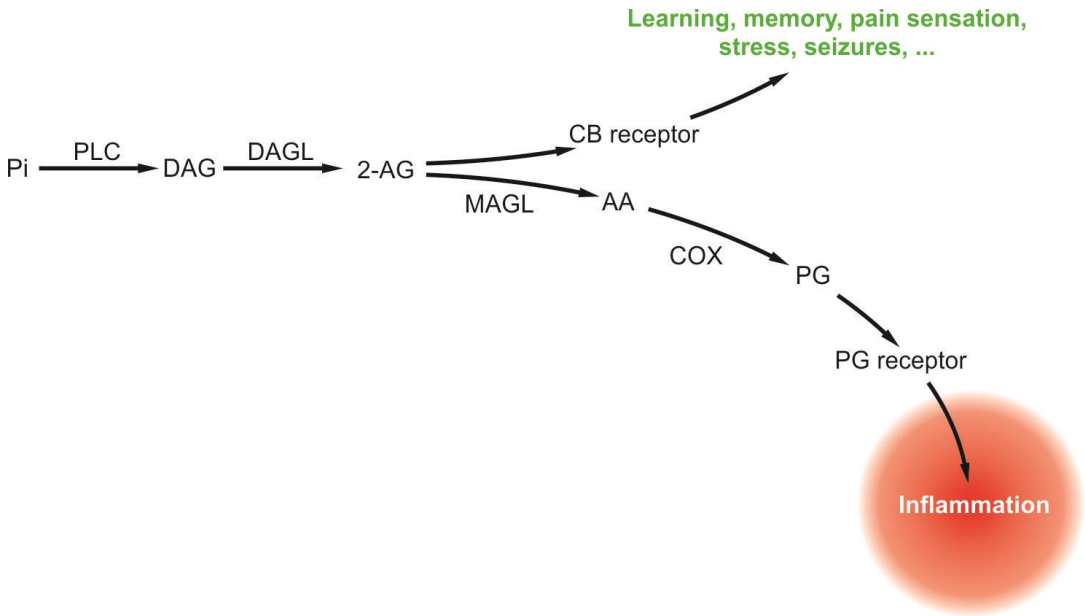

Figure 4.2. MAGL contributes to inflammation. Phospholipase C (PLC) produces diacylglycerol (DAG) from the precursor molecule phosphoinositol (Pi). Diacylglycerol is further converted to 2-AG by diacylglycerol lipase (DAGL). In the brain, arachidonic acid (AA) is primarily produced by MAGL. Cyclooxygenase (COX) then converts arachidonic acid into pro-inflammatory prostaglandins (PG). Prostaglandins induce inflammation and neurodegeneration. CB, cannabinoid.

Global application of MAGL inhibitors induces an anxiolytic effect in rodents (Kinsey et al., 2011; Sciolino et al., 2011), which is consistent with enhanced CB1 receptor signaling mediated by CB1 receptor agonists (Zanettini et al., 2011). The exposure to chronic stress initiates a progressive increase in 2-AG content in the medial prefrontal cortex, amygdala, hippocampus, and hypothalamus, presumably mediated via downregulation of MAGL (Patel et al., 2005; Rademacher et al., 2008; Patel et al., 2009; Sumislawski et al., 2011;

Dubreucq et al., 2012). Pharmacological inhibition of MAGL attenuates the anxiety-like phenotype induced by chronic stress, suggesting that 2-AG signaling is involved in the behavioral adaptations to chronic stress (Sumislawski et al., 2011). Additionally, MAGL blockade diminishes cancer pathogenicity (Kopp et al., 2010; Nomura et al., 2011a) and opioid or cannabis withdrawal responses (Schlosburg et al., 2009; Ramesh et al., 2011). The impact of MAGL activity on memory consolidation is controversial because MAGL inhibitors have no effect on hippocampal memory performance (Busquets-Garcia et al., 2011) but MAGL knockout mice exhibited enhanced LTP accompanied by improved performance in hippocampal learning tasks (Pan et al., 2011).

In conclusion, MAGL is a potential target for the treatment of pain, inflammation, neurodegeneration, anxiety, addiction, cancer and stress disorders. But besides the many beneficial effects of chronic pharmacological blockade or genetic deletion of MAGL, it was shown that elevated 2-AG levels in the brain result in desensitization and downregulation of the CB1 receptor (Schlosburg et al., 2010). Hence, chronic inhibition or disruption of MAGL-mediated 2-AG hydrolysis displays a functional antagonism of the brain endocannabinoid system leading to a loss of cannabinoid-mediated behavioral effects, such as analgesia and hypomotility (Chanda et al., 2010; Schlosburg et al., 2010).

Altogether, 2-AG-mediated endocannabinoid signaling participates in several physiological processes. Studies using MAGL inhibitors or MAGL knockout mice revealed the effects of elevated 2-AG contents on the physiological and behavioral level. But these global approaches provoked compensatory mechanisms and do not allow discriminating the heterogeneous effects of endocannabinoid signaling on distinct neuronal populations, which is for instance associated with the biphasic effect of cannabinoids (Rey et al., 2012). Hence, we aimed at specifically interfering with the on-demand availability of the endocannabinoid 2-AG at synaptic terminals of a defined neuronal population within a brain region with well-established contribution to endocannabinoid system function. To this end, we developed a mouse model which affords an elevation of MAGL activity specifically at glutamatergic axon terminals of the hippocampus, by combining viral-mediated gene delivery and Cre-mediated recombination to ensure brain region- and cell type-specificity (Guggenhuber et al., 2010). Transgenic mice showed highly increased MAGL activity resulting in a 50 % decrease in hippocampal 2-AG levels without affecting other endocannabinoid and arachidonic acid content. Elevated 2-AG hydrolysis at glutamatergic terminals abolished DSE, while DSI was unchanged. At the behavioral level, MAGL-overexpressing mice showed an increase in anxiety, but surprisingly no changes in aversive learning and in the severity of chemically-induced epileptiform seizures.

5.2 Results

For N-terminal tagging of the mouse MAGL, HpaI-linkers were introduced by PCR. The PCR product was sequenced and inserted downstream and in frame of a human influenza hemagglutinin (HA) epitope tag in our pAAV-Stop vector to receive pAAV-Stop-MAGL (Fig. 4.3). Hereby, MAGL protein carries an HA tag at the N-terminus, which facilitates immunological detection of the transgene and allows specific assessment of ectopic versus endogenous MAGL protein. The incorporation of a transcriptional Stop sequence flanked by loxP sites between the ubiquitous cytomegalovirus enhancer/chicken beta-actin (CAG) promoter and the transgene allows targeting specific neuronal populations mediated by Cre recombination (Guggenhuber et al., 2010). After confirming the functionality of the HA tag in pAAV-Stop-MAGL by HEK cell transfection and immunocytochemistry (data not shown), a viral vector was produced (named as AAV-Stop-MAGL) and subjected to standard quality controls, such as Coomassie gel staining and qPCR analysis to quantify the vector titer.

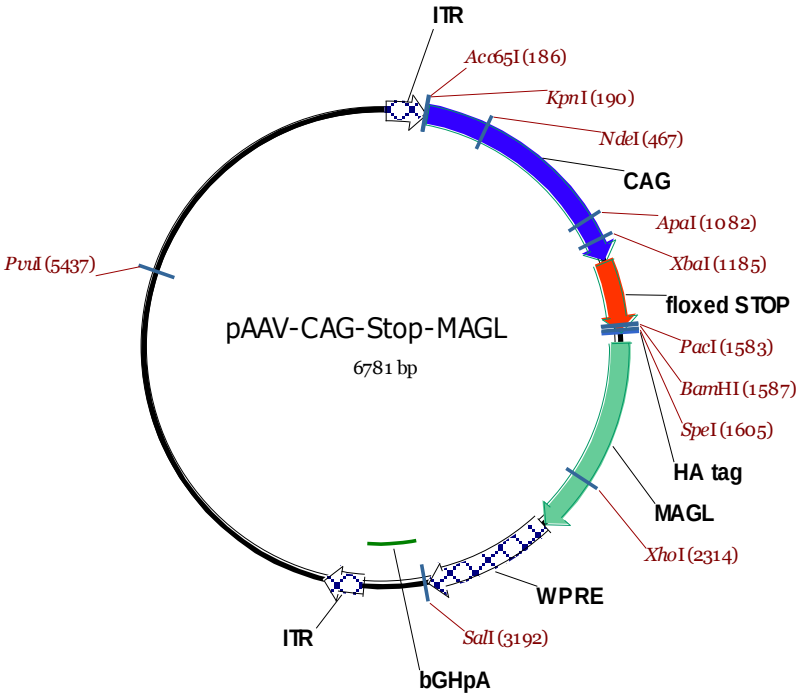

Figure 4.3. Plasmid map of pAAV-Stop-MAGL. bGHpA, bovine growth hormone polyadenylation signal; CAG, cytomegalovirus enhancer/chicken beta-actin promoter; floxed Stop, transcriptional terminator flanked by loxP sites; ITR, inverted terminal repeats; MAGL, monoacylglycerol lipase (mouse); WPRE, woodchuck hepatitis virus post-transcriptional regulatory element.

5.2.1 The level of ectopic MAGL expression directly correlates with inflammation

By degrading 2-AG to glycerol and arachidonic acid, MAGL contributes to controlling the primary precursor pool of arachidonic acid for pro-inflammatory prostaglandin production (Mulvihill and Nomura, 2012). A recent study showed that global deletion of MAGL caused reductions in several prostaglandins and other eicosanoids in the brain (Nomura et al., 2011b). Hence, an elevation in MAGL expression and concomitantly an enhanced 2-AG hydrolysis might increase the precursor pool of arachidonic acid and induce neuroinflammation, a process that we want to avoid.

To elaborate the impact of elevated MAGL levels on inflammatory processes, we aimed at injecting different viral vector copy numbers in a constant volume of one microliter, which will guarantee a sufficient viral vector spread in the hippocampus. Hence, a high titer AAV-Stop-MAGL vector was diluted to obtain 9.0E+08, 4.5E+08, 1.8E+08 and 9.0E+07 vector copy numbers per microliter of AAV solution. The distinct AAV-Stop-MAGL dilutions were injected into the hippocampus of adult NEX-Cre mice and wild-type littermates (Goebbels et al., 2006). Four weeks post injection, mice were sacrificed and brain sections were stained for the HA tag of the transgene and for glial fibrillary acidic protein (GFAP), a marker for reactive astrocytes. Astrogliosis is commonly observed during neuroinflammation and it was shown that astrocytes respond to prostaglandins with an enhanced GFAP production (Mohri et al., 2006). Fluorescence intensities of GFAP and ectopic MAGL were quantified around the injection site (square in Fig. 4.4D`).

Injection of high titer AAV-Stop-MAGL (9.0E+08 vector copies) provoked very strong GFAP expression, indicating an immense activation of astrocytes (Fig. 4.4A). Furthermore, fluorescence intensity of the HA immunostaining was reduced in mice injected with 9.0E+08 vector copies compared to 4.5E+08 vector copies, presumably due to the degeneration of transduced neurons (Fig. 4.4E; one-way ANOVA, $p < 0.001$). In dentate gyrus granule cells, expression of the transgene was inhibited by the Stop cassette as Cre recombinase is not expressed in these cells at adult stages (Goebbels et al., 2006). Here, reactive astrogliosis is completely absent, and thus, neuroinflammation can be allocated to ectopic MAGL expression. Importantly, high-titer AAV-Stop-MAGL injection into wild-type littermates of NEX-Cre mice, which subsequently do not express ectopic MAGL proteins because of the lack of Cre recombinase, did not cause astrogliosis (data not shown), excluding viral vector administration and viral vector transduction per se from inducing neuroinflammation.

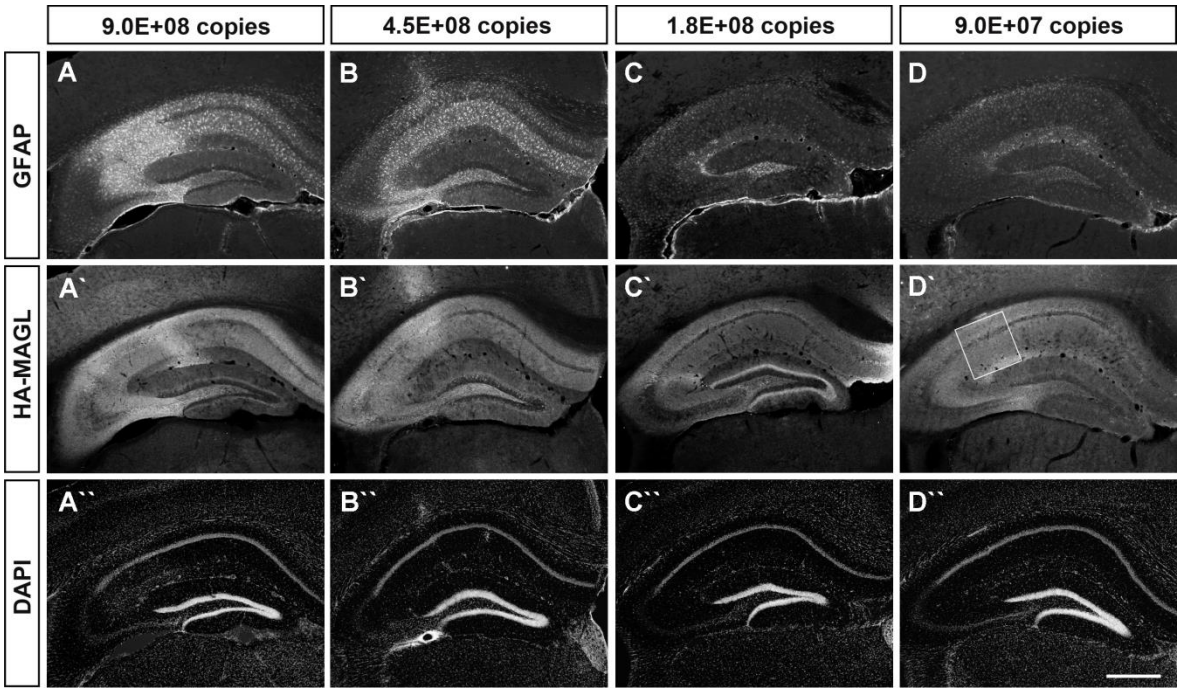

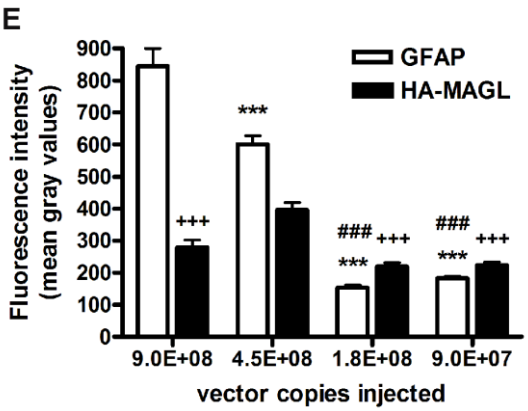

Figure 4.4. Assessment of MAGL-induced neuroinflammation. A-D, Four different concentrations of the AAV-Stop-MAGL vector were injected into the hippocampus of NEX-Cre mice and astrogliosis (GFAP) and transgene expression (HA-MAGL) were analyzed four weeks after vector administration. **A,** Injection of high titer AAV-Stop-MAGL vector resulted in a strong elevation of GFAP expression, indicating reactive astrogliosis and concomitantly neuroinflammation. **B-D,** Decreasing vector copy numbers are accompanied by a reduction of astrogliosis (GFAP). Bar in D`` 500µm. Images were acquired using a constant exposure time (n = 2 per group, 6 sections of each hippocampus were analyzed). **E,** Fluorescence intensities of GFAP and HA-MAGL were quantified around the injection site (square in D') disclosing low astrocyte activity and robust transgene expression at 1.8E+08 injected vector copies. One-way ANOVA analysis, *** $p < 0.001$, GFAP intensity compared to the 9.0E+08 group; ### $p < 0.001$, GFAP intensity compared to the 4.5E+08 group; +++ $p < 0.001$, HA-MAGL intensity compared to the 4.5E+08 group. No statistically significant differences were observed between 1.8E+08 and 9.0E+07 groups. Data are presented as means ± SEM.

A decrease in injected vector copy numbers is accompanied by a reduction in astrogliosis (Fig. 4.4E), reaching stable levels at 1.8E+08 vector copies injected. To bridge an efficient MAGL transgene expression and unwanted processes, such as neuroinflammation and neurodegeneration, we chose to inject 1.5E+08 vector copies in a volume of one microliter per hippocampal hemisphere for further studies.

5.2.2 Efficient overexpression of MAGL in hippocampal pyramidal neurons

In order to provoke a conditional MAGL overexpression in hippocampal pyramidal neurons, the AAV-Stop-MAGL vector (1.5E+08 vector copies) was stereotaxically injected bilaterally into the hippocampus of adult NEX-Cre mice (Goebbels et al., 2006), which express Cre recombinase specifically in cortical and hippocampal glutamatergic neurons (named as AAV-Glu-MAGL mice). The control group was generated by injection of the AAV-Stop-MAGL virus into the hippocampus of wild-type littermates of the NEX-Cre mouse line, which do not express Cre recombinase (named as AAV-WT mice). Ectopic MAGL expression was visualized by immunostaining for the HA tag, revealing widespread transgene expression in the hippocampal formation, which was exclusive to hippocampal pyramidal neurons (Fig. 4.5A). Immunostaining was ample in the stratum radiatum and stratum oriens of CA1 and CA3, while cell bodies were vastly spared, resembling the expression pattern of endogenous MAGL protein (Gulyas et al., 2004). To associate ectopic MAGL with glutamatergic axon terminals, co-localization of the HA staining and VGluT1, a marker for glutamatergic presynaptic sites, was successfully assessed (Fig. 4.5B).

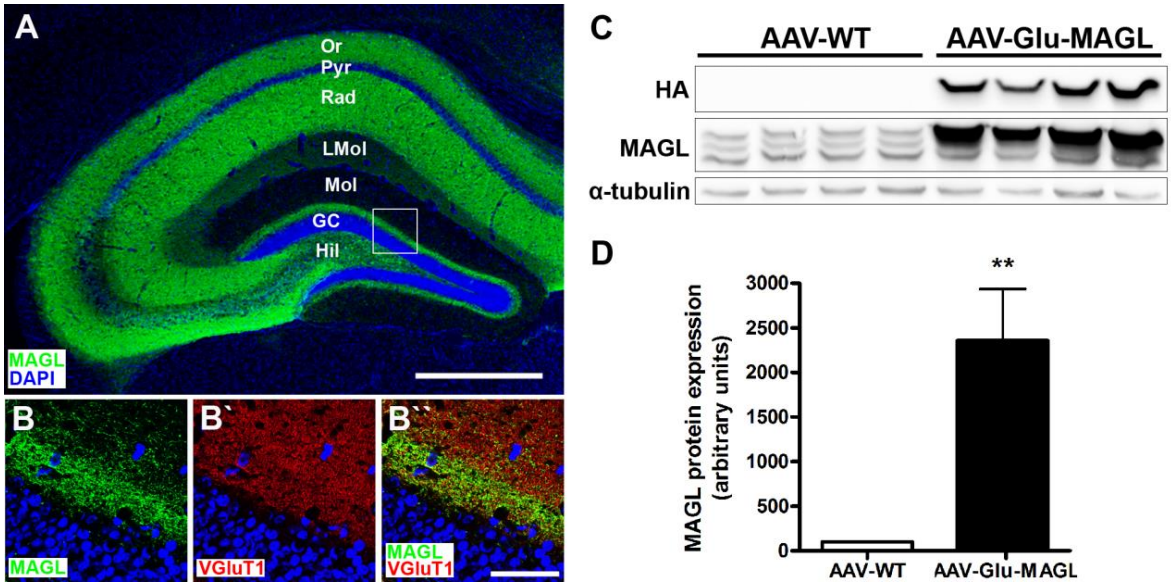

Figure 4.5. MAGL overexpression in hippocampal pyramidal neurons. A, Immunostaining against the HA tag shows strong MAGL transgene expression in pyramidal neurons of the hippocampus in AAV-Glu-MAGL mice. Bar in A, 500µm; GC, granule cell layer of the dentate gyrus; Hil, hilar region; LMol, stratum lacunosum-moleculare; Mol, stratum moleculare; Or, stratum oriens; Pyr, CA1/CA3 pyramidal cell layer; Rad, stratum radiatum. **B,** Higher magnification micrographs of dentate gyrus granule cells (square in A). Co-localization of HA and VGluT1 immunostaining in the inner molecular layer demonstrates MAGL localization at glutamatergic presynaptic sites. Bar in B``, 50 µm. **C,** Western blot analysis of AAV-WT and AAV-Glu-MAGL animals reveals exclusive transgene expression in AAV-Glu-MAGL mice using a HA antibody. MAGL immunoblot indicates the magnitude of MAGL overexpression. **D,** Quantification of MAGL protein in hippocampal homogenates shows a more than 20-fold increase of MAGL in AAV-Glu-MAGL mice compared to AAV-WT controls (AAV-WT, 100.8% ± 8.1, n = 4; AAV-Glu-MAGL 2360% ± 574.2, n = 4; unpaired t test, two-tailed, $p < 0.01$). Data are normalized for α-tubulin and are means ± SEM. ** $p < 0.01$.

Western blot analysis of hippocampal lysates of AAV-WT and AAV-Glu-MAGL mice against the HA tag confirmed exclusive transgene expression in AAV-Glu-MAGL mice (Fig. 4.5C). To determine the magnitude of MAGL overexpression in AAV-Glu-MAGL mice as compared to AAV-WT mice, MAGL expression in relation to α-tubulin was quantified by immunoblot using a MAGL antibody. It is known that different isoforms of MAGL are present in the brain, however, the amount and the molecular weights of MAGL isoforms are still controversial comprising two to three isoforms including 30 kD, 33kD, 35kD, and 37kD bands (Long et al., 2009; Mulder et al., 2011; Jung et al., 2012). Western blot analysis revealed that three isoforms of MAGL are expressed in the hippocampus (Fig. 4.5C, AAV-WT). Importantly, MAGL protein levels were highly increased in AAV-Glu-MAGL animals compared to AAV-WT controls (Fig. 4.5D; unpaired t test, two-tailed, $p < 0.01$).

5.2.3 Increased MAGL activity lowers exclusively 2-AG levels

MAGL activity was examined by Michaelis-Menten enzyme kinetics analysis using hippocampal homogenates. In AAV-Glu-MAGL mice, the turnover rate of the substrate 4-nitrophenyl acetate to 4-nitrophenol was strongly elevated, and thus, AAV-Glu-MAGL mice exhibited significantly enhanced MAGL activity relative to AAV-WT controls (Fig. 4.6A; two-way repeated measures ANOVA, $p < 0.0001$). The mean maximum turnover rate in AAV-Glu-MAGL animals was 784.1 ± 55.1 µmol/min/mg protein and highly increased as compared to AAV-WT mice reaching 59.9 ± 6.8 µmol/min/mg protein (Fig. 4.6B; unpaired t test, two-tailed, $p < 0.001$).

Because MAGL controls the degradation of the endocannabinoid 2-AG to glycerol and arachidonic acid, the content of 2-AG, AEA and arachidonic acid in the dorsal hippocampus was measured by liquid chromatography followed by mass spectrometry. These measurements were performed by Raissa Lerner and Claudia Schwitter in our laboratory. As expected, 2-AG levels were significantly lower in the hippocampus of AAV-Glu-MAGL mice than in AAV-WT controls (Fig. 4.6C; unpaired t test, two-tailed, $p < 0.001$). Importantly, levels of AEA (Fig. 4.6D), arachidonic acid (Fig. 4.6E) and other endocannabinoid-like compounds, such as palmitoyl ethanolamide and oleoyl ethanolamide (data not shown) were unaltered, indicating that MAGL overexpression exclusively affects the levels of 2-AG.

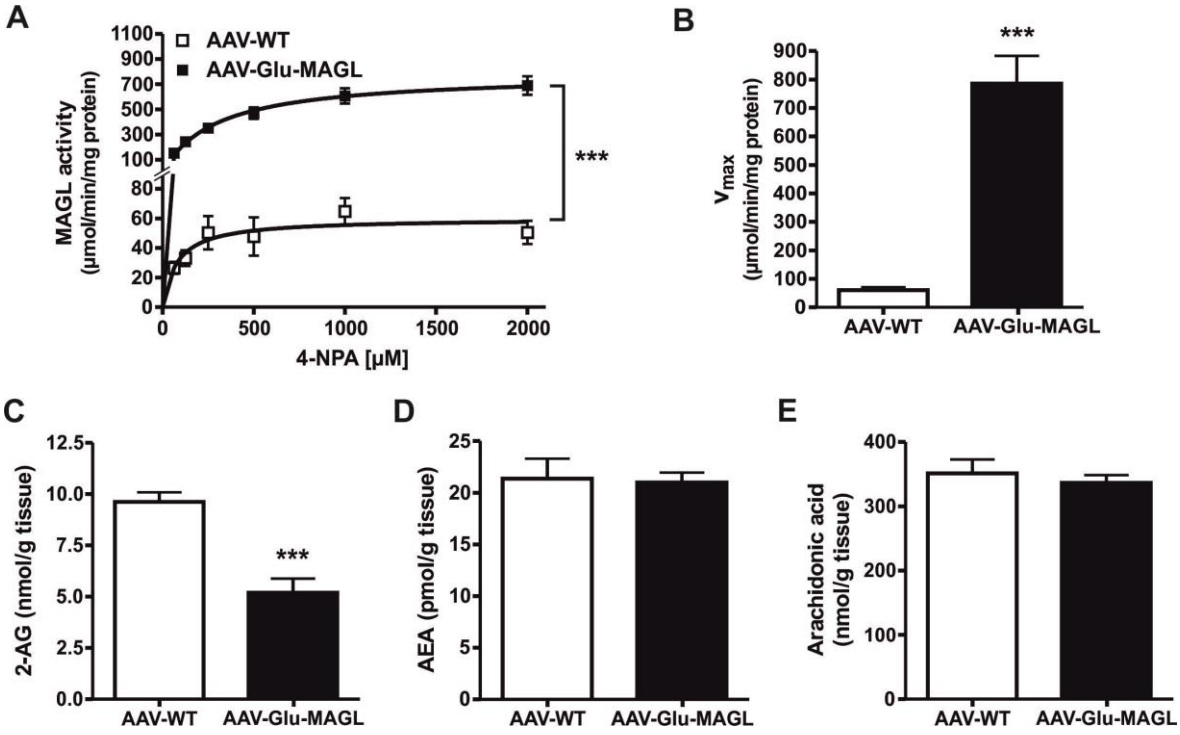

Figure 4.6. Biochemical characterization of AAV-Glu-MAGL mice. A, Michaelis-Menten enzyme kinetics revealed highly elevated MAGL activity in AAV-Glu-MAGL mice as compared to AAV-WT controls (non-linear regression curve fit, two-way repeated measures ANOVA, interaction effect $F(5, 30) = 50.89$, $p < 0.0001$; genotype effect $F(1, 30) = 94.31$, $p < 0.0001$; $n = 4$). **B,** AAV-Glu-MAGL mice showed a highly increased maximum turnover rate (unpaired t test, two-tailed, $p < 0.001$; $n = 4$). **C-E,** In the dorsal hippocampus of AAV-Glu-MAGL mice, 2-AG levels were significantly reduced (AAV-WT, 9.6 ± 0.5 nmol/g tissue, $n = 6$; AAV-Glu-MAGL, 5.2 ± 0.7 nmol/g tissue, $n = 6$; unpaired t test, two-tailed, $p < 0.001$), while the content of AEA and arachidonic acid was unchanged. Data are presented as means ± SEM. *** $p < 0.001$.

5.2.4 Elevated MAGL levels at glutamatergic terminals abolishes DSE in CA1 pyramidal neurons while DSI is not affected

A well-known analytical test for endocannabinoid signaling effects on neurotransmitter release is the depolarization-induced suppression of excitation (DSE) and of inhibition (DSI), respectively. An enhanced degradation of 2-AG at glutamatergic presynaptic sites may compromise these phenomena. Thus, DSE and DSI protocols were analyzed in hippocampal CA1 pyramidal neurons of AAV-WT and AAV-Glu-MAGL mice. Electrophysiological recordings were performed by Hector Romo-Parra in collaboration with the laboratory of Hans-Christian Pape (Institute of Physiology I, Westfälische Wilhelms-University, Münster). Postsynaptic excitatory (eEPSCs) or inhibitory (eIPSCs) currents were evoked in CA1 pyramidal cells upon electrical stimulation of Schaffer collaterals and the effect of a three second depolarization step (from -70 to 0 mV) was measured. In AAV-WT controls, the postsynaptic depolarization reduced eEPCSs to 86.7 ± 0.2 % (Fig. 4.7A), amounting to a DSE magnitude of -12.92 ± 2.29 % (Fig. 4.7B). By comparison in AAV-Glu-MAGL mice, none of the tested neurons displayed a suppression of eEPSCs upon the postsynaptic depolarization step (97.5 ± 0.02 %), indicating that DSE was abolished in this group (Fig. 4.7A, B; AAV-WT, -12.92 ± 2.29 %, n = 6 cells; AAV-Glu-MAGL, -3.65 ± 1.89 %, n = 10 cells; unpaired t test, two-tailed, $p < 0.01$). Moreover, glutamatergic MAGL overexpression did not influence DSI, as indicated by a similar suppression of eIPSCs after depolarization in AAV-WT controls (suppression to 57.0 ± 0.07 %) and AAV-Glu-MAGL mice (suppression to 68.8 ± 0.11 %) (Fig. 4.7C). DSI magnitudes were not statistically different between the two groups (Fig. 4.7D; AAV-WT, -42.50 ± 8.20 %, n = 5 cells; AAV-Glu-MAGL, -33.91 ± 10.23 %, n = 5 cells; unpaired t test, two-tailed, $p = 0.53$). Altogether, these findings indicate that 2-AG plays a major role in mediating retrograde neurotransmitter suppression at hippocampal CA1 synapses (Gao et al., 2010; Tanimura et al., 2010; Zhong et al., 2011; Pan et al., 2011). The results further suggest that MAGL precisely controls retrograde suppression at central synapses and that a divergent regulation of MAGL protein levels in either cell population enables to modify DSE and DSI, respectively.

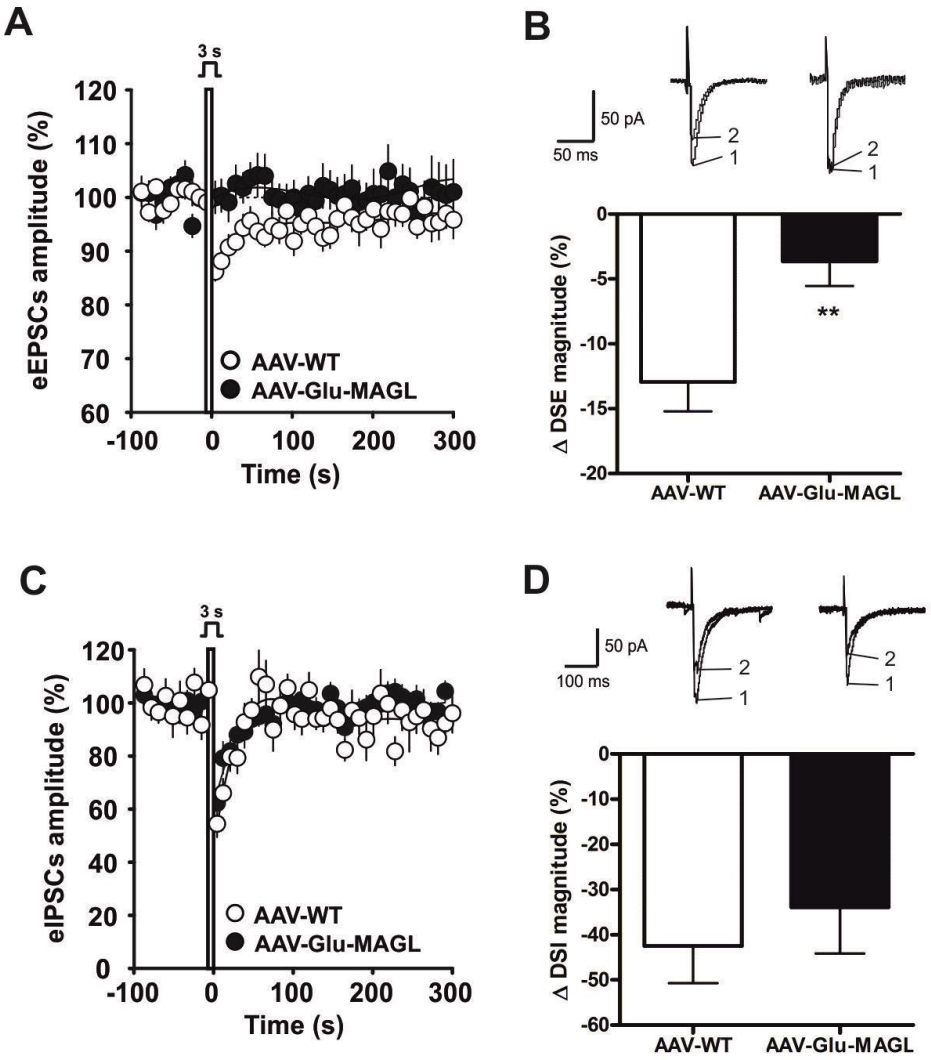

Figure 4.7. DSE and DSI in hippocampal CA1 pyramidal neurons of AAV-WT and AAV-Glu-MAGL mice. A, eEPSCs averaged from recordings in AAV-WT (open circles) and AAV-Glu-MAGL (closed circles) mice. Each dot represents the average of three consecutively evoked responses. Application of 3 s depolarization as indicated by the bar at time point 0. Note that DSE was present in AAV-WT controls, but not in AAV-Glu-MAGL mice. **B,** Top, averaged eEPSCs immediately before (1; n = 5 traces) and after (2; n = 3 traces) the 3 s depolarization step, recorded in AAV-WT (left) and AAV-Glu-MAGL (right) mice. Bottom, summary bar graph showing the magnitude of DSE (Wilson and Nicoll, 2001; see Methods). **C,** eIPSCs averaged from recordings in AAV-WT (open circles) and AAV-Glu-MAGL (closed circles) mice. Note that DSI is not different in the two groups. **D,** Top, same as in B but for eIPSCs. Bottom, summary bar graph showing the magnitude of DSI. Values are expressed as mean ± SEM. ** $p < 0.01$.

5.2.5 AAV-Glu-MAGL mice exhibit an increase in anxiety-like behavior

Cell type-specific overexpression of MAGL at glutamatergic terminals in the hippocampus led to significant changes in MAGL activity, resulting in the absence of DSE without affecting DSI. These appropriate alterations may entail abnormalities at the behavioral level, and thus, AAV-WT and AAV-Glu-MAGL mice were subjected to a battery of behavioral tests including elevated plus maze, light/dark avoidance test, open field, passive avoidance task and kainic acid-induced epileptiform seizures (performed in this order).

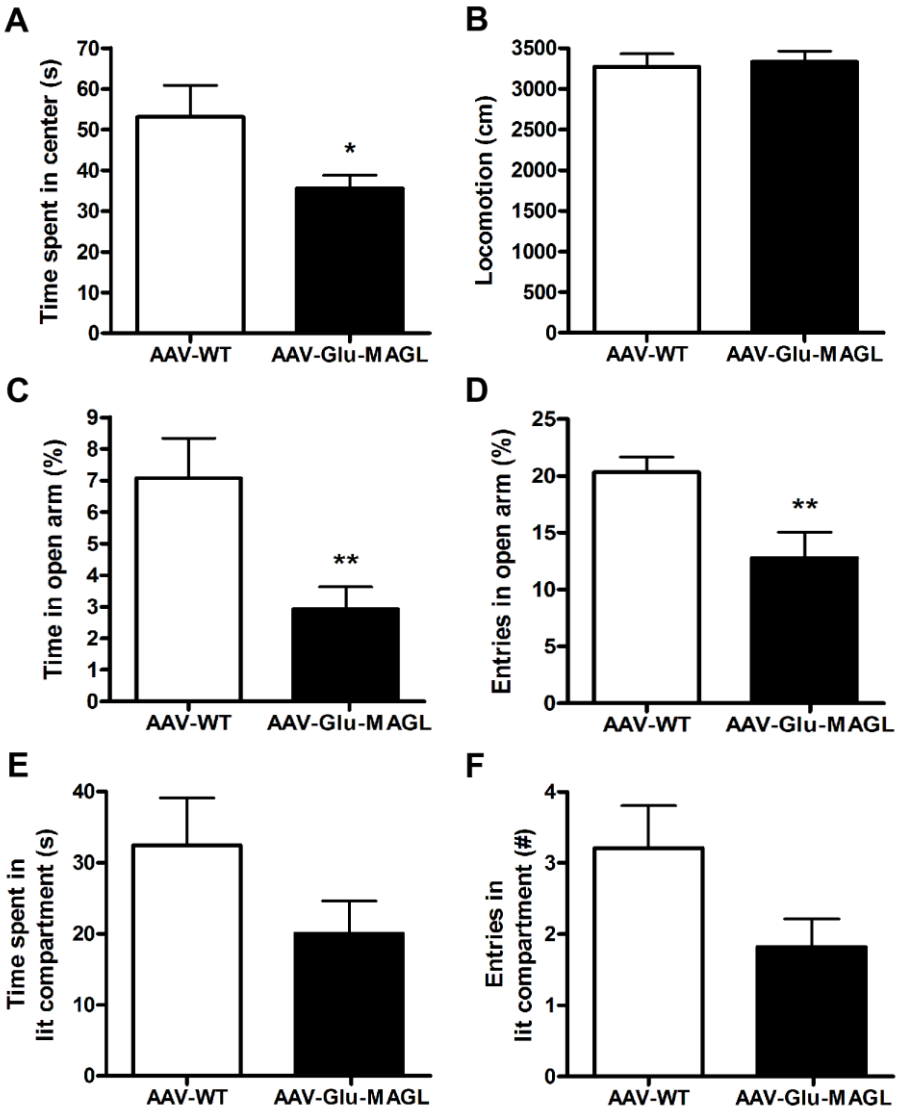

Figure 4.8. AAV-Glu-MAGL mice exhibit enhanced anxiety. A, AAV-Glu-MAGL mice spent less time in the center in the open field test (unpaired t test, two-tailed, $p < 0.05$). **B,** Locomotion did not differ in the open field between AAV-WT and AAV-Glu-MAGL mice. **C and D,** In the elevated plus maze, there was a reduction in the time spent in the open arm and in entries in the open arm of AAV-Glu-MAGL mice compared to AAV-WT controls (unpaired t test, two-tailed, $p < 0.01$). **E and F,** The light/dark avoidance test revealed that AAV-Glu-MAGL mice showed a decreasing trend in time spent in the lit compartment (unpaired t test, two-tailed, $p = 0.1332$) and in entries into the lit compartment (unpaired t test, two-tailed, $p = 0.0635$), which did not reach statistical significance. Values are expressed as means ± SEM. n = 20 to 24 mice per group. * $p < 0.05$; ** $p < 0.01$.

The open field test revealed a significant difference in the time spent in the center of AAV-Glu-MAGL mice relative to AAV-WT controls (Fig. 4.8A; unpaired t test, two-tailed, $p < 0.05$), whereas locomotor activity was unchanged (Fig. 4.8B). The center compartment represents the most illuminated and most unsheltered area in an open field box, and therefore, the time spent in this area is an indicator of anxiety behavior. Accordingly, AAV-Glu-MAGL mice were more anxious than AAV-WT controls. Anxiety was furthermore addressed in the elevated plus maze and the light/dark avoidance test. In the elevated plus maze, AAV-Glu-MAGL mice spent significantly less time in the open arm (Fig. 4.8C; unpaired t test, two-tailed, $p < 0.01$) and entered the open arm less frequently than AAV-WT controls (Fig. 4.8D; unpaired t test, two-tailed, $p < 0.01$). An analogous behavior was found in the light/dark avoidance test in which the entries and the time spent in the aversive lit compartment were altered in AAV-Glu-MAGL mice without reaching statistical significance (Fig. 4.8E, F; unpaired t test, two-tailed, time in lit compartment $p = 0.1332$, entries in lit compartment $p = 0.0635$). The trend to an anxious behavior in the light/dark test can be explained by the less aversive properties of this test as compared to the elevated plus maze that seem to be required to reveal anxiety behavior in these transgenic mice. Taken together, these findings clearly indicate an increased anxiety of AAV-Glu-MAGL mice as compared to AAV-WT controls.

It is known that anxiety can be affected by chronic stress resulting in an anxious phenotype (Hill et al., 2011). Moreover, chronic stress induces a progressive increase in 2-AG content within several brain regions including the hippocampus (Rademacher et al., 2008; Patel et al., 2009; Wang et al., 2012; Dubreucq et al., 2012). Recent publications hypothesized that the endocannabinoid system serves as an endogenous regulatory system in anxiety and stress responses (Sumislawski et al., 2011; Ruehle et al., 2012). As AAV-Glu-MAGL mice show decreased 2-AG levels accompanied by an anxiety-like phenotype, we asked if these alterations are due to a disturbed stress response. Hence, blood samples were taken under basal conditions from AAV-WT and AAV-Glu-MAGL mice by using the vena facialis blood collection technique, which facilitates quick and painless proceedings thereby minimizing stress to the animal. Blood plasma was separated by centrifugation and corticosterone levels were analyzed using an ELISA kit (IBL international, Hamburg, Germany). Plasma

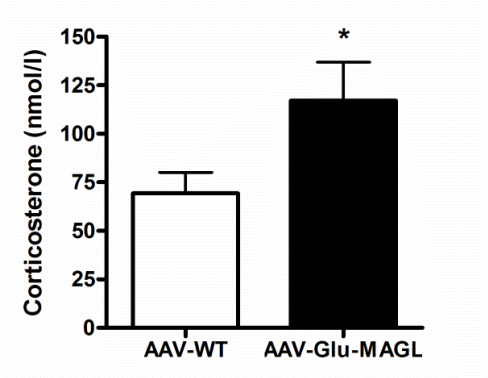

Figure 4.9. Increased 2-AG hydrolysis in the hippocampus impairs an adequate stress response. Corticosterone levels of AAV-Glu-MAGL mice were increased as compared to AAV-WT controls (unpaired t test, two-tailed, $p < 0.05$). Data are presented as means ± SEM. n = 7 to 8 mice per group. * $p < 0.05$.

corticosterone levels were significantly elevated in AAV-Glu-MAGL mice compared to AAV-WT controls (Fig. 4.9; unpaired t test, two-tailed, $p < 0.05$), suggesting that a reduction of 2-AG levels in the hippocampus by MAGL overexpression disturbs endocannabinoid system-mediated adaptation to stressful stimuli.

Analysis of hippocampal memory in the passive avoidance test did not show any difference between AAV-WT and AAV-Glu-MAGL mice (Fig. 4.10A), indicating that the elimination of DSE at glutamatergic synapses in the hippocampus has no impact on the formation of aversive memory. Because glutamatergic CB1 receptor activation in the hippocampus is important for the protection against epileptiform seizures (Monory et al., 2006), chemically-induced seizures were evoked by injection of kainic acid (35 mg/kg, i.p.). Surprisingly, seizure severity was not altered in AAV-Glu-MAGL mice as compared to AAV-WT controls (Fig. 4.10B). Kaplan-Meier survival curves depict a similar survival rate of AAV-WT and AAV-Glu-MAGL mice during the course of the experiment (Fig. 4.10C). This finding indicates that 2-AG signaling at hippocampal glutamatergic synapses is not essential for the protection against epileptiform seizures.

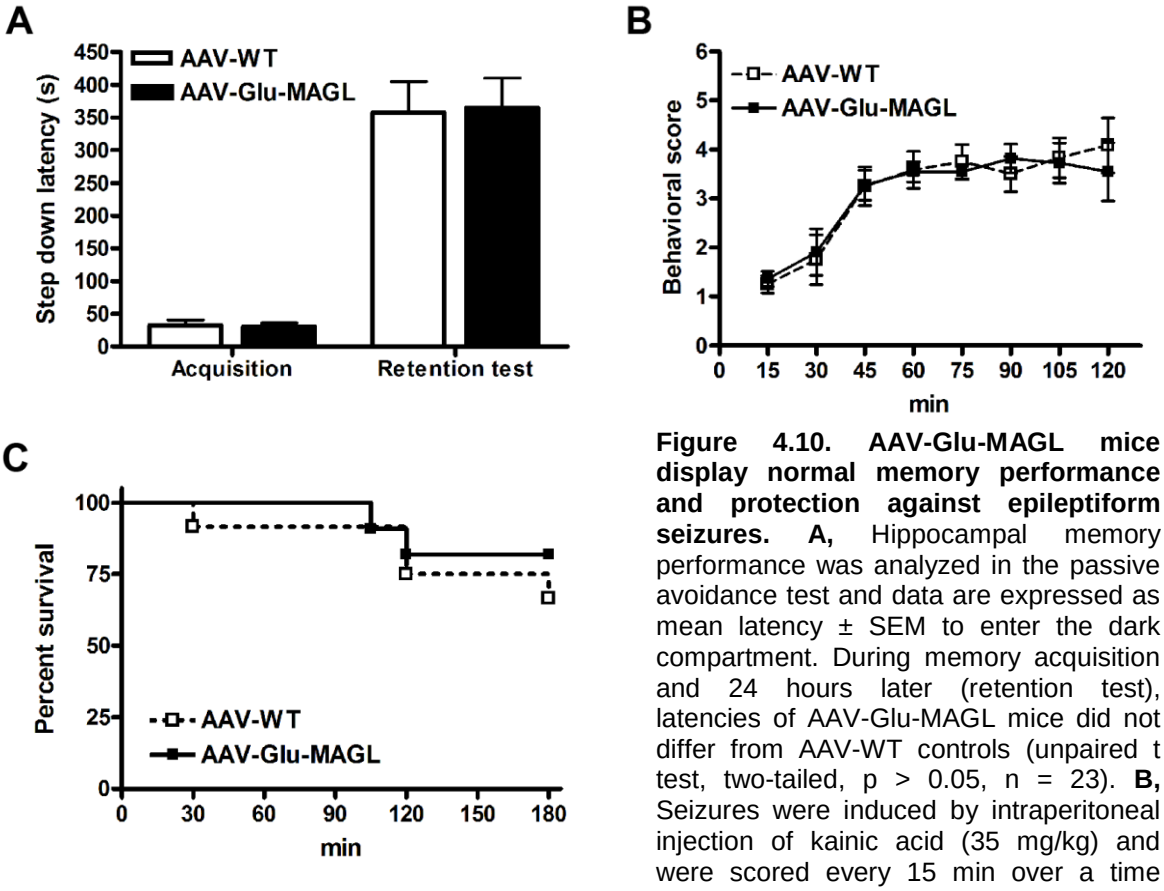

Figure 4.10. AAV-Glu-MAGL mice display normal memory performance and protection against epileptiform seizures. A, Hippocampal memory performance was analyzed in the passive avoidance test and data are expressed as mean latency ± SEM to enter the dark compartment. During memory acquisition and 24 hours later (retention test), latencies of AAV-Glu-MAGL mice did not differ from AAV-WT controls (unpaired t test, two-tailed, $p > 0.05$, $n = 23$). **B,** Seizures were induced by intraperitoneal injection of kainic acid (35 mg/kg) and were scored every 15 min over a time course of 120 min. Seizure severity was not altered in AAV-Glu-MAGL mice as compared to AAV-WT controls (Mann-Whitney U test, two-tailed, $p > 0.05$, $n = 11$-12). **C,** Kaplan-Meier survival curves during KA treatment did not differ between both groups (log rank test, $p > 0.05$, $n = 11$-12). Data are expressed as means ± SEM.

5.3 Discussion

In the present study, we investigated the effect of elevated MAGL protein levels at glutamatergic terminals in hippocampal pyramidal neurons on 2-AG hydrolysis, retrograde suppression of neurotransmitter release and selected behaviors. This manipulation caused a decrease in 2-AG levels in the hippocampus and diminished DSE without affecting DSI. Additionally, AAV-Glu-MAGL mice displayed elevated corticosterone levels under basal conditions accompanied by an enhanced anxiety, while aversive hippocampal memory and severity of chemically-induced seizures did not differ from AAV-WT controls.

MAGL hydrolyzes 2-AG to glycerol and arachidonic acid, and thus, provides arachidonic acid molecules as substrates for other enzymes which produce pro-inflammatory prostaglandins and other signaling lipids (Mulvihill and Nomura, 2012). In MAGL knockout mice, 2-AG levels are elevated, accompanied by a reduction in arachidonic acid and prostaglandin levels (Nomura et al., 2011b). Hence, MAGL activity controls the magnitude of prostaglandin synthesis and coherent neuroinflammation. In a preliminary experiment, the effect of MAGL overexpression on inflammation was assessed by injecting distinct vector genome copy numbers of the AAV-Stop-MAGL vector into the hippocampus of NEX-Cre mice and wild-type littermates. In the brain, inflammation and neurologic insults induce an increase in the number and size of astrocytes expressing glial fibrillary acidic protein (GFAP), a phenomenon generally referred to as astrogliosis (Eddleston and Mucke, 1993). Astrocytes express prostaglandin receptors and respond to prostaglandins with an enhanced GFAP production (Mohri et al., 2006). Strong GFAP immunostaining was found in CA1 and CA3 of mouse hippocampi injected with the highest vector copy number (Fig. 4.4A, E). In contrast, reactive astrocytes were not detected in areas, which were infected with the AAV-Stop-MAGL vector, but due to the absence of Cre recombinase did not express the transgene, as seen in denate gyrus granule cells of AAV-Glu-MAGL mice and in the hippocampus of AAV-WT animals. This finding excludes viral transduction as the cause of astrogliosis and neurodegeneration. However, it is known that the process of AAV injection and that AAV vectors per se can cause an activation of astrocytes (McCown et al., 2005). Thus, mild astrogliosis was still found in the hippocampus of mice injected with the lowest vector copy number (9.0E+07). However, GFAP staining was significantly reduced as compared to 9.0E+08 vector copy numbers injected (Fig. 4.4E). Taken together, high levels of MAGL protein induce neuroinflammation, presumably by increasing the pool of arachidonic acid, which further gets converted to pro-inflammatory eicosanoids, such as prostaglandins. However, this unwanted process was abolished by reducing the number of injected vector copies.

2-AG is considered the major endocannabinoid mediating retrograde synaptic suppression of neurotransmitter release (Katona and Freund, 2008). To selectively investigate the functions of 2-AG *in vivo*, two mouse models were generated that either lack the 2-AG synthetic enzyme DAGLα or the 2-AG degrading enzyme MAGL. Ablation of DAGLα reduces 2-AG content, which results in the elimination of DSE and DSI, respectively (Gao et al., 2010; Tanimura et al., 2010). A major drawback of this genetic model is the accompanied reduction of AEA and arachidonic acid levels (Gao et al., 2010), which excluded allocating the effects of DAGLα deletion exclusively to 2-AG signaling. On the other hand, MAGL knockout mice exhibit increased 2-AG levels which caused CB1 receptor desensitization and tolerance to the effects of cannabinoid agonists (Chanda et al., 2010; Schlosburg et al., 2010). Furthermore, MAGL deletion lowered the pool of arachidonic acid (Schlosburg et al., 2010; Nomura et al., 2011b), which serves as a substrate for a number of enzymes to generate other lipid signaling molecules, in particular eicosanoids. As DAGLα and MAGL knockout mice showed the above mentioned compensatory effects, the usefulness of these mouse lines as models to exclusively define the functions of 2-AG in the brain is limited. A recent study established a transgenic mouse line that selectively overexpressed MAGL under the control of the CaMKIIα promoter in principal forebrain neurons (Jung et al., 2012). Here, 2-AG content was reduced by 50 % without affecting AEA and arachidonic acid levels. These mice display a series of metabolic changes including leanness, elevated energy expenditure and resistance to diet-induced obesity (Jung et al., 2012). However, this study did not provide insights into the changes of retrograde synaptic depression mediated by MAGL overexpression. Alterations of DSE and DSI would be in particular interesting in this mouse model as the CaMKIIα promoter allocates MAGL overexpression to glutamatergic neurons (Liu and Jones, 1996; Tighilet et al., 1998).

In the present report, we used a genetic approach, which exploits viral-mediated gene delivery and Cre-mediated recombination (Guggenhuber et al., 2010), to exclusively overexpress MAGL in hippocampal pyramidal neurons. Elevated MAGL protein levels in the hippocampus led to an enhanced MAGL activity (Fig. 4.6). Importantly, the resulting decrement in 2-AG availability did not elicit alterations in the levels of AEA and arachidonic acid (Fig. 4.6), confirming that compensatory mechanisms do not emerge in this mouse model. This enables us to directly correlate changes on the cellular and behavioral level to hippocampal 2-AG signaling.

MAGL overexpression was aimed to be specific for glutamatergic hippocampal pyramidal neurons and excluded from GABAergic cells, which allowed us to selectively attenuate 2-AG-mediated synaptic depression at glutamatergic terminals in the hippocampus without

affecting 2-AG action on GABAergic transmission (Fig. 4.7). This finding indicates that presynaptic MAGL can precisely control the activation of CB1 receptor located on the same synaptic site by quenching postsynaptically synthesized and released 2-AG before it can activate perisynaptic CB1 receptor. Given that 2-AG content was reduced but AEA content was unchanged in AAV-Glu-MAGL mice, 2-AG can be considered as the main mediator of DSE. Thus, we created a mouse model that allows a cell type-specific diminution of 2-AG-mediated effects and that will proof useful to discriminate the functions of DSE and DSI on the physiological and behavioral level.

The exposure to aversive stimuli or to stress is characterized by a pronounced increase in glutamate release (Millan, 2003) and the blockade of glutamatergic neurotransmission causes antidepressant and anxiolytic responses and a downmodulation of HPA axis activity (Simon and Gorman, 2006; Palucha and Pilc, 2007). Thus, hyperfunction of glutamatergic signaling is associated with the development of depression and anxiety disorders (Palucha and Pilc, 2007). Furthermore, it was shown that stress enhances glutamatergic release in the hippocampus (Bagley and Moghaddam., 1997). The endocannabinoid system counteracts to this stress-mediated enhanced excitatory activity with compensatory mechanisms in the hippocampus such as downregulation of the CB1 receptor exclusively on GABAergic terminals, which is accompanied by impaired DSI (Hu et al., 2011), and elevation of 2-AG levels (Wang et al., 2012). Hill and colleagues suggested that an increase in 2-AG levels is highly important for the adaptation to stress (Hill et al., 2010). AAV-mediated MAGL overexpression at glutamatergic terminals in the hippocampus attenuates 2-AG signaling exclusively at glutamatergic CB1 receptors. A consequence is the missing DSE likely resulting in prolonged glutamatergic transmission at synaptic connections within and from the hippocampus. This alteration may result in an unbalance between excitatory and inhibitory transmission precluding an adaptation to stressful and aversive stimuli and leading to elevated corticosterone levels and an increased anxiety. Interestingly, control over a stressful event has been found to relate to changes in glutamatergic excitability in pyramidal neurons of the prefrontal cortex, particularly the prelimbic area (Varela et al., 2012). Given the tight functional links between the prelimbic prefrontal cortex and the hippocampus in high fear situations (Sotres-Bayon et al., 2012), and the role of endocannabinoid signaling in behavioral adaptation (Kamprath et al., 2009), it is tempting to conclude that excessive glutamatergic activity in these pathways will mobilize endocannabinoid synthesis leading to a suppression of glutamate release (Katona and Freund, 2008), thereby contributing to the control over a stressful or aversive event.

The endocannabinoid system is further involved in memory processing because CB1 receptor agonists, such as Δ^9-tetrahydrocannabinol (THC), produce deficits in memory and cognition (Messinis et al., 2006; Boucher et al., 2009; Puighermanal et al., 2009). Consistently, dual inhibition of MAGL and FAAH increases endocannabinoid levels and impairs spatial memory performance in a manner similar to that of THC (Wise et al., 2012). Hence, a reduction in 2-AG levels and the absence of DSE induced by increased MAGL activity may affect memory. But the analysis of AAV-Glu-MAGL and AAV-WT mice in the passive avoidance task revealed that hippocampal memory performance of AAV-Glu-MAGL mice did not differ from wild-type controls (Fig. 4.10). Interestingly, MAGL knockout animals exhibit enhanced hippocampal LTP and enhanced performance in the Morris water maze and novel object recognition test (Pan et al., 2011). In these mice, DSI is prolonged and it was reported that DSI enables the induction of LTP (Carlson et al., 2002). Thus, DSI seems to be involved in memory formation and that's why AAV-Glu-MAGL mice did not display changes in hippocampal memory performance because DSI is not affected in these mice. Moreover, a recent study showed that FAAH inhibition impairs memory consolidation while MAGL inhibition has no effect on this process (Busquets-Garcia et al., 2011). In addition, it was reported that FAAH knockout mice show improved memory acquisition and extinction (Varvel et al., 2007). Hence, AEA, but not 2-AG, may be the major endocannabinoid modulating memory performance.

Systemic application of kainic acid drives excitatory synaptic activity in hippocampal circuits resulting in the development of seizures (Ben-Ari and Cossart, 2000). The endocannabinoid system has been implied as a therapeutical target in epilepsy as CB1 receptor activation has anticonvulsant and neuroprotective effects in acute and chronic seizure models (Marsicano et al., 2003; Wallace et al., 2003). Importantly, it was shown that CB1 receptors on hippocampal glutamatergic but not GABAergic neurons are required for the protection against excitotoxic seizures (Marsicano et al., 2003; Monory et al., 2006). Seizure activity is accompanied by increased synthesis of the endocannabinoids AEA (Marsicano et al., 2003) and 2-AG (Wallace et al., 2003; Wettschureck et al., 2006). Surprisingly, seizure severity of AAV-Glu-MAGL mice did not differ from wild-type controls (Fig. 4.10). This finding is in contrast to the proposed model of Katona and Freund (2008), assigning retrograde 2-AG signaling as a protective mechanism against excessive presynaptic activity. It is thought that excessive glutamatergic activity mobilizes endocannabinoid synthesis leading to the suppression of glutamate release (DSE). Thus, the finding that the lack of hippocampal DSE in AAV-Glu-MAGL mice had no effect on seizure severity is rather astonishing. One possible explanation would be the distinct signaling properties of 2-AG and AEA, respectively.

A recent study showed that bath application of KA to hippocampal slices does not change the levels of 2-AG, but increases AEA levels (Lourenco et al., 2011). Accordingly, the KA-induced depression of eIPSCs is prolonged by application of a FAAH inhibitor, whereas no alterations occur in presence of a MAGL inhibitor (Lourenco et al., 2011). Although it was reported that FAAH knockout mice are more susceptible to KA-induced seizures (Clement et al., 2003), several studies showed that injection of a FAAH inhibitor prior to the induction of seizures markedly reduced the seizure score (Karanian et al., 2007; Coomber at al., 2008; Naderi et al., 2008; Naidoo et al., 2011; Vilela et al., 2013). Moreover, AEA content is decreased in cerebrospinal fluid of patients suffering from temporal lobe epilepsy, while 2-AG levels are not affected (Romigi et al., 2010). Altogether, these findings point to AEA as potential initiator of endocannabinoid-mediated protection against epileptiform seizures and our results support this hypothesis.

Taken together, we developed a transgenic mouse model that allows specific analyses of 2-AG signaling in the brain at a particular neuronal population. AAV-mediated MAGL overexpression in hippocampal pyramidal neurons reduced 2-AG levels, which was accompanied by an abolition of DSE without affecting DSI. This lacking suppression of glutamate release in the hippocampus manifested in an enhanced stress response comprising elevated corticosterone levels and an increased anxiety. However, the alterations in 2-AG signaling did not affect hippocampal memory and seizure severity. Thus, MAGL in hippocampal pyramidal neurons may represent a target to treat anxiety and stress disorders. Furthermore, AAV-mediated overexpression of components of the endocannabinoid system in a particular cell population will proof useful to discriminate between 2-AG- and AEA-mediated signaling effects. Moreover, stereotaxic injection of viral vectors enables to dissect endocannabinoid signaling in a specific brain region and its participation to a behavioral output.

6 Doxycycline-inducible transgene expression mediated by a single AAV vector

6.1 Introduction

Specific control of gene activities *in vivo* has become a promising strategy in biological research to investigate gene functions at particular time points. Precisely regulating gene expression by switching it on and off is an elegant tool for gene function studies and an essential safety feature for gene therapy applications. A unique system allowing for reversible control of gene expression is the tetracycline (tet)-inducible system originally developed by Gossen and Bujard (Gossen and Bujard, 1992).

Classically, the tet system comprises two major components: (1) the tetracycline controlled transcriptional activator (tTA), a fusion of the bacterial tet repressor (tetR) and the transcriptional activating domain VP16 from herpes simplex virus, and (2) the tetracycline responsive element (TRE), which consists of seven repeats of the tetracycline resistant operon (tetO) of *Escherichia coli* fused to a minimal cytomegalovirus (CMV) promoter. TRE is located upstream of the gene of interest and controls its expression upon activation. To afford tissue specificity, tTA is expressed under control of a cell type-specific promoter. tTA molecules form homodimers which bind constitutively to the tetO sequence of TRE and thereby induce gene expression (Fig. 5.1). In presence of tetracycline or of its derivative doxycycline (dox), tTA changes its conformation, which precludes tTA binding to TRE, and gene expression is turned off ("tet-off system").

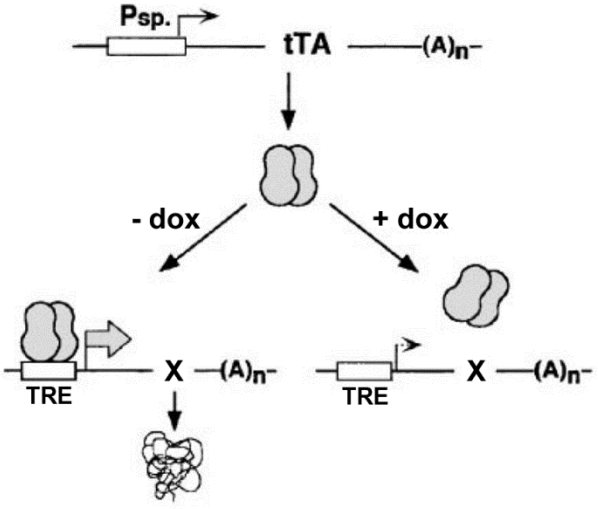

Figure 5.1. Scheme of the tTA regulatory system. In absence of the effector molecule dox, tTA binds to the tetO sequence within TRE and activates transcription of gene X. Addition of dox prevents tTA from binding, and thus, abolishes the initiation of transcription. $(A)_n$, polyadenylation signal; Psp, tissue-specific promoter; TRE, minimal promoter fused downstream of seven repeats of the tet operator (modified from Gossen and Bujard, 2002).

This technology owes its remarkable specificity to dissimilar components derived from prokaryotes and is nevertheless fully functional in eukaryotes. A key disadvantage of the tet-off system is the need for chronic dox treatment to silence gene expression. Chronic dox treatment might cause side effects such as renal toxicity, photosensitivity and emergence of antibiotic-resistant organisms (Stieger et al., 2009).

To circumvent this issue, Gossen and colleagues developed a reverse tTA (rtTA) with opposite function (Gossen et al., 1995). Here, gene expression is constitutively silent in the absence of dox (Fig. 5.2). Addition of dox enables binding of rtTA to TRE, and thus, gene transcription is activated ("tet-on system").

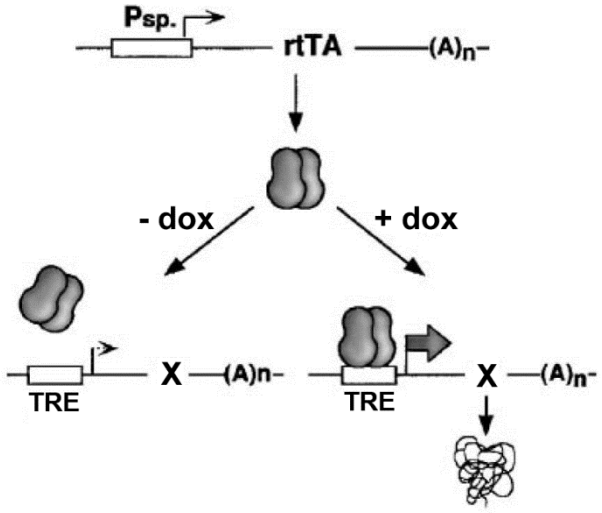

Figure 5.2. Scheme of the rtTA regulatory system. rtTA requires dox for binding to tetO sequences within TRE in order to activate transcription of gene X. $(A)_n$, polyadenylation signal; Psp, tissue-specific promoter; TRE, minimal promoter fused downstream of seven repeats of the tet operator (modified from Gossen and Bujard, 2002).

A major drawback of transactivators of the tet systems is their leakiness which results from nonspecific binding of the transactivator to the operator in the uninduced state. This issue has been partially addressed by improving the specificity of transactivators by mutagenesis (Urlinger et al., 2000). A distinct strategy was the replacement of the transcriptional activating domain VP16 in tTA by the transcriptional repressing domain Krueppel-associated box (KRAB) of the human Zink finger protein Kox-1 (Deuschle et al., 1995) or of the rodent Zink finger protein Kid-1 (Freundlieb et al., 1999). The fusion of KRAB domains to the tetracycline repressor led to the development of tetracycline-regulatable transcriptional silencers (tTS). Here, a tetracycline-controlled transcriptional silencer binds as homodimer to TRE in absence of the effector molecule dox (Fig. 5.3). Thus, tTS actively shields the promoter from outside stimulatory influence resulting in repression of transcription. Addition of dox prevents binding of tTS, thus relieving repression, and thereby switching the promoter from a repressed to a dynamic state in terms of transcriptional control.

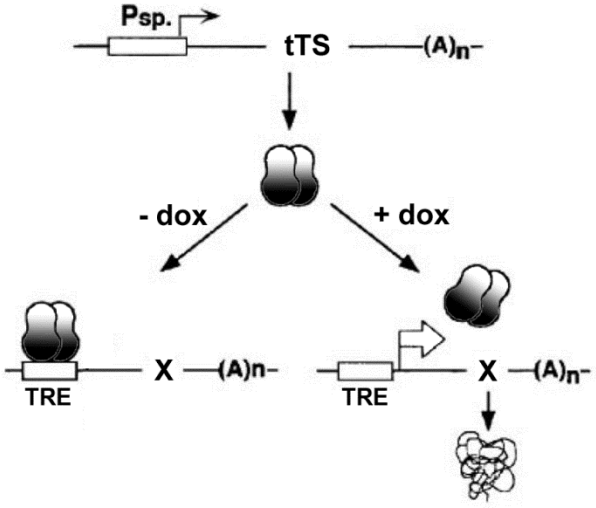

Figure 5.3. Scheme of the tTS regulatory system. In absence of dox, tTS binds to the tetO sequence within TRE and inhibits transcription of gene X. Addition of dox prevents tTS from binding to TRE, and thus, releases the repression of transcription. $(A)_n$, polyadenylation signal; Psp, tissue-specific promoter; TRE, minimal promoter fused downstream of seven repeats of the tet operator (modified from Gossen and Bujard, 2002).

To achieve inducible, reversible and cell type-specific transgene expression mediated by viral gene delivery, several studies used two distinct viral vectors, a transactivator vector and a tet-response vector (Wang et al., 2005; Ebert et al., 2005; Matsui et al., 2012). In the transactivator vector, a tissue specific promoter controls the expression of the tetracycline transactivator, whereas in the tet-response vector, TRE fused upstream to a ubiquitous promoter controls the transcription of the gene of interest. Hence, tissue-specific transactivator expression leads to TRE-controlled transcription of the gene of interest, which can be regulated by administration of dox. However, a single vector carrying both units and leading to uniform expression would considerably facilitate research applications *in vivo*. Regarding the transcriptional silencer approach, it is essential to use a single vector construct as the application of two separate vectors (transsilencer vector and tet-response vector) would result in constitutive gene expression in non-target cells. Because tTS is expressed under control of a cell type-specific promoter in the transsilencer vector, tTS is absent from non-target cells, in which the cell type-specific promoter is not active. In this case, it is mandatory to utilize an autoregulatory system that expresses the transsilencer under control of the TRE element.

A single vector needs to enable the expression of two separate proteins, a tet-controlled molecule such as tTS and a reporter protein to assess the functionality of the system. A practical strategy comprises a dual expression cassette, in which each transgene is expressed under control of a TRE element (Haberman et al., 1998). However, two TRE elements in one AAV vector genome would enlarge the vector size, which is stringently restricted in AAVs.

A promising approach encompasses the expression of two proteins from a bicistronic mRNA. Here, the two DNA sequences of the transgenes need to be linked by a nucleotide sequence which affords the expression of two separate proteins. A nucleotide sequence, which meets this criterion, is the internal ribosome entry site (IRES). IRES was first discovered in poliovirus RNA and initiates translation by directly binding to ribosomes (Pelletier and Sonenberg, 1988). The translation of the protein located on the 5' end of the mRNA molecule is commenced by the 5' cap structure, while translation initiation of the proximate protein is mediated by the IRES sequence located in the intercistronic spacer region between the two protein coding regions. Hence, IRES-mediated separation of two proteins from a bicistronic mRNA is a post-transcriptional mechanism. A major drawback of IRES-mediated protein coexpression from a single open reading frame (ORF) is that the upstream element is more strongly transcribed than the IRES-controlled downstream protein (Hennecke et al., 2001).

Another capable linker segment to afford expression of separate proteins from a bicistronic mRNA is the 2A peptide sequence, which comprises 18 amino acids (EGRGSLLTCGDVEENPG**P**). 2A is a self-processing peptide bridge and is referred to as *cis*-acting hydrolase element (Doronina et al., 2008). Here, a ribosomal-skip mechanism mediates the cleavage between the C-terminal glycine (underlined) and the N-terminal proline (bold) of the downstream peptide sequence (Donnelly et al., 2001). Thus, 2A-mediated peptide cleavage constitutes a post-translational mechanism and is described in detail in Fig. 5.4. In contrast to IRES-mediated protein coexpression, 2A peptide linkage results in cellular expression of discrete proteins in essentially equimolar quantities (de Felipe et al., 2006). However, it was reported that C-terminal 2A peptide sequences caused impaired protein function (Lengler et al., 2005; Hasegawa et al., 2007). To circumvent this issue, a recent study used a slightly modified 2A peptide bridge containing a short C-terminal linker sequence composed of four amino acid residues, APGS (Tang et al., 2009). Tang and colleagues demonstrated that their 2A peptide approach resulted in reliable and quantitative peptide coexpression after AAV-mediated gene delivery to the brain.

Altogether, the tet system is supposed to be an optimal method for tightly regulated reversible transgene expression mediated by AAV in eukaryotes. Because it is entirely prokaryotic and dox can be used at low doses to induce gene transcription, pleiotropic effects are precluded. In recent studies, we employed the Cre/loxP system in AAVs to facilitate transgene expression in a cell type-specific manner (Guggenhuber et al., 2010). But Cre recombinase-mediated induction of transgene expression is irreversible. To extend the application spectrum of AAVs, we aimed at developing a AAV system that

enables conditional, inducible and reversible gene expression. To this end, we combined the Cre/loxP system and the tTS system to develop an autoregulatory AAV that contains all components in one vector.

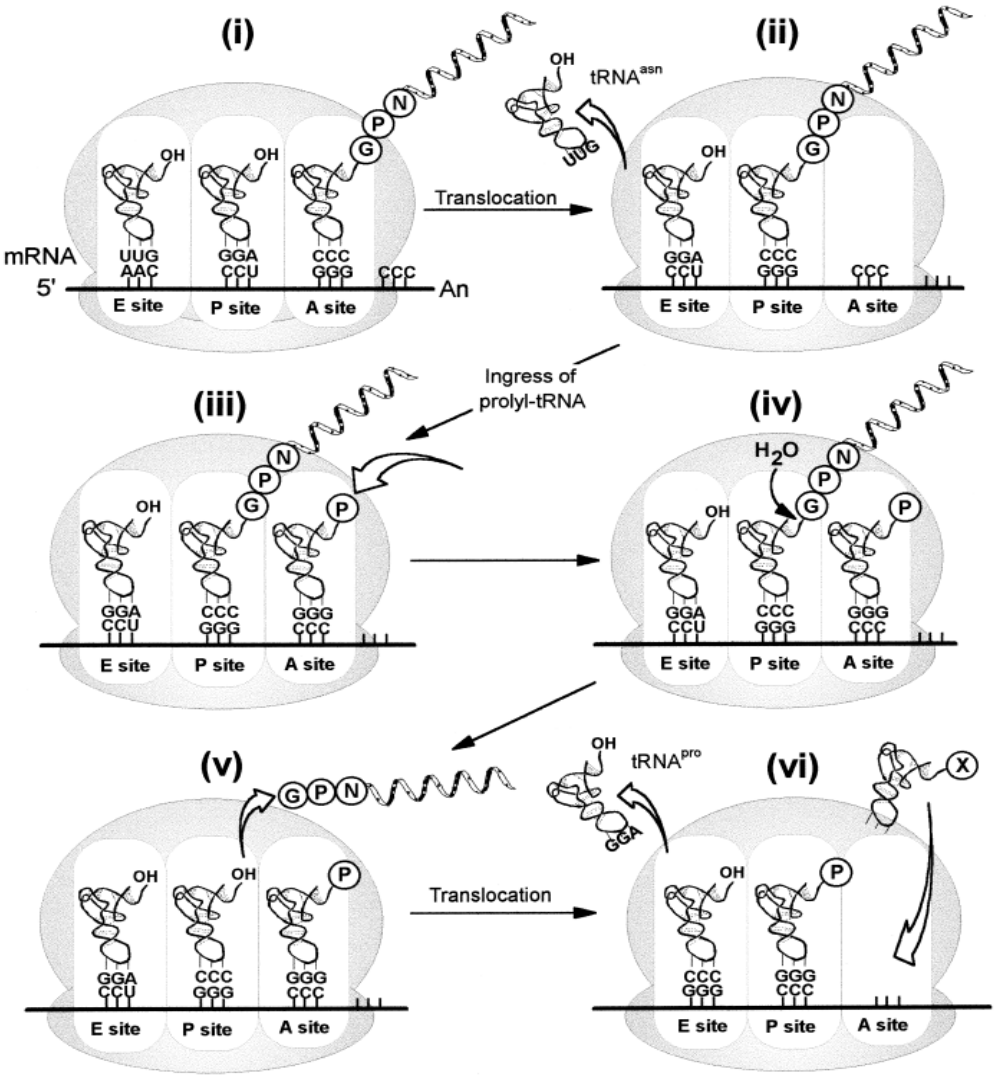

Figure 5.4. Scheme of 2A-mediated peptide cleavage. The stage following the addition of the ultimate residue of 2A is shown (step i). Peptidyl(2A)-tRNA is translocated from the A to the P site of the ribosome (step ii), allowing the ingress of prolyl-tRNA (step iii). Prolyl-tRNA is unable to attack the peptidyl(2A)-tRNA-Gly ester linkage. Hydrolysis of the peptidyl(2A)-tRNA-Gly ester linkage occurs, releasing the nascent peptide from the ribosome (steps iv and v). Deacylated tRNA is now present in the P site (mimicking peptide bond formation) and would allow the translocation of prolyl-tRNA (rather than the normal peptidyl-tRNA) from the A to P sites (step vi). Synthesis of the peptide C-terminal of 2A would proceed as normal, although recommencing (rather than initiating) with proline (from Donnelly et al., 2001).

6.2 Results

6.2.1 Doxycycline-inducible AAV vector design

The vector design entailed the following *cis*-acting recombinant elements: TRE, synapsin I promoter, floxed Stop cassette, reporter gene, 2A and tTS (Fig. 5.5). The construction of the vector included the following steps: a tetracycline responsive element (TRE), which consists of seven repeats of the 19bp bacterial tetO sequence without any promoter, was amplified by PCR to introduce PstI sites (Fig. 5.5, primer TRE) and inserted in between the 5'-ITR and the neuron-specific synapsin I promoter (Kugler et al., 2003). Furthermore, the floxed Stop cassette was incorporated downstream of the promoter to allow for conditional transgene expression.

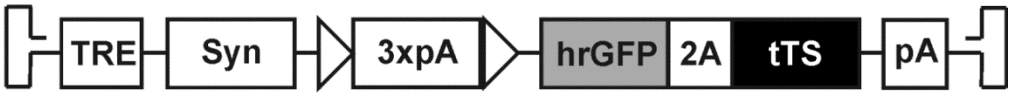

Primer TRE fw		PstI		
	CATC	CTGCAG	TAAAACGACGGCCAGTGAAT	
Primer TRE rev		PstI		
	TTTT	CTGCAG	GGGTACCGAGCTCTGCTTAT	
Primer 1 OE-PCR fw		SpeI	HindIII	complementary to hrGFP
	TTTT	ACTAGT	AAGCTT	ATGGTGAGCAAGCAGATCCTGA
Primer 2 OE-PCR rev	complementary to 2A-tTS		HindIII	complementary to hrGFP
	GAGCCAGGGGTCCTCTCCTT		AAGCTT	CACCCACTCGTGCAGGC
Primer 3 OE-PCR fw	complementary to hrGFP		HindIII	complementary to 2A-tTS
	GCAGCCTGCACGAGTGGGTG		AAGCTT	GGCAGAGGAAGTCTTCT
Primer 4 OE-PCR rev		SpeI	Stop	complementary to 2A-tTS
	TTTT	ACTAGT	TCA	CCAGGGGTCCTCTCCTT

Figure 5.5. Vector design and primer sequences for the construction of pAAV-TRE-Syn-Stop-hrGFP-2A-tTS. 2A, peptide linker; 3xpA, three polyadenylation signals ("Stop"), triangles indicate loxP sites; hrGFP, humanized renilla green fluorescent protein; pA; polyadenylation signal; Syn, synapsin promoter; TRE, tetracycline-responsive element; tTS, tetracycline-controlled transcriptional silencer.

For the *in vivo* approach, humanized renilla green fluorescent protein (hrGFP) was used as reporter gene. As two independent proteins (hrGFP and tTS) need to be transcribed from a single ORF, the two proteins were linked by the self-processing 2A peptide sequence (Tang et al., 2009). To generate a DNA construct, in which the sequences of hrGFP, 2A and tTS are in frame, overlap extension PCR (OE-PCR) was performed. This technique comprises two PCR steps (Warrens et al., 1997). The first PCR step amplified the target sequences using one general primer (Fig. 5.5; primer 1 for hrGFP, primer 4 for 2A-tTS) and one specific primer at the 3' end of hrGFP and the 5' start of 2A-tTS, respectively, which possesses a 5' overhang complementary to the start/end of the other molecule (Fig. 5.5; primer 2 for hrGFP, primer 3 for 2A-tTS). In the second PCR reaction, only primers 1 & 4 were used and products of the first PCR step served as templates. The final construct is synthesized in this step and is flanked by SpeI-linkers to facilitate introduction in the AAV expression cassette. The hrGFP-2A-tTS sequence was incorporated in between the floxed Stop cassette and a short form of the woodchuck hepatitis virus post-transcriptional regulatory element (WPRE2). Finally, the vector plasmid was sequenced to confirm the absence of PCR-induced mutations (Fig. 5.6).

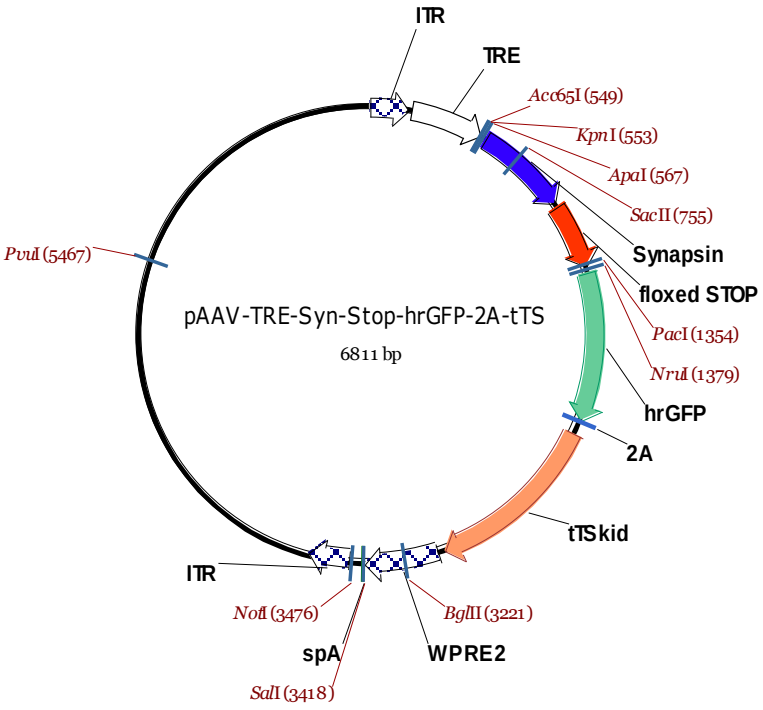

Figure 5.6. Plasmid map of the tetracycline-inducible AAV expression vector (pAAV-TRE-Syn-Stop-hrGFP-2A-tTS). 2A, peptide linker; floxed Stop, transcriptional terminator flanked by loxP sites; hrGFP, humanized renilla green fluorescent protein; ITR, inverted terminal repeats; spA, short bovine growth hormone poly-adenylation signal; Synapsin, synapsin I promoter; TRE, tetracycline responsive element; tTS^{kid}, tetracycline-controlled transcriptional silencer; WPRE2, short woodchuck hepatitis virus post-transcriptional regulatory element.

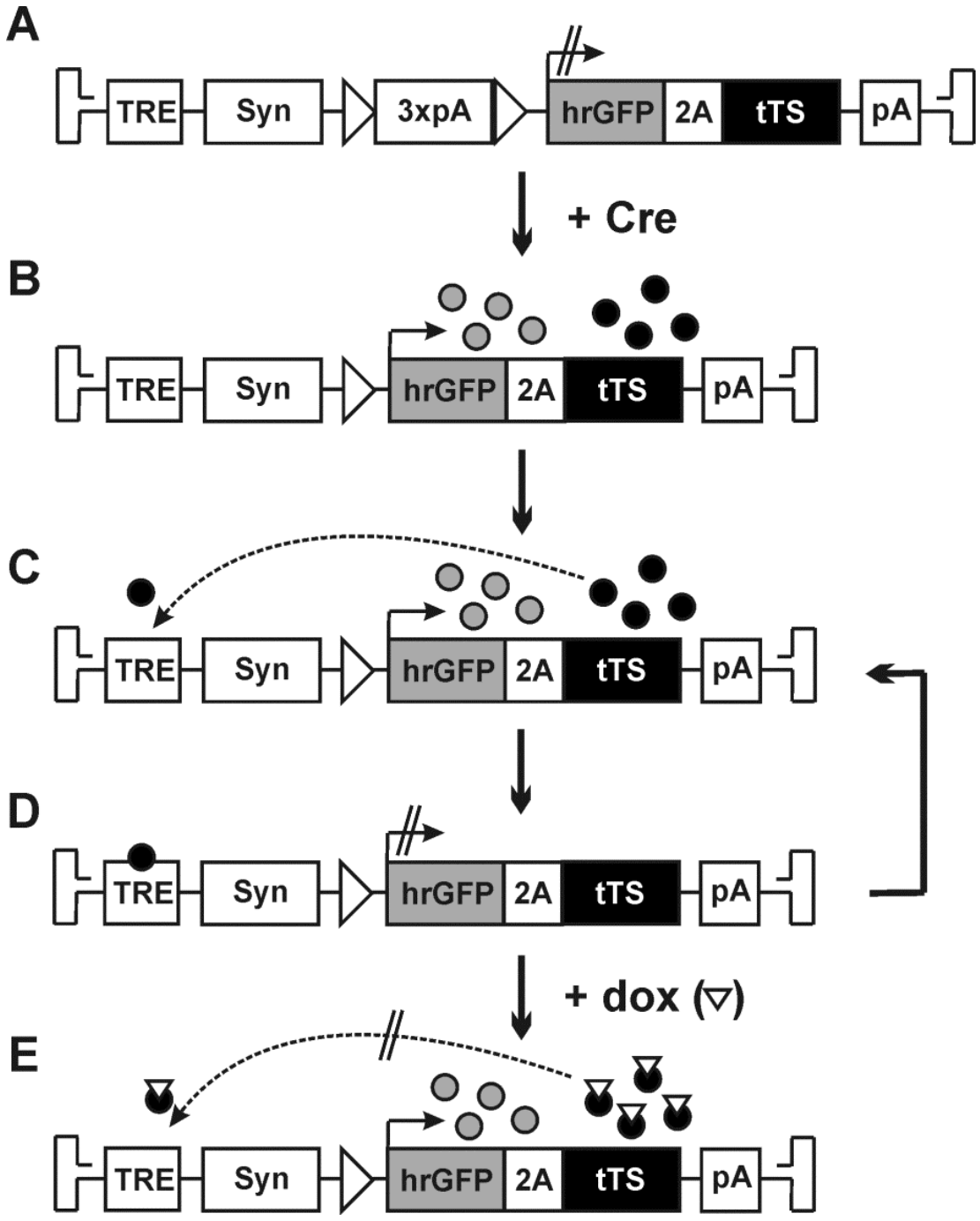

Figure 5.7. Scheme of the tetracycline-regulated expression system in a single AAV vector. A, In absence of Cre recombinase, the Stop cassette inhibits transcription of the transgene. **B,** After Cre-mediated excision of the Stop element, hrGFP and tTS are expressed. **C,** tTS binds to TRE. **D,** tTS bound to TRE shields the promoter and represses transcription. tTS regulates its particular expression, and thus, this system represents an autoregulatory loop. **E,** Application of dox prevents binding of tTS to TRE and induces transgene expression. 2A, peptide linker; 3xpA, three polyadenylation signals ("Stop"), triangles indicate loxP sites; dox, doxycycline; hrGFP, humanized renilla green fluorescent protein; pA, bovine growth hormone polyadenylation site; Syn, synapsin promoter; TRE, tetracycline-responsive element; tTS, tetracycline controlled transcriptional silencer.

In theory, this construct offers the following functionality (Fig. 5.7): in absence of Cre recombinase, the Stop element terminates transcription (Fig. 5.7A). After Cre-mediated excision of the Stop cassette, transcription is initiated under control of the synapsin promoter leading to expression of the discrete proteins hrGFP and tTS (Fig. 5.7B). tTS then binds to TRE (Fig. 5.7C) and silences transcription (Fig. 5.7D). Consequentially, tTS itself is no longer expressed and after degradation of previously synthesized tTS molecules, transcription will be turned on again, which leads to the expression of novel tTS molecules (Fig. 5.7C). Accordingly, this system is based on an autoregulatory loop, in which tTS is expressed under control of a promoter responsive for tTS. Thereby the silencer regulates its own expression. Thus, the autoregulatory loop implicates low basal transgene expression in the uninduced state. Addition of dox prevents tTS from binding to TRE. Hence, the synapsin promoter is exempt from repression and the transgene is expressed (Fig. 5.7E).

6.2.2 Transgene expression is efficiently turned on *in vivo* after dox application

In order to assess the functionality of this system *in vivo*, the AAV-TRE-Syn-Stop-hrGFP-2A-tTS virus was stereotaxically injected into the hippocampus of adult NEX-Cre mice (Goebbels et al., 2006). Four weeks after AAV injection, mice received daily intraperitoneal injections of doxycycline (40 mg/kg, dox group) or saline (vehicle group) at a volume of 10 ml/kg for two weeks. On the day of the last i.p. injection, mice were sacrificed via transcardial perfusion in deep anesthesia. Brains were removed from the skull and cut (40 µm) in the coronal plane on a cryostat after postfixation and subsequent cryoprotection.

Brain sections were stained with 4',6-diamidino-2-phenylindole (DAPI) and epifluorescence of hrGFP was analyzed under a fluorescence microscope to reveal transgene expression in a quantitative manner (Fig. 5.8). In vehicle treated animals, epifluorescence of hrGFP was not detected in Fig. 5.8A`, which indicates efficient repression of transcription by tTS. Under high magnification, hrGFP expression was only sporadically found in scattered cells of the hippocampus (Fig. 5.8A`` arrowhead), which confirms a very low background activity of the system in the uninduced state. Importantly, the application of dox efficiently released repression of transcription and induced extensive expression of hrGFP in hippocampal pyramidal neurons (Fig. 5.8B). Dentate gyrus granule cells do not express Cre recombinase at adult stages (Goebbels et al., 2006) and were spared from hrGFP expression, further demonstrating cell type-specificity caused by Cre-mediated excision of the Stop cassette. Fluorescence intensity was quantified in an area of the dorsal hippocampus, which comprises regions CA1-3 and the

dentate gyrus, and background values were systematically subtracted (Fig. 5.8C). Dox-treated animals showed a highly significant increase in mean fluorescence intensity compared to vehicle-treated animals (unpaired t test, two-tailed, $p < 0.0001$), furthermore demonstrating the functionality of the tet system in a single AAV vector.

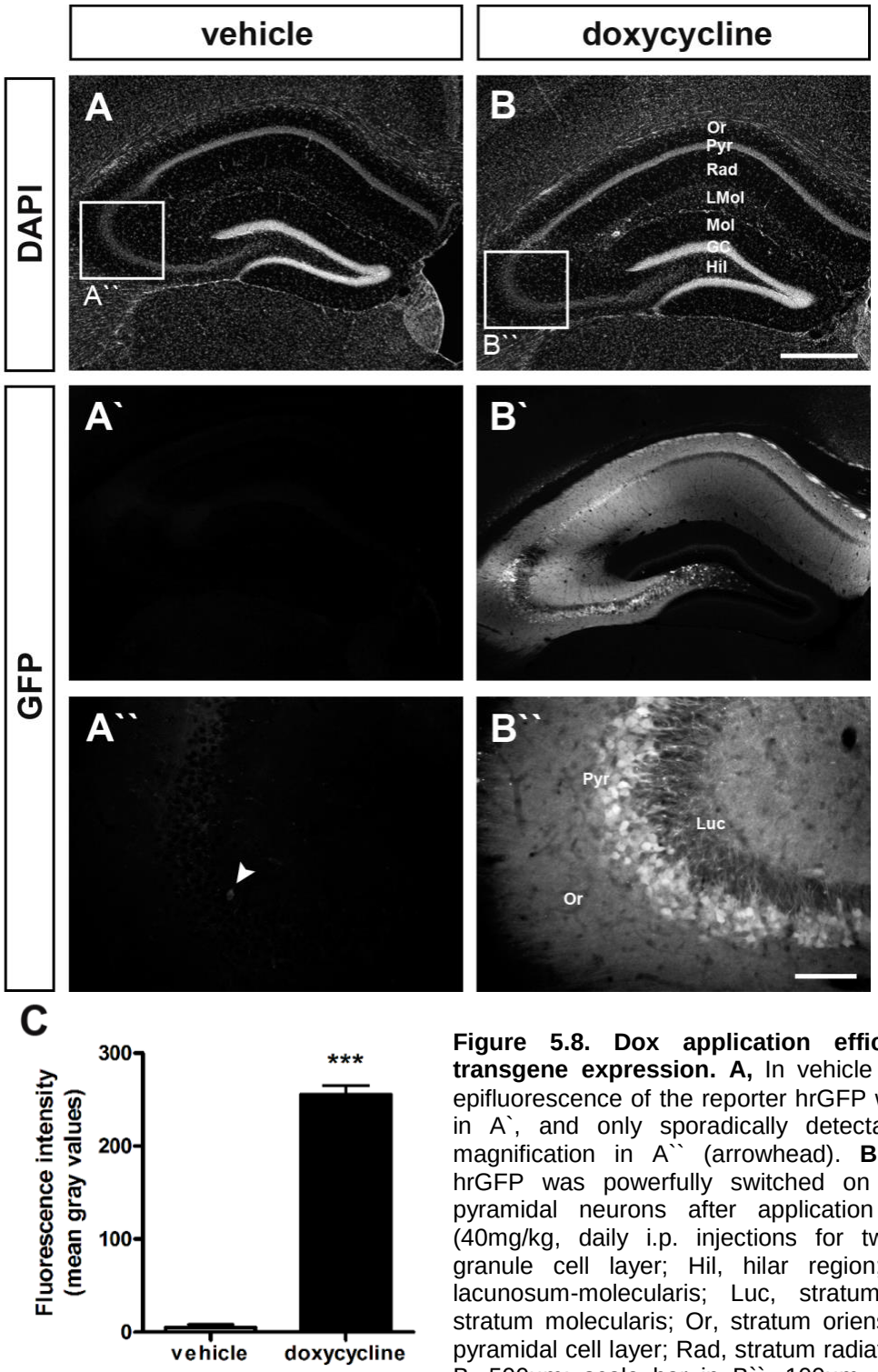

Figure 5.8. Dox application efficiently induces transgene expression. A, In vehicle treated animals, epifluorescence of the reporter hrGFP was not detected in A`, and only sporadically detectable under high magnification in A`` (arrowhead). **B,** Expression of hrGFP was powerfully switched on in hippocampal pyramidal neurons after application of doxycycline (40mg/kg, daily i.p. injections for two weeks). GC, granule cell layer; Hil, hilar region; LMol, stratum lacunosum-molecularis; Luc, stratum lucidum; Mol, stratum molecularis; Or, stratum oriens; Pyr, CA1/CA3 pyramidal cell layer; Rad, stratum radiatum. Scale bar in B, 500µm; scale bar in B``, 100µm. **C,** Fluorescence intensity was highly increased in dox-treated animals compared to vehicle-treated controls (veh, 5.2 ± 3.3 mean gray values; dox, 255.4 ± 9.8 mean gray values; unpaired t test, two-tailed, $p < 0.0001$). Images were acquired using a constant exposure time. Data are expressed as mean ± SEM. n = 3 to 4 mice per group. *** $p < 0.0001$.

6.3 Discussion

To understand the function of genes in the adult nervous system, it is essential to modulate transgene expression by switching it on and off. The tet system is exceptional for reversible control of gene expression in higher eukaryotes (Gossen and Bujard, 2002). Several studies took advantage of the tet systems and incorporated it into viral vectors to target brain tissue. For obvious reasons, a preferential strategy was the use of two vectors, in which one drives expression of the transactivator and one drives expression of the transgene (Wang et al., 2005; Ebert et al., 2005; Matsui et al., 2012). This strategy allows the incorporation of large transgenes but requires co-infection of the cell with both vectors at an optimal stoichiometry, which is difficult to achieve *in vivo* (Davidson and McCray, 2011; Hadaczek et al., 2011). Furthermore, the two vector strategy exclusively promotes the usage of the transactivator system and precludes the usage of transsilencers as here the transsilencer is expressed under control of a cell type-specific promoter. Hence, cells, in which the cell type-specific promoter is not active, do not express the transsilencer leading to uncontrolled transgene expression in these non-target cells.

Ideally, all components of the regulatory system are assembled in one vector genome requiring a cell to be transduced by only one vector. The use of the tet system in a single AAV vector genome was established in previous studies, in which the expression of the transactivator was controlled by TRE fused to a ubiquitous CMV promoter (Haberman et al., 1998; Fitzsimons et al., 2001; Chtarto et al., 2003; Chen et al., 2008). Incorporation of the tetracycline transactivator in a single vector construct under control of a constitutive promoter suffers from high basal expression of the gene of interest in the uninduced state (Haberman et al., 1998). This background activity might result from basal activity of the CMV promoter, transcription initiated by the minimal promoter activity of the ITRs and nonspecific binding of the transactivator, respectively (Chtarto et al., 2003).

To reduce background activity to a minimum, we used the tetracycline-regulatable transcriptional silencer (tTS) to control transgene expression because here unspecific activation of the system in the uninduced state is eliminated and transcription is actively repressed. Another advantage of tTS is a reduced immunogenicity compared to tTA, as recent studies showed that tTA causes a strong cellular and humoral immune response in nonhuman primates, which was directed to the immunogenic viral part of the transactivator fusion protein, the transcriptional activating domain VP16 from herpes simplex virus (Latta-Mahieu et al., 2002, Le Guiner et al., 2007). This domain was replaced in tetracycline-regulatable transcriptional silencers with the transrepressing

domain KRAB (Deuschle et al., 1995, Freundlieb et al., 1999). Furthermore, we replaced the ubiquitous CMV promoter with the neuron-specific synapsin I promoter (Kugler et al., 2003). As AAV has a packaging limit of 5 kb (Dong et al., 1996), we aspired to minimize the size of *cis* elements in the expression vector. The synapsin I promoter enables cell type-specific transgene expression and is a rather short promoter element (480 bp). Although the tet system is relatively small, our single vector design limits the size of the transgene to approximately 2 - 2.5 kb.

Injection of the AAV-TRE-Syn-Stop-hrGFP-2A-tTS vector into the hippocampus of NEX-Cre mice resulted in efficient inhibition of transgene expression by tTS in the uninduced state (Fig. 5.8A`). High power microscopy revealed sporadic and very low expression of the reporter hrGFP (Fig. 5.8A``). This low background activity was expected as our expression system is based on an autoregulatory loop. The turnover of tTS, which actively participate in the repression of transcription, leads to the abolishment of repression and thus the onset of transcription. Importantly, our system shows very low background activity when compared to studies using the transactivator in a single autoregulatory AAV vector *in vivo* (Chtarto et al., 2003). As we initially performed a proof-of-concept study using hrGFP as reporter gene, minimal transgene expression in the uninduced state can hardly be determined because of tissue background autofluorescence and photobleaching. Thus, basal expression needs to be characterized in detail in further approaches, e.g. by using luciferase as reporter gene following quantification by a luciferase assay.

Two weeks of dox treatment efficiently induced hrGFP expression in glutamatergic pyramidal neurons while dentate gyrus granule cells were spared (Fig. 5.8B). At adult stages the NEX promoter is not active in dentate gyrus granule cells and thus Cre recombinase is not expressed in these cells (Goebbels et al., 2006). Here, the Stop cassette cannot get excised and inhibits transcription. Hence, this finding verifies cell type-specific expression mediated by the Stop cassette. Most importantly, this result confirms the functionality of the tet-regulatable system to induce transgene expression by application of a tetracycline analog. However, chronic intraperitoneal drug application is a stressful event for mice leading to impaired mouse behavior and should be avoided if possible. In several studies, dox was administered via drinking water or food pellets (Szulc et al., 2006; Zhu et al., 2007). We leveraged this non-invasive approach and exposed, which were injected with our viral vector, to drinking water supplemented with 5% sucrose and dox (2 mg/ml). One week of dox treatment did not induce transgene expression (data not shown) possibly due to poor solubility of dox in water resulting in low dox uptake. The

optimal dox delivery route, which fits best to the experiment, needs to be investigated further.

Accordingly, the onset of transgene expression following dox administration will be an important issue if this system is used in studies investigating tightly regulated gene function. Hence, the assessment of a time course of transgene expression following dox application would be beneficial. Additionally, a dose-response curve is mandatory to fully characterize the relation between applied dox and the level of transgene expression.

The reversibility of the tet system in the AAV vector was not assessed in this study and needs to be analyzed consequently after dox withdrawal. Dox has a relatively slow tissue clearance which causes transgene repression to be an essentially slower process than activation (Naidoo and Young, 2012). To improve the reversibility process, dox can be substituted by the tetracycline derivative methacycline, which has similar induction potency but a shorter half-life compared to dox allowing for faster tissue clearance (Agwuh and MacGowan, 2006). Additionally, the termination of tet-mediated gene expression can be accelerated by application of a tetracycline antagonist that competitively binds to tet-controlled molecules (Chrast-Balz and Hooft van Huijsduijnen, 1996). Importantly, it must be considered that the assessment of the system's reversibility is compromised by the turnover rate of the transgenic protein, which is very poor for artificial proteins such as hrGFP.

AAV-delivered and dox-inducible transgene expression constitutes a very promising strategy for gene therapy approaches. The use of controllable viral vectors would allow to restrict therapeutic gene expression to specified periods and to stop the treatment in the case of adverse events related to the vector-mediated transgene expression (Manfredsson et al., 2012). According to Chtarto and colleagues, an ideal regulatory system for gene therapy should comprehend (a) a low basal activity in the uninduced state, (b) a high and dose-dependent level of transgene expression in the induced state, (c) a rapid response to the administration or removal of the inducer drug, (d) a negligible toxicity, inflammatory response or immunogenicity associated with the regulatory elements and (e) absence of toxicity and good bioavailability of the inducing drug (Chtarto et al., 2013). The present study and previous surveys showed that our system is able to fulfill some of the mentioned criteria. However, this system shows great potential to fulfill all criteria but needs to be investigated in more detail. Besides dox, other tetracyclines can be used to induce gene expression and in addition afford beneficial properties, such as the previously mentioned methacycline. Further exemplary tetracycline analogs are minocycline, which exhibits an anti-inflammatory effect (Bantubungi et al., 2005), and 4-epidoxycycline, which lacks the antibiotic activity of dox (Zhu et al., 2007).

For gene therapy approaches, the floxed Stop cassette in our tet-inducible AAV vector needs to be removed as it requires transgenic Cre driver mice to initiate gene expression. Cell type-specificity is guaranteed by the utilization of particular promoter elements such as the synapsin promoter, which drives transgene expression specifically in neurons. To target other cell types in the CNS, for example oligodendrocytes, a oligodendrocyte-specific promoter, such as the myelin basic protein promoter, can be incorporated in the tet-inducible AAV vector. This strategy would allow to compensate loss-of-function gene mutations in oligodendrocytes and to provide a promising treatment against leukodystrophies such as Canavan disease.

Taken together, we established a viral vector system that allows expressing a transgene in an inducible, cell type-specific and population-specific manner. This system will facilitate studying CNS gene function under a highly specific temporal and spatial control. Moreover, it enables to turn the expression of the transgene on and off whenever it is desired and thus it will proof useful in advancing gene therapy studies. However, a detailed characterization of the system will have to be addressed in further studies.

Conclusion and outlook

Transgenic mouse lines expressing Cre recombinase under control of a cell type-specific promoter are important tools to explore the role of the endocannabinoid system either by generating conditional knockout mice or by creating a conditional overexpression pattern. The present study aimed at investigating the effect of genetically modified endocannabinoid signaling in the hippocampus and delineated the generation and characterization of transgenic mouse models, which display a gain-of-function of a particular constituent of the endocannabinoid system exclusively in glutamatergic pyramidal neurons of the hippocampus. These transgenic mice were generated by combining AAV-mediated gene delivery and Cre-mediated recombination.

Using this method, endocannabinoid signaling in the mouse hippocampus was amplified in glutamatergic pyramidal neurons by AAV-mediated overexpression of the CB1 receptor, which resulted in an impaired hippocampal memory performance and an increased protection against chemically-induced seizures and excitotoxicity. This approach identified CB1 receptor on glutamatergic hippocampal neurons as potential target for novel agents to restrain excitotoxic events and to treat neurodegenerative diseases.

On the other hand, overexpression of the 2-AG-degrading enzyme MAGL in hippocampal pyramidal neurons alleviated exclusively 2-AG signaling in this particular cell population and enabled to dissect the specific signaling effects of the endocannabinoid 2-AG. This genetic modification exclusively eliminated depolarization-induced suppression of excitation (DSE) in hippocampal CA1 pyramidal neurons, which manifested in elevated corticosterone levels and an increased anxiety-like behavior. Thus, specific inhibition of MAGL expressed in hippocampal pyramidal neurons may represent a potential treatment for anxiety and stress disorders.

Taken together, endocannabinoid signaling was bidirectionally modified in this study leading to completely different phenotypes. However, the genetic modification was restricted to glutamatergic pyramidal neurons of the hippocampus. In order to further dissect the effect of endocannabinoid signaling in distinct brain regions, AAV vectors afford brain region-specific manipulations by stereotaxic injections. Moreover, the novel system is versatile regarding the use of different transgenic mouse lines to target distinct cell-types. Community research projects for the generation of new cell type-specific Cre transgenic mouse lines have been promoted (e.g. CREATE European Project, *http://dev.creline.org/home*; Mouse Clinical Institute, *http://www.ics-mci.fr/mousecre*).

Thus, the number of available Cre driver lines has significantly increased over the last decade and their utilization allows for efficient targeting of AAV-mediated transgene expression to a specific cell-type (e.g. dlx-Cre for GABAergic neurons, tph2(tryptophan hydroxylase 2)-Cre for serotonergic neurons, GFAP-Cre for astrocytes, …). For instance, stereotaxic injection of the AAV-Stop-MAGL vector into the amygdala of dlx-Cre mice would enable to investigate the consequences of abolished 2-AG-mediated DSI in several amygdala-dependent paradigms, such as anxiety and fear extinction.

AAV-mediated, Cre-inducible transgene expression further affords commutability of the transgene, which will be useful to analyze the function of other constituents of the endocannabinoid system. The endocannabinoid system comprises two major signaling molecules, 2-AG and AEA. Several studies identified 2-AG as the key player mediating retrograde synaptic signaling, which is supported by the subcellular segregation of 2-AG-metabolizing enzymes with DAGLα at postsynaptic and MAGL at presynaptic domains (Gulyas et al., 2004; Yoshida et al., 2006; Yoshida et al., 2011; Ludanyi et al., 2011). In contrast, the AEA-degrading enzyme FAAH is localized at postsynaptic sites (Gulyas et al., 2004), which may indicate distinct signaling properties of AEA and 2-AG, respectively. However, it was shown that AEA also acts through CB1 receptors in several neurobiological paradigms (Clapper et al., 2010, Straiker et al., 2011) and that tonic endocannabinoid signaling involves the mobilization of both 2-AG and AEA at hippocampal GABAergic synapses (Hashimotodani et al., 2007; Kim and Alger, 2010). Thus, cell type-specific overexpression of FAAH would be particularly interesting to discriminate between 2-AG- and AEA-mediated signaling effects.

In conclusion, AAV-mediated and Cre recombinase-inducible transgene expression offers a lot of potential for neurobiological research. With the establishment of increasing numbers of transgenic mouse lines, this method represents a general strategy to systematically (over)express a gene of interest in a specific cell population *in vivo*. Cre-activated viral gene expression increases the impact of Cre driver mouse lines, and represents a significant technical progress in studying neuronal circuit organization and function. The generation of an AAV vector, which allows for inducible and reversible transgene expression by drug administration, advances the application spectrum of viral vectors and affords tight temporal control over AAV transgene expression. This vector needs to be investigated in more detail, however, it shows great promise for research applications and gene therapy approaches.

References

Afione, S. A., Conrad, C. K., Kearns, W. G., Chunduru, S., Adams, R., Reynolds, T. C., Guggino, W. B., Cutting, G. R., Carter, B. J. & Flotte, T. R. (1996) In vivo model of adeno-associated virus vector persistence and rescue. *J Virol,* 70, 3235-41.

Agwuh, K. N. & MacGowan, A. (2006) Pharmacokinetics and pharmacodynamics of the tetracyclines including glycylcyclines. *J Antimicrob Chemother,* 58, 256-65.

Albayram, O., Alferink, J., Pitsch, J., Piyanova, A., Neitzert, K., Poppensieker, K., Mauer, D., Michel, K., Legler, A., Becker, A., Monory, K., Lutz, B., Zimmer, A. & Bilkei-Gorzo, A. (2011) Role of CB1 cannabinoid receptors on GABAergic neurons in brain aging. *Proc Natl Acad Sci U S A,* 108, 11256-61.

Asokan, A., Hamra, J. B., Govindasamy, L., Agbandje-McKenna, M. & Samulski, R. J. (2006) Adeno-associated virus type 2 contains an integrin alpha5beta1 binding domain essential for viral cell entry. *J Virol,* 80, 8961-9.

Bagley, J. & Moghaddam, B. (1997) Temporal dynamics of glutamate efflux in the prefrontal cortex and in the hippocampus following repeated stress: effects of pretreatment with saline or diazepam. *Neuroscience,* 77, 65-73.

Bantubungi, K., Jacquard, C., Greco, A., Pintor, A., Chtarto, A., Tai, K., Galas, M. C., Tenenbaum, L., Deglon, N., Popoli, P., Minghetti, L., Brouillet, E., Brotchi, J., Levivier, M., Schiffmann, S. N. & Blum, D. (2005) Minocycline in phenotypic models of Huntington's disease. *Neurobiol Dis,* 18, 206-17.

Batista-Brito, R., Machold, R., Klein, C. & Fishell, G. (2008) Gene expression in cortical interneuron precursors is prescient of their mature function. *Cereb Cortex,* 18, 2306-17.

Bellocchio, L., Lafenetre, P., Cannich, A., Cota, D., Puente, N., Grandes, P., Chaouloff, F., Piazza, P. V. & Marsicano, G. (2010) Bimodal control of stimulated food intake by the endocannabinoid system. *Nat Neurosci,* 13, 281-3.

Ben-Ari, Y. & Cossart, R. (2000) Kainate, a double agent that generates seizures: two decades of progress. *Trends Neurosci,* 23, 580-7.

Benito, C., Romero, J. P., Tolon, R. M., Clemente, D., Docagne, F., Hillard, C. J., Guaza, C. & Romero, J. (2007) Cannabinoid CB1 and CB2 receptors and fatty acid amide hydrolase are specific markers of plaque cell subtypes in human multiple sclerosis. *J Neurosci,* 27, 2396-402.

Bisogno, T., Howell, F., Williams, G., Minassi, A., Cascio, M. G., Ligresti, A., Matias, I., Schiano-Moriello, A., Paul, P., Williams, E. J., Gangadharan, U., Hobbs, C., Di Marzo, V. & Doherty, P. (2003) Cloning of the first sn1-DAG lipases points to the spatial and temporal regulation of endocannabinoid signaling in the brain. *J Cell Biol,* 163, 463-8.

Blacklow, N. R., Hoggan, M. D. & Rowe, W. P. (1968) Serologic evidence for human infection with adenovirus-associated viruses. *J Natl Cancer Inst,* 40, 319-27.

Blankman, J. L., Simon, G. M. & Cravatt, B. F. (2007) A comprehensive profile of brain enzymes that hydrolyze the endocannabinoid 2-arachidonoylglycerol. *Chem Biol,* 14, 1347-56.

Bliss, T. V. & Collingridge, G. L. (1993) A synaptic model of memory: long-term potentiation in the hippocampus. *Nature,* 361, 31-9.

Boucher, A. A., Vivier, L., Metna-Laurent, M., Brayda-Bruno, L., Mons, N., Arnold, J. C. & Micheau, J. (2009) Chronic treatment with Delta(9)-tetrahydrocannabinol impairs spatial memory and reduces zif268 expression in the mouse forebrain. *Behav Pharmacol,* 20, 45-55.

Branda, C. S. & Dymecki, S. M. (2004) Talking about a revolution: The impact of site-specific recombinases on genetic analyses in mice. *Dev Cell,* 6, 7-28.

Breivogel, C. (2006) Cannabinoid receptor binding to membrane homogenates and cannabinoid-stimulated [35S]GTPgammaS binding to membrane homogenates or intact cultured cells. *Methods Mol Med,* 123, 149-62.

Buning, H., Perabo, L., Coutelle, O., Quadt-Humme, S. & Hallek, M. (2008) Recent developments in adeno-associated virus vector technology. *J Gene Med,* 10, 717-33.

Burger, C., Nash, K. & Mandel, R. J. (2005) Recombinant adeno-associated viral vectors in the nervous system. *Hum Gene Ther,* 16, 781-91.

Busquets-Garcia, A., Puighermanal, E., Pastor, A., de la Torre, R., Maldonado, R. & Ozaita, A. (2011) Differential role of anandamide and 2-arachidonoylglycerol in memory and anxiety-like responses. *Biol Psychiatry,* 70, 479-86.

Campolongo, P. & Trezza, V. (2012) The endocannabinoid system: a key modulator of emotions and cognition. *Front Behav Neurosci,* 6, 73.

Cardin, J. A., Carlen, M., Meletis, K., Knoblich, U., Zhang, F., Deisseroth, K., Tsai, L. H. & Moore, C. I. (2009) Driving fast-spiking cells induces gamma rhythm and controls sensory responses. *Nature,* 459, 663-7.

Carlson, G., Wang, Y. & Alger, B. E. (2002) Endocannabinoids facilitate the induction of LTP in the hippocampus. *Nat Neurosci,* 5, 723-4.

Cearley, C. N. & Wolfe, J. H. (2006) Transduction characteristics of adeno-associated virus vectors expressing cap serotypes 7, 8, 9, and Rh10 in the mouse brain. *Mol Ther,* 13, 528-37.

Chanda, P. K., Gao, Y., Mark, L., Btesh, J., Strassle, B. W., Lu, P., Piesla, M. J., Zhang, M. Y., Bingham, B., Uveges, A., Kowal, D., Garbe, D., Kouranova, E. V., Ring, R. H., Bates, B., Pangalos, M. N., Kennedy, J. D., Whiteside, G. T. & Samad, T. A. (2010) Monoacylglycerol lipase activity is a critical modulator of the tone and integrity of the endocannabinoid system. *Mol Pharmacol,* 78, 996-1003.

Chen, C. L., Jensen, R. L., Schnepp, B. C., Connell, M. J., Shell, R., Sferra, T. J., Bartlett, J. S., Clark, K. R. & Johnson, P. R. (2005) Molecular characterization of adeno-associated viruses infecting children. *J Virol,* 79, 14781-92.

Chen, Q., Xiong, X., Lee, T. H., Liu, Y., Sun, Q. A., Wetsel, W. & Zhang, X. (2008) Adeno-associated virus-mediated ILK gene silencing in the rat NAc core. *J Neurosci Methods,* 173, 208-14.

Chirmule, N., Propert, K., Magosin, S., Qian, Y., Qian, R. & Wilson, J. (1999) Immune responses to adenovirus and adeno-associated virus in humans. *Gene Ther,* 6, 1574-83.

Chrast-Balz, J. & Hooft van Huijsduijnen, R. (1996) Bi-directional gene switching with the tetracycline repressor and a novel tetracycline antagonist. *Nucleic Acids Res,* 24, 2900-4.

Christensen, R., Kristensen, P. K., Bartels, E. M., Bliddal, H. & Astrup, A. (2007) Efficacy and safety of the weight-loss drug rimonabant: a meta-analysis of randomised trials. *Lancet,* 370, 1706-13.

Chtarto, A., Bender, H. U., Hanemann, C. O., Kemp, T., Lehtonen, E., Levivier, M., Brotchi, J., Velu, T. & Tenenbaum, L. (2003) Tetracycline-inducible transgene expression mediated by a single AAV vector. *Gene Ther,* 10, 84-94.

Chtarto, A., Bockstael, O., Tshibangu, T., Dewitte, O., Levivier, M. & Tenenbaum, L. (2013) A next step in adeno-associated virus (AAV)-mediated gene therapy for neurological diseases: regulation and targeting. *Br J Clin Pharmacol*.

Clapper, J. R., Moreno-Sanz, G., Russo, R., Guijarro, A., Vacondio, F., Duranti, A., Tontini, A., Sanchini, S., Sciolino, N. R., Spradley, J. M., Hohmann, A. G., Calignano, A., Mor, M., Tarzia, G. & Piomelli, D. (2010) Anandamide suppresses pain initiation through a peripheral endocannabinoid mechanism. *Nat Neurosci,* 13, 1265-70.

Clement, A. B., Hawkins, E. G., Lichtman, A. H. & Cravatt, B. F. (2003) Increased seizure susceptibility and proconvulsant activity of anandamide in mice lacking fatty acid amide hydrolase. *J Neurosci,* 23, 3916-23.

Coomber, B., O'Donoghue, M. F. & Mason, R. (2008) Inhibition of endocannabinoid metabolism attenuates enhanced hippocampal neuronal activity induced by kainic acid. *Synapse,* 62, 746-55.

Cristino, L., Starowicz, K., De Petrocellis, L., Morishita, J., Ueda, N., Guglielmotti, V. & Di Marzo, V. (2008) Immunohistochemical localization of anabolic and catabolic enzymes for anandamide and other putative endovanilloids in the hippocampus and cerebellar cortex of the mouse brain. *Neuroscience,* 151, 955-68.

Cryan, J. F. & Holmes, A. (2005) The ascent of mouse: advances in modelling human depression and anxiety. *Nature Reviews Drug Discovery,* 4, 775-90.

Davidson, B. L. & McCray, P. B., Jr. (2011) Current prospects for RNA interference-based therapies. *Nat Rev Genet,* 12, 329-40.

Daya, S. & Berns, K. I. (2008) Gene therapy using adeno-associated virus vectors. *Clin Microbiol Rev,* 21, 583-93.

de Felipe, P., Luke, G. A., Hughes, L. E., Gani, D., Halpin, C. & Ryan, M. D. (2006) E unum pluribus: multiple proteins from a self-processing polyprotein. *Trends Biotechnol,* 24, 68-75.

De Petrocellis, L. & Di Marzo, V. (2010) Non-CB1, non-CB2 receptors for endocannabinoids, plant cannabinoids, and synthetic cannabimimetics: focus on G-protein-coupled receptors and transient receptor potential channels. *J Neuroimmune Pharmacol,* 5, 103-21.

Degroot, A., Kofalvi, A., Wade, M. R., Davis, R. J., Rodrigues, R. J., Rebola, N., Cunha, R. A. & Nomikos, G. G. (2006) CB1 receptor antagonism increases hippocampal acetylcholine release: site and mechanism of action. *Mol Pharmacol,* 70, 1236-45.

Deuschle, U., Meyer, W. K. & Thiesen, H. J. (1995) Tetracycline-reversible silencing of eukaryotic promoters. *Mol Cell Biol,* 15, 1907-14.

Devane, W. A., Dysarz, F. A., 3rd, Johnson, M. R., Melvin, L. S. & Howlett, A. C. (1988) Determination and characterization of a cannabinoid receptor in rat brain. *Mol Pharmacol,* 34, 605-13.

Devane, W. A., Hanus, L., Breuer, A., Pertwee, R. G., Stevenson, L. A., Griffin, G., Gibson, D., Mandelbaum, A., Etinger, A. & Mechoulam, R. (1992) Isolation and structure of a brain constituent that binds to the cannabinoid receptor. *Science,* 258, 1946-9.

Di, S., Boudaba, C., Popescu, I. R., Weng, F. J., Harris, C., Marcheselli, V. L., Bazan, N. G. & Tasker, J. G. (2005) Activity-dependent release and actions of endocannabinoids in the rat hypothalamic supraoptic nucleus. *J Physiol,* 569, 751-60.

Dinh, T. P., Carpenter, D., Leslie, F. M., Freund, T. F., Katona, I., Sensi, S. L., Kathuria, S. & Piomelli, D. (2002) Brain monoglyceride lipase participating in endocannabinoid inactivation. *Proc Natl Acad Sci U S A,* 99, 10819-24.

Domenici, M. R., Azad, S. C., Marsicano, G., Schierloh, A., Wotjak, C. T., Dodt, H. U., Zieglgansberger, W., Lutz, B. & Rammes, G. (2006) Cannabinoid receptor type 1 located on presynaptic terminals of principal neurons in the forebrain controls glutamatergic synaptic transmission. *J Neurosci,* 26, 5794-9.

Dong, J. Y., Fan, P. D. & Frizzell, R. A. (1996) Quantitative analysis of the packaging capacity of recombinant adeno-associated virus. *Hum Gene Ther,* 7, 2101-12.

Donnelly, M. L., Luke, G., Mehrotra, A., Li, X., Hughes, L. E., Gani, D. & Ryan, M. D. (2001) Analysis of the aphthovirus 2A/2B polyprotein 'cleavage' mechanism indicates not a proteolytic reaction, but a novel translational effect: a putative ribosomal 'skip'. *J Gen Virol,* 82, 1013-25.

Doronina, V. A., de Felipe, P., Wu, C., Sharma, P., Sachs, M. S., Ryan, M. D. & Brown, J. D. (2008) Dissection of a co-translational nascent chain separation event. *Biochem Soc Trans,* 36, 712-6.

Dubreucq, S., Matias, I., Cardinal, P., Haring, M., Lutz, B., Marsicano, G. & Chaouloff, F. (2012) Genetic dissection of the role of cannabinoid type-1 receptors in the emotional consequences of repeated social stress in mice. *Neuropsychopharmacology,* 37, 1885-900.

During, M. J., Young, D., Baer, K., Lawlor, P. & Klugmann, M. (2003) Development and optimization of adeno-associated virus vector transfer into the central nervous system. *Methods Mol Med,* 76, 221-36.

Ebert, A. D., Chen, F., He, X., Cryns, V. L. & Bohn, M. C. (2005) A tetracycline-regulated adenovirus encoding dominant-negative caspase-9 is regulated in rat brain and protects against neurotoxin-induced cell death in vitro, but not in vivo. *Exp Neurol,* 191 Suppl 1, S80-94.

Eddleston, M. & Mucke, L. (1993) Molecular profile of reactive astrocytes--implications for their role in neurologic disease. *Neuroscience,* 54, 15-36.

Falenski, K. W., Blair, R. E., Sim-Selley, L. J., Martin, B. R. & DeLorenzo, R. J. (2007) Status epilepticus causes a long-lasting redistribution of hippocampal cannabinoid type 1 receptor expression and function in the rat pilocarpine model of acquired epilepsy. *Neuroscience,* 146, 1232-44.

Fitzsimons, H. L., McKenzie, J. M. & During, M. J. (2001) Insulators coupled to a minimal bidirectional tet cassette for tight regulation of rAAV-mediated gene transfer in the mammalian brain. *Gene Ther,* 8, 1675-81.

Fowler, C. J. & Jacobsson, S. O. (2002) Cellular transport of anandamide, 2-arachidonoylglycerol and palmitoylethanolamide--targets for drug development? *Prostaglandins Leukot Essent Fatty Acids,* 66, 193-200.

Freundlieb, S., Schirra-Muller, C. & Bujard, H. (1999) A tetracycline controlled activation/repression system with increased potential for gene transfer into mammalian cells. *J Gene Med,* 1, 4-12.

Fu, J., Bottegoni, G., Sasso, O., Bertorelli, R., Rocchia, W., Masetti, M., Guijarro, A., Lodola, A., Armirotti, A., Garau, G., Bandiera, T., Reggiani, A., Mor, M., Cavalli, A. & Piomelli, D. (2012) A catalytically silent FAAH-1 variant drives anandamide transport in neurons. *Nat Neurosci,* 15, 64-9.

Fuxe, K., Chadi, G., Tinner, B., Agnati, L. F., Pettersson, R. & David, G. (1994) On the regional distribution of heparan sulfate proteoglycan immunoreactivity in the rat brain. *Brain Res,* 636, 131-8.

Gaetani, S., Dipasquale, P., Romano, A., Righetti, L., Cassano, T., Piomelli, D. & Cuomo, V. (2009) The endocannabinoid system as a target for novel anxiolytic and antidepressant drugs. *Int Rev Neurobiol,* 85, 57-72.

Gallia, G. L. & Khalili, K. (1998) Evaluation of an autoregulatory tetracycline regulated system. *Oncogene,* 16, 1879-84.

Gao, Y., Vasilyev, D. V., Goncalves, M. B., Howell, F. V., Hobbs, C., Reisenberg, M., Shen, R., Zhang, M. Y., Strassle, B. W., Lu, P., Mark, L., Piesla, M. J., Deng, K., Kouranova, E. V., Ring, R. H., Whiteside, G. T., Bates, B., Walsh, F. S., Williams, G., Pangalos, M. N., Samad, T. A. & Doherty, P. (2010) Loss of retrograde endocannabinoid signaling and reduced adult neurogenesis in diacylglycerol lipase knock-out mice. *J Neurosci,* 30, 2017-24.

Gaoni, Y. & Mechoulam, R. (1964) Isolation, structure and partial synthesis of an active constituent of hashish. *J Am Chem Soc,* 86, 1646-47.

Gaveriaux-Ruff, C. & Kieffer, B. L. (2007) Conditional gene targeting in the mouse nervous system: Insights into brain function and diseases. *Pharmacol Ther,* 113, 619-34.

Goebbels, S., Bormuth, I., Bode, U., Hermanson, O., Schwab, M. H. & Nave, K. A. (2006) Genetic targeting of principal neurons in neocortex and hippocampus of NEX-Cre mice. *Genesis,* 44, 611-21.

Goff, S. P. & Berg, P. (1976) Construction of hybrid viruses containing SV40 and lambda phage DNA segments and their propagation in cultured monkey cells. *Cell,* 9, 695-705.

Gossen, M. & Bujard, H. (1992) Tight control of gene expression in mammalian cells by tetracycline-responsive promoters. *Proc Natl Acad Sci U S A,* 89, 5547-51.

Gossen, M., Freundlieb, S., Bender, G., Muller, G., Hillen, W. & Bujard, H. (1995) Transcriptional activation by tetracyclines in mammalian cells. *Science,* 268, 1766-9.

Gossen, M. & Bujard, H. (2002) Studying gene function in eukaryotes by conditional gene inactivation. *Annu Rev Genet,* 36, 153-73.

Guggenhuber, S., Monory, K., Lutz, B. & Klugmann, M. (2010) AAV vector-mediated overexpression of CB1 cannabinoid receptor in pyramidal neurons of the hippocampus protects against seizure-induced excitoxicity. *PLoS One,* 5, e15707.

Guindon, J., Guijarro, A., Piomelli, D. & Hohmann, A. G. (2011) Peripheral antinociceptive effects of inhibitors of monoacylglycerol lipase in a rat model of inflammatory pain. *Br J Pharmacol,* 163, 1464-78.

Gulyas, A. I., Cravatt, B. F., Bracey, M. H., Dinh, T. P., Piomelli, D., Boscia, F. & Freund, T. F. (2004) Segregation of two endocannabinoid-hydrolyzing enzymes into pre- and postsynaptic compartments in the rat hippocampus, cerebellum and amygdala. *Eur J Neurosci,* 20, 441-58.

Haberman, R. P., McCown, T. J. & Samulski, R. J. (1998) Inducible long-term gene expression in brain with adeno-associated virus gene transfer. *Gene Ther,* 5, 1604-11.

Hadaczek, P., Eberling, J. L., Pivirotto, P., Bringas, J., Forsayeth, J. & Bankiewicz, K. S. (2010) Eight years of clinical improvement in MPTP-lesioned primates after gene therapy with AAV2-hAADC. *Mol Ther,* 18, 1458-61.

Hadaczek, P., Beyer, J., Kells, A., Narrow, W., Bowers, W., Federoff, H. J., Forsayeth, J. & Bankiewicz, K. S. (2011) Evaluation of an AAV2-based rapamycin-regulated glial cell line-derived neurotrophic factor (GDNF) expression vector system. *PLoS One,* 6, e27728.

Han, J., Kesner, P., Metna-Laurent, M., Duan, T., Xu, L., Georges, F., Koehl, M., Abrous, D. N., Mendizabal-Zubiaga, J., Grandes, P., Liu, Q., Bai, G., Wang, W., Xiong, L., Ren, W., Marsicano, G. & Zhang, X. (2012) Acute cannabinoids impair working memory through astroglial CB1 receptor modulation of hippocampal LTD. *Cell,* 148, 1039-50.

Haring, M., Marsicano, G., Lutz, B. & Monory, K. (2007) Identification of the cannabinoid receptor type 1 in serotonergic cells of raphe nuclei in mice. *Neuroscience,* 146, 1212-9.

Hasegawa, K., Cowan, A. B., Nakatsuji, N. & Suemori, H. (2007) Efficient multicistronic expression of a transgene in human embryonic stem cells. *Stem Cells,* 25, 1707-12.

Hashimotodani, Y., Ohno-Shosaku, T. & Kano, M. (2007) Presynaptic monoacylglycerol lipase activity determines basal endocannabinoid tone and terminates retrograde endocannabinoid signaling in the hippocampus. *J Neurosci,* 27, 1211-9.

Hauck, B., Chen, L. & Xiao, W. (2003) Generation and characterization of chimeric recombinant AAV vectors. *Mol Ther,* 7, 419-25.

Hennecke, M., Kwissa, M., Metzger, K., Oumard, A., Kroger, A., Schirmbeck, R., Reimann, J. & Hauser, H. (2001) Composition and arrangement of genes define the strength of IRES-driven translation in bicistronic mRNAs. *Nucleic Acids Res,* 29, 3327-34.

Hill, M. N., Froc, D. J., Fox, C. J., Gorzalka, B. B. & Christie, B. R. (2004) Prolonged cannabinoid treatment results in spatial working memory deficits and impaired long-term potentiation in the CA1 region of the hippocampus in vivo. *Eur J Neurosci,* 20, 859-63.

Hill, M. N., McLaughlin, R. J., Bingham, B., Shrestha, L., Lee, T. T., Gray, J. M., Hillard, C. J., Gorzalka, B. B. & Viau, V. (2010) Endogenous cannabinoid signaling is essential for stress adaptation. *Proc Natl Acad Sci U S A,* 107, 9406-11.

Hill, M. N., Hillard, C. J. & McEwen, B. S. (2011) Alterations in corticolimbic dendritic morphology and emotional behavior in cannabinoid CB1 receptor-deficient mice parallel the effects of chronic stress. *Cereb Cortex,* 21, 2056-64.

Hoggan, M. D., Blacklow, N. R. & Rowe, W. P. (1966) Studies of small DNA viruses found in various adenovirus preparations: physical, biological, and immunological characteristics. *Proc Natl Acad Sci U S A,* 55, 1467-74.

Hopkins, K. J., Wang, G. & Schmued, L. C. (2000) Temporal progression of kainic acid induced neuronal and myelin degeneration in the rat forebrain. *Brain Res,* 864, 69-80.

Howlett, A. C., Barth, F., Bonner, T. I., Cabral, G., Casellas, P., Devane, W. A., Felder, C. C., Herkenham, M., Mackie, K., Martin, B. R., Mechoulam, R. & Pertwee, R. G. (2002) International Union of Pharmacology. XXVII. Classification of cannabinoid receptors. *Pharmacol Rev,* 54, 161-202.

Howlett, A. C., Blume, L. C. & Dalton, G. D. (2010) CB(1) cannabinoid receptors and their associated proteins. *Curr Med Chem,* 17, 1382-93.

Hu, C., Busuttil, R. W. & Lipshutz, G. S. (2010) RH10 provides superior transgene expression in mice when compared with natural AAV serotypes for neonatal gene therapy. *J Gene Med,* 12, 766-78.

Hu, W., Zhang, M., Czeh, B., Zhang, W. & Flugge, G. (2011) Chronic restraint stress impairs endocannabinoid mediated suppression of GABAergic signaling in the hippocampus of adult male rats. *Brain Res Bull,* 85, 374-9.

Jacob, W., Marsch, R., Marsicano, G., Lutz, B. & Wotjak, C. T. (2012) Cannabinoid CB1 receptor deficiency increases contextual fear memory under highly aversive conditions and long-term potentiation in vivo. *Neurobiol Learn Mem,* 98, 47-55.

Johnson, J. S. & Samulski, R. J. (2009) Enhancement of adeno-associated virus infection by mobilizing capsids into and out of the nucleolus. *J Virol,* 83, 2632-44.

Jung, K. M., Clapper, J. R., Fu, J., D'Agostino, G., Guijarro, A., Thongkham, D., Avanesian, A., Astarita, G., DiPatrizio, N. V., Frontini, A., Cinti, S., Diano, S. & Piomelli, D. (2012) 2-arachidonoylglycerol signaling in forebrain regulates systemic energy metabolism. *Cell Metab,* 15, 299-310.

Kaludov, N., Brown, K. E., Walters, R. W., Zabner, J. & Chiorini, J. A. (2001) Adeno-associated virus serotype 4 (AAV4) and AAV5 both require sialic acid binding for hemagglutination and efficient transduction but differ in sialic acid linkage specificity. *J Virol,* 75, 6884-93.

Kamprath, K., Plendl, W., Marsicano, G., Deussing, J. M., Wurst, W., Lutz, B. & Wotjak, C. T. (2009) Endocannabinoids mediate acute fear adaptation via glutamatergic neurons independently of corticotropin-releasing hormone signaling. *Genes Brain Behav,* 8, 203-11.

Kano, M., Ohno-Shosaku, T., Hashimotodani, Y., Uchigashima, M. & Watanabe, M. (2009) Endocannabinoid-mediated control of synaptic transmission. *Physiol Rev,* 89, 309-80.

Kaplitt, M. G., Leone, P., Samulski, R. J., Xiao, X., Pfaff, D. W., O'Malley, K. L. & During, M. J. (1994) Long-term gene expression and phenotypic correction using adeno-associated virus vectors in the mammalian brain. *Nat Genet,* 8, 148-54.

Karanian, D. A., Karim, S. L., Wood, J. T., Williams, J. S., Lin, S., Makriyannis, A. & Bahr, B. A. (2007) Endocannabinoid enhancement protects against kainic acid-induced seizures and associated brain damage. *J Pharmacol Exp Ther,* 322, 1059-66.

Karlen, A., Karlsson, T. E., Mattsson, A., Lundstromer, K., Codeluppi, S., Pham, T. M., Backman, C. M., Ogren, S. O., Aberg, E., Hoffman, A. F., Sherling, M. A., Lupica, C. R., Hoffer, B. J., Spenger, C., Josephson, A., Brene, S. & Olson, L. (2009) Nogo receptor 1 regulates formation of lasting memories. *Proc Natl Acad Sci U S A,* 106, 20476-81.

Kathuria, S., Gaetani, S., Fegley, D., Valino, F., Duranti, A., Tontini, A., Mor, M., Tarzia, G., La Rana, G., Calignano, A., Giustino, A., Tattoli, M., Palmery, M., Cuomo, V. & Piomelli, D. (2003) Modulation of anxiety through blockade of anandamide hydrolysis. *Nat Med,* 9, 76-81.

Katona, I., Sperlagh, B., Sik, A., Kafalvi, A., Vizi, E. S., Mackie, K. & Freund, T. F. (1999) Presynaptically located CB1 cannabinoid receptors regulate GABA release from axon terminals of specific hippocampal interneurons. *J Neurosci,* 19, 4544-58.

Katona, I. & Freund, T. F. (2008) Endocannabinoid signaling as a synaptic circuit breaker in neurological disease. *Nat Med,* 14, 923-30.

Katona, I. & Freund, T. F. (2012) Multiple functions of endocannabinoid signaling in the brain. *Annual Review of Neuroscience,* 35, 529-58.

Kawamura, Y., Fukaya, M., Maejima, T., Yoshida, T., Miura, E., Watanabe, M., Ohno-Shosaku, T. & Kano, M. (2006) The CB1 cannabinoid receptor is the major cannabinoid receptor at excitatory presynaptic sites in the hippocampus and cerebellum. *J Neurosci,* 26, 2991-3001.

Kim, J., Isokawa, M., Ledent, C. & Alger, B. E. (2002) Activation of muscarinic acetylcholine receptors enhances the release of endogenous cannabinoids in the hippocampus. *J Neurosci,* 22, 10182-91.

Kim, J. & Alger, B. E. (2010) Reduction in endocannabinoid tone is a homeostatic mechanism for specific inhibitory synapses. *Nat Neurosci,* 13, 592-600.

Kinsey, S. G., Long, J. Z., O'Neal, S. T., Abdullah, R. A., Poklis, J. L., Boger, D. L., Cravatt, B. F. & Lichtman, A. H. (2009) Blockade of endocannabinoid-degrading enzymes attenuates neuropathic pain. *J Pharmacol Exp Ther,* 330, 902-10.

Kinsey, S. G., O'Neal, S. T., Long, J. Z., Cravatt, B. F. & Lichtman, A. H. (2011) Inhibition of endocannabinoid catabolic enzymes elicits anxiolytic-like effects in the marble burying assay. *Pharmacol Biochem Behav,* 98, 21-7.

Klein, R. L., Dayton, R. D., Tatom, J. B., Henderson, K. M. & Henning, P. P. (2008) AAV8, 9, Rh10, Rh43 vector gene transfer in the rat brain: effects of serotype, promoter and purification method. *Mol Ther,* 16, 89-96.

Klugmann, M., Symes, C. W., Leichtlein, C. B., Klaussner, B. K., Dunning, J., Fong, D., Young, D. & During, M. J. (2005) AAV-mediated hippocampal expression of short and long Homer 1 proteins differentially affect cognition and seizure activity in adult rats. *Mol Cell Neurosci,* 28, 347-60.

Klugmann, M., Leichtlein, C. B., Symes, C. W., Klaussner, B. C., Brooks, A. I., Young, D. & During, M. J. (2006) A novel role of circadian transcription factor DBP in hippocampal plasticity. *Mol Cell Neurosci,* 31, 303-14.

Kopp, F., Komatsu, T., Nomura, D. K., Trauger, S. A., Thomas, J. R., Siuzdak, G., Simon, G. M. & Cravatt, B. F. (2010) The glycerophospho metabolome and its influence on amino acid homeostasis revealed by brain metabolomics of GDE1(-/-) mice. *Chem Biol,* 17, 831-40.

Kozak, K. R., Prusakiewicz, J. J. & Marnett, L. J. (2004) Oxidative metabolism of endocannabinoids by COX-2. *Curr Pharm Des,* 10, 659-67.

Kronenberg, S., Bottcher, B., von der Lieth, C. W., Bleker, S. & Kleinschmidt, J. A. (2005) A conformational change in the adeno-associated virus type 2 capsid leads to the exposure of hidden VP1 N termini. *J Virol,* 79, 5296-303.

Kugler, S., Kilic, E. & Bahr, M. (2003) Human synapsin 1 gene promoter confers highly neuron-specific long-term transgene expression from an adenoviral vector in the adult rat brain depending on the transduced area. *Gene Ther,* 10, 337-47.

Labar, G., Wouters, J. & Lambert, D. M. (2010) A review on the monoacylglycerol lipase: at the interface between fat and endocannabinoid signalling. *Curr Med Chem,* 17, 2588-607.

Latta-Mahieu, M., Rolland, M., Caillet, C., Wang, M., Kennel, P., Mahfouz, I., Loquet, I., Dedieu, J. F., Mahfoudi, A., Trannoy, E. & Thuillier, V. (2002) Gene transfer of a chimeric trans-activator is immunogenic and results in short-lived transgene expression. *Hum Gene Ther,* 13, 1611-20.

Le Guiner, C., Stieger, K., Snyder, R. O., Rolling, F. & Moullier, P. (2007) Immune responses to gene product of inducible promoters. *Curr Gene Ther,* 7, 334-46.

Lengler, J., Holzmuller, H., Salmons, B., Gunzburg, W. H. & Renner, M. (2005) FMDV-2A sequence and protein arrangement contribute to functionality of CYP2B1-reporter fusion protein. *Anal Biochem,* 343, 116-24.

Lenz, R. A. & Alger, B. E. (1999) Calcium dependence of depolarization-induced suppression of inhibition in rat hippocampal CA1 pyramidal neurons. *J Physiol,* 521 Pt 1, 147-57.

LeWitt, P. A., Rezai, A. R., Leehey, M. A., Ojemann, S. G., Flaherty, A. W., Eskandar, E. N., Kostyk, S. K., Thomas, K., Sarkar, A., Siddiqui, M. S., Tatter, S. B., Schwalb, J. M., Poston, K. L., Henderson, J. M., Kurlan, R. M., Richard, I. H., Van Meter, L., Sapan, C. V., During, M. J., Kaplitt, M. G. & Feigin, A. (2011) AAV2-GAD gene therapy for advanced Parkinson's disease: a double-blind, sham-surgery controlled, randomised trial. *Lancet Neurol,* 10, 309-19.

Lichtman, A. H., Dimen, K. R. & Martin, B. R. (1995) Systemic or intrahippocampal cannabinoid administration impairs spatial memory in rats. *Psychopharmacology (Berl),* 119, 282-90.

Lichtman, A. H. (2000) SR 141716A enhances spatial memory as assessed in a radial-arm maze task in rats. *Eur J Pharmacol,* 404, 175-9.

Liu, X. B. & Jones, E. G. (1996) Localization of alpha type II calcium calmodulin-dependent protein kinase at glutamatergic but not gamma-aminobutyric acid (GABAergic) synapses in thalamus and cerebral cortex. *Proc Natl Acad Sci U S A,* 93, 7332-6.

Long, J. Z., Li, W., Booker, L., Burston, J. J., Kinsey, S. G., Schlosburg, J. E., Pavon, F. J., Serrano, A. M., Selley, D. E., Parsons, L. H., Lichtman, A. H. & Cravatt, B. F. (2009) Selective blockade of 2-arachidonoylglycerol hydrolysis produces cannabinoid behavioral effects. *Nat Chem Biol,* 5, 37-44.

Lourenco, J., Cannich, A., Carta, M., Coussen, F., Mulle, C. & Marsicano, G. (2010) Synaptic activation of kainate receptors gates presynaptic CB(1) signaling at GABAergic synapses. *Nat Neurosci,* 13, 197-204.

Lourenco, J., Matias, I., Marsicano, G. & Mulle, C. (2011) Pharmacological activation of kainate receptors drives endocannabinoid mobilization. *J Neurosci,* 31, 3243-8.

Ludanyi, A., Eross, L., Czirjak, S., Vajda, J., Halasz, P., Watanabe, M., Palkovits, M., Magloczky, Z., Freund, T. F. & Katona, I. (2008) Downregulation of the CB1 cannabinoid receptor and related molecular elements of the endocannabinoid system in epileptic human hippocampus. *J Neurosci,* 28, 2976-90.

Ludanyi, A., Hu, S. S., Yamazaki, M., Tanimura, A., Piomelli, D., Watanabe, M., Kano, M., Sakimura, K., Magloczky, Z., Mackie, K., Freund, T. F. & Katona, I. (2011) Complementary synaptic distribution of enzymes responsible for synthesis and inactivation of the endocannabinoid 2-arachidonoylglycerol in the human hippocampus. *Neuroscience,* 174, 50-63.

Lutz, B. (2004) On-demand activation of the endocannabinoid system in the control of neuronal excitability and epileptiform seizures. *Biochem Pharmacol,* 68, 1691-8.

Lutz, B. (2009) Endocannabinoid signals in the control of emotion. *Curr Opin Pharmacol,* 9, 46-52.

Mackie, K. (2005) Distribution of cannabinoid receptors in the central and peripheral nervous system. *Handb Exp Pharmacol*, 299-325.

Maejima, T., Hashimoto, K., Yoshida, T., Aiba, A. & Kano, M. (2001) Presynaptic inhibition caused by retrograde signal from metabotropic glutamate to cannabinoid receptors. *Neuron,* 31, 463-75.

Magloczky, Z., Toth, K., Karlocai, R., Nagy, S., Eross, L., Czirjak, S., Vajda, J., Rasonyi, G., Kelemen, A., Juhos, V., Halasz, P., Mackie, K. & Freund, T. F. (2010) Dynamic changes of CB1-receptor expression in hippocampi of epileptic mice and humans. *Epilepsia,* 51 Suppl 3, 115-20.

Mandel, R. J., Manfredsson, F. P., Foust, K. D., Rising, A., Reimsnider, S., Nash, K. & Burger, C. (2006) Recombinant adeno-associated viral vectors as therapeutic agents to treat neurological disorders. *Mol Ther,* 13, 463-83.

Manfredsson, F. P., Bloom, D. C. & Mandel, R. J. (2012) Regulated protein expression for in vivo gene therapy for neurological disorders: progress, strategies, and issues. *Neurobiol Dis,* 48, 212-21.

Marrs, W. R., Blankman, J. L., Horne, E. A., Thomazeau, A., Lin, Y. H., Coy, J., Bodor, A. L., Muccioli, G. G., Hu, S. S., Woodruff, G., Fung, S., Lafourcade, M., Alexander, J. P., Long, J. Z., Li, W., Xu, C., Moller, T., Mackie, K., Manzoni, O. J., Cravatt, B. F. & Stella, N. (2010) The serine hydrolase ABHD6 controls the accumulation and efficacy of 2-AG at cannabinoid receptors. *Nat Neurosci,* 13, 951-7.

Marsicano, G. & Lutz, B. (1999) Expression of the cannabinoid receptor CB1 in distinct neuronal subpopulations in the adult mouse forebrain. *Eur J Neurosci,* 11, 4213-25.

Marsicano, G., Wotjak, C. T., Azad, S. C., Bisogno, T., Rammes, G., Cascio, M. G., Hermann, H., Tang, J., Hofmann, C., Zieglgansberger, W., Di Marzo, V. & Lutz, B. (2002) The endogenous cannabinoid system controls extinction of aversive memories. *Nature,* 418, 530-4.

Marsicano, G., Goodenough, S., Monory, K., Hermann, H., Eder, M., Cannich, A., Azad, S. C., Cascio, M. G., Gutierrez, S. O., van der Stelt, M., Lopez-Rodriguez, M. L., Casanova, E., Schutz, G., Zieglgansberger, W., Di Marzo, V., Behl, C. & Lutz, B. (2003) CB1 cannabinoid receptors and on-demand defense against excitotoxicity. *Science,* 302, 84-8.

Marsicano, G. & Lafenetre, P. (2009) Roles of the endocannabinoid system in learning and memory. *Curr Top Behav Neurosci,* 1, 201-30.

Matsuda, L. A., Lolait, S. J., Brownstein, M. J., Young, A. C. & Bonner, T. I. (1990) Structure of a cannabinoid receptor and functional expression of the cloned cDNA. *Nature,* 346, 561-4.

Matsui, R., Tanabe, Y. & Watanabe, D. (2012) Avian adeno-associated virus vector efficiently transduces neurons in the embryonic and post-embryonic chicken brain. *PLoS One,* 7, e48730.

McCown, T. J., Xiao, X., Li, J., Breese, G. R. & Samulski, R. J. (1996) Differential and persistent expression patterns of CNS gene transfer by an adeno-associated virus (AAV) vector. *Brain Res,* 713, 99-107.

McCown, T. J. (2005) Adeno-associated virus (AAV) vectors in the CNS. *Curr Gene Ther,* 5, 333-8.

McFarland, N. R., Lee, J. S., Hyman, B. T. & McLean, P. J. (2009) Comparison of transduction efficiency of recombinant AAV serotypes 1, 2, 5, and 8 in the rat nigrostriatal system. *J Neurochem,* 109, 838-45.

Mechoulam, R., Ben-Shabat, S., Hanus, L., Ligumsky, M., Kaminski, N. E., Schatz, A. R., Gopher, A., Almog, S., Martin, B. R., Compton, D. R. & et al. (1995) Identification of an endogenous 2-monoglyceride, present in canine gut, that binds to cannabinoid receptors. *Biochem Pharmacol,* 50, 83-90.

Mechoulam, R. & Lichtman, A. H. (2003) Neuroscience. Stout guards of the central nervous system. *Science,* 302, 65-7.

Mechoulam, R. & Parker, L. A. (2013) The endocannabinoid system and the brain. *Annu Rev Psychol,* 64, 21-47.

Messinis, L., Kyprianidou, A., Malefaki, S. & Papathanasopoulos, P. (2006) Neuropsychological deficits in long-term frequent cannabis users. *Neurology,* 66, 737-9.

Millan, M. J. (2003) The neurobiology and control of anxious states. *Prog Neurobiol,* 70, 83-244.

Mishima, K., Egashira, N., Hirosawa, N., Fujii, M., Matsumoto, Y., Iwasaki, K. & Fujiwara, M. (2001) Characteristics of learning and memory impairment induced by delta9-tetrahydrocannabinol in rats. *Jpn J Pharmacol,* 87, 297-308.

Mohri, I., Taniike, M., Taniguchi, H., Kanekiyo, T., Aritake, K., Inui, T., Fukumoto, N., Eguchi, N., Kushi, A., Sasai, H., Kanaoka, Y., Ozono, K., Narumiya, S., Suzuki, K. & Urade, Y. (2006) Prostaglandin D2-mediated microglia/astrocyte interaction enhances astrogliosis and demyelination in twitcher. *J Neurosci,* 26, 4383-93.

Monory, K., Massa, F., Egertova, M., Eder, M., Blaudzun, H., Westenbroek, R., Kelsch, W., Jacob, W., Marsch, R., Ekker, M., Long, J., Rubenstein, J. L., Goebbels, S., Nave, K. A., During, M., Klugmann, M., Wolfel, B., Dodt, H. U., Zieglgansberger, W., Wotjak, C. T., Mackie, K., Elphick, M. R., Marsicano, G. & Lutz, B. (2006) The endocannabinoid system controls key epileptogenic circuits in the hippocampus. *Neuron,* 51, 455-66.

Monory, K., Blaudzun, H., Massa, F., Kaiser, N., Lemberger, T., Schutz, G., Wotjak, C. T., Lutz, B. & Marsicano, G. (2007) Genetic dissection of behavioural and autonomic effects of Delta(9)-tetrahydrocannabinol in mice. *PLoS Biol,* 5, e269.

Moreira, F. A. & Lutz, B. (2008) The endocannabinoid system: emotion, learning and addiction. *Addict Biol,* 13, 196-212.

Moreira, F. A. & Wotjak, C. T. (2010) Cannabinoids and anxiety. *Curr Top Behav Neurosci,* 2, 429-50.

Morozov, Y. M., Torii, M. & Rakic, P. (2009) Origin, early commitment, migratory routes, and destination of cannabinoid type 1 receptor-containing interneurons. *Cereb Cortex,* 19 Suppl 1, i78-89.

Morris, R. G., Garrud, P., Rawlins, J. N. & O'Keefe, J. (1982) Place navigation impaired in rats with hippocampal lesions. *Nature,* 297, 681-3.

Morris, R. G., Anderson, E., Lynch, G. S. & Baudry, M. (1986) Selective impairment of learning and blockade of long-term potentiation by an N-methyl-D-aspartate receptor antagonist, AP5. *Nature,* 319, 774-6.

Mulder, J., Zilberter, M., Pasquare, S. J., Alpar, A., Schulte, G., Ferreira, S. G., Kofalvi, A., Martin-Moreno, A. M., Keimpema, E., Tanila, H., Watanabe, M., Mackie, K., Hortobagyi, T., de Ceballos, M. L. & Harkany, T. (2011) Molecular reorganization of endocannabinoid signalling in Alzheimer's disease. *Brain,* 134, 1041-60.

Mulvihill, M. M. & Nomura, D. K. (2012) Therapeutic potential of monoacylglycerol lipase inhibitors. *Life Sci*.

Munro, S., Thomas, K. L. & Abu-Shaar, M. (1993) Molecular characterization of a peripheral receptor for cannabinoids. *Nature,* 365, 61-5.

Murray, A. J., Sauer, J. F., Riedel, G., McClure, C., Ansel, L., Cheyne, L., Bartos, M., Wisden, W. & Wulff, P. (2011) Parvalbumin-positive CA1 interneurons are required for spatial working but not for reference memory. *Nat Neurosci,* 14, 297-9.

Naderi, N., Aziz Ahari, F., Shafaghi, B., Najarkolaei, A. H. & Motamedi, F. (2008) Evaluation of interactions between cannabinoid compounds and diazepam in electroshock-induced seizure model in mice. *J Neural Transm,* 115, 1501-11.

Naidoo, J. & Young, D. (2012) Gene regulation systems for gene therapy applications in the central nervous system. *Neurol Res Int,* 2012, 595410.

Naidoo, V., Nikas, S. P., Karanian, D. A., Hwang, J., Zhao, J., Wood, J. T., Alapafuja, S. O., Vadivel, S. K., Butler, D., Makriyannis, A. & Bahr, B. A. (2011) A new generation fatty acid amide hydrolase inhibitor protects against kainate-induced excitotoxicity. *J Mol Neurosci,* 43, 493-502.

Nasehi, M., Piri, M., Jamali-Raeufy, N. & Zarrindast, M. R. (2010) Influence of intracerebral administration of NO agents in dorsal hippocampus (CA1) on cannabinoid state-dependent memory in the step-down passive avoidance test. *Physiol Behav,* 100, 297-304.

Navarrete, M. & Araque, A. (2010) Endocannabinoids potentiate synaptic transmission through stimulation of astrocytes. *Neuron,* 68, 113-26.

Nevalainen, T. & Irving, A. J. (2010) GPR55, a lysophosphatidylinositol receptor with cannabinoid sensitivity? *Curr Top Med Chem,* 10, 799-813.

Nomura, D. K., Lombardi, D. P., Chang, J. W., Niessen, S., Ward, A. M., Long, J. Z., Hoover, H. H. & Cravatt, B. F. (2011a) Monoacylglycerol lipase exerts dual control over endocannabinoid and fatty acid pathways to support prostate cancer. *Chem Biol,* 18, 846-56.

Nomura, D. K., Morrison, B. E., Blankman, J. L., Long, J. Z., Kinsey, S. G., Marcondes, M. C., Ward, A. M., Hahn, Y. K., Lichtman, A. H., Conti, B. & Cravatt, B. F. (2011b) Endocannabinoid hydrolysis generates brain prostaglandins that promote neuroinflammation. *Science,* 334, 809-13.

Nonnenmacher, M. & Weber, T. (2012) Intracellular transport of recombinant adeno-associated virus vectors. *Gene Ther,* 19, 649-58.

O'Sullivan, S. E. & Kendall, D. A. (2010) Cannabinoid activation of peroxisome proliferator-activated receptors: potential for modulation of inflammatory disease. *Immunobiology,* 215, 611-6.

Oropeza, V. C., Mackie, K. & Van Bockstaele, E. J. (2007) Cannabinoid receptors are localized to noradrenergic axon terminals in the rat frontal cortex. *Brain Res,* 1127, 36-44.

Ortolano, S., Spuch, C. & Navarro, C. (2012) Present and future of adeno associated virus based gene therapy approaches. *Recent Pat Endocr Metab Immune Drug Discov,* 6, 47-66.

Palucha, A. & Pilc, A. (2007) Metabotropic glutamate receptor ligands as possible anxiolytic and antidepressant drugs. *Pharmacol Ther,* 115, 116-47.

Pan, B., Wang, W., Long, J. Z., Sun, D., Hillard, C. J., Cravatt, B. F. & Liu, Q. S. (2009) Blockade of 2-arachidonoylglycerol hydrolysis by selective monoacylglycerol lipase inhibitor 4-nitrophenyl 4-(dibenzo[d][1,3]dioxol-5-yl(hydroxy)methyl)piperidine-1-carboxylate (JZL184) Enhances retrograde endocannabinoid signaling. *J Pharmacol Exp Ther,* 331, 591-7.

Pan, B., Wang, W., Zhong, P., Blankman, J. L., Cravatt, B. F. & Liu, Q. S. (2011) Alterations of endocannabinoid signaling, synaptic plasticity, learning, and memory in monoacylglycerol lipase knock-out mice. *J Neurosci,* 31, 13420-30.

Patel, S., Roelke, C. T., Rademacher, D. J. & Hillard, C. J. (2005) Inhibition of restraint stress-induced neural and behavioural activation by endogenous cannabinoid signalling. *Eur J Neurosci,* 21, 1057-69.

Patel, S., Kingsley, P. J., Mackie, K., Marnett, L. J. & Winder, D. G. (2009) Repeated homotypic stress elevates 2-arachidonoylglycerol levels and enhances short-term endocannabinoid signaling at inhibitory synapses in basolateral amygdala. *Neuropsychopharmacology,* 34, 2699-709.

Peel, A. L. & Klein, R. L. (2000) Adeno-associated virus vectors: activity and applications in the CNS. *J Neurosci Methods,* 98, 95-104.

Pelletier, J. & Sonenberg, N. (1988) Internal initiation of translation of eukaryotic mRNA directed by a sequence derived from poliovirus RNA. *Nature,* 334, 320-5.

Piomelli, D. (2003) The molecular logic of endocannabinoid signalling. *Nat Rev Neurosci,* 4, 873-84.

Puighermanal, E., Marsicano, G., Busquets-Garcia, A., Lutz, B., Maldonado, R. & Ozaita, A. (2009) Cannabinoid modulation of hippocampal long-term memory is mediated by mTOR signaling. *Nat Neurosci,* 12, 1152-8.

Qing, K., Mah, C., Hansen, J., Zhou, S., Dwarki, V. & Srivastava, A. (1999) Human fibroblast growth factor receptor 1 is a co-receptor for infection by adeno-associated virus 2. *Nat Med,* 5, 71-7.

Rabinowitz, J. E., Rolling, F., Li, C., Conrath, H., Xiao, W., Xiao, X. & Samulski, R. J. (2002) Cross-packaging of a single adeno-associated virus (AAV) type 2 vector genome into multiple AAV serotypes enables transduction with broad specificity. *J Virol,* 76, 791-801.

Rabinowitz, J. E., Bowles, D. E., Faust, S. M., Ledford, J. G., Cunningham, S. E. & Samulski, R. J. (2004) Cross-dressing the virion: the transcapsidation of adeno-associated virus serotypes functionally defines subgroups. *J Virol,* 78, 4421-32.

Rademacher, D. J., Meier, S. E., Shi, L., Ho, W. S., Jarrahian, A. & Hillard, C. J. (2008) Effects of acute and repeated restraint stress on endocannabinoid content in the amygdala, ventral striatum, and medial prefrontal cortex in mice. *Neuropharmacology,* 54, 108-16.

Ramesh, D., Ross, G. R., Schlosburg, J. E., Owens, R. A., Abdullah, R. A., Kinsey, S. G., Long, J. Z., Nomura, D. K., Sim-Selley, L. J., Cravatt, B. F., Akbarali, H. I. & Lichtman, A. H. (2011) Blockade of endocannabinoid hydrolytic enzymes attenuates precipitated opioid withdrawal symptoms in mice. *J Pharmacol Exp Ther,* 339, 173-85.

Reibaud, M., Obinu, M. C., Ledent, C., Parmentier, M., Bohme, G. A. & Imperato, A. (1999) Enhancement of memory in cannabinoid CB1 receptor knock-out mice. *Eur J Pharmacol,* 379, R1-2.

Rey, A. A., Purrio, M., Viveros, M. P. & Lutz, B. (2012) Biphasic effects of cannabinoids in anxiety responses: CB1 and GABA(B) receptors in the balance of GABAergic and glutamatergic neurotransmission. *Neuropsychopharmacology,* 37, 2624-34.

Richichi, C., Lin, E. J., Stefanin, D., Colella, D., Ravizza, T., Grignaschi, G., Veglianese, P., Sperk, G., During, M. J. & Vezzani, A. (2004) Anticonvulsant and antiepileptogenic effects mediated by adeno-associated virus vector neuropeptide Y expression in the rat hippocampus. *J Neurosci,* 24, 3051-9.

Romigi, A., Bari, M., Placidi, F., Marciani, M. G., Malaponti, M., Torelli, F., Izzi, F., Prosperetti, C., Zannino, S., Corte, F., Chiaramonte, C. & Maccarrone, M. (2010) Cerebrospinal fluid levels of the endocannabinoid anandamide are reduced in patients with untreated newly diagnosed temporal lobe epilepsy. *Epilepsia,* 51, 768-72.

Ruehle, S., Rey, A. A., Remmers, F. & Lutz, B. (2012) The endocannabinoid system in anxiety, fear memory and habituation. *J Psychopharmacol,* 26, 23-39.

Samulski, R. J., Berns, K. I., Tan, M. & Muzyczka, N. (1982) Cloning of adeno-associated virus into pBR322: rescue of intact virus from the recombinant plasmid in human cells. *Proc Natl Acad Sci U S A,* 79, 2077-81.

Sanlioglu, S., Benson, P. K., Yang, J., Atkinson, E. M., Reynolds, T. & Engelhardt, J. F. (2000) Endocytosis and nuclear trafficking of adeno-associated virus type 2 are controlled by rac1 and phosphatidylinositol-3 kinase activation. *J Virol,* 74, 9184-96.

Schlosburg, J. E., Carlson, B. L., Ramesh, D., Abdullah, R. A., Long, J. Z., Cravatt, B. F. & Lichtman, A. H. (2009) Inhibitors of endocannabinoid-metabolizing enzymes reduce precipitated withdrawal responses in THC-dependent mice. *AAPS J,* 11, 342-52.

Schlosburg, J. E., Blankman, J. L., Long, J. Z., Nomura, D. K., Pan, B., Kinsey, S. G., Nguyen, P. T., Ramesh, D., Booker, L., Burston, J. J., Thomas, E. A., Selley, D. E., Sim-Selley, L. J., Liu, Q. S., Lichtman, A. H. & Cravatt, B. F. (2010) Chronic monoacylglycerol lipase blockade causes functional antagonism of the endocannabinoid system. *Nat Neurosci,* 13, 1113-9.

Schmued, L. C., Stowers, C. C., Scallet, A. C. & Xu, L. (2005) Fluoro-Jade C results in ultra high resolution and contrast labeling of degenerating neurons. *Brain Res,* 1035, 24-31.

Schnepp, B. C., Jensen, R. L., Chen, C. L., Johnson, P. R. & Clark, K. R. (2005) Characterization of adeno-associated virus genomes isolated from human tissues. *J Virol,* 79, 14793-803.

Schulte, K., Steingruber, N., Jergas, B., Redmer, A., Kurz, C. M., Buchalla, R., Lutz, B., Zimmer, A. & Schlicker, E. (2012) Cannabinoid CB1 receptor activation, pharmacological blockade, or genetic ablation affects the function of the muscarinic auto- and heteroreceptor. *Naunyn Schmiedebergs Arch Pharmacol,* 385, 385-96.

Sciolino, N. R., Zhou, W. & Hohmann, A. G. (2011) Enhancement of endocannabinoid signaling with JZL184, an inhibitor of the 2-arachidonoylglycerol hydrolyzing enzyme monoacylglycerol lipase, produces anxiolytic effects under conditions of high environmental aversiveness in rats. *Pharmacol Res,* 64, 226-34.

Sigel, E., Baur, R., Racz, I., Marazzi, J., Smart, T. G., Zimmer, A. & Gertsch, J. (2011) The major central endocannabinoid directly acts at GABA(A) receptors. *Proc Natl Acad Sci U S A,* 108, 18150-5.

Simon, A. B. & Gorman, J. M. (2006) Advances in the treatment of anxiety: targeting glutamate. *NeuroRx,* 3, 57-68.

Somia, N. & Verma, I. M. (2000) Gene therapy: trials and tribulations. *Nat Rev Genet,* 1, 91-9.

Sonntag, F., Bleker, S., Leuchs, B., Fischer, R. & Kleinschmidt, J. A. (2006) Adeno-associated virus type 2 capsids with externalized VP1/VP2 trafficking domains are generated prior to passage through the cytoplasm and are maintained until uncoating occurs in the nucleus. *J Virol,* 80, 11040-54.

Sotres-Bayon, F., Sierra-Mercado, D., Pardilla-Delgado, E. & Quirk, G. J. (2012) Gating of fear in prelimbic cortex by hippocampal and amygdala inputs. *Neuron,* 76, 804-12.

Steindel, F., Lerner, R., Haring, M., Ruehle, S., Marsicano, G., Lutz, B. & Monory, K. (2013) Neuron-type specific cannabinoid-mediated G protein signalling in mouse hippocampus. *J Neurochem,* 124, 795-807.

Stieger, K., Belbellaa, B., Le Guiner, C., Moullier, P. & Rolling, F. (2009) In vivo gene regulation using tetracycline-regulatable systems. *Adv Drug Deliv Rev,* 61, 527-41.

Straiker, A., Wager-Miller, J., Hu, S. S., Blankman, J. L., Cravatt, B. F. & Mackie, K. (2011) COX-2 and fatty acid amide hydrolase can regulate the time course of depolarization-induced suppression of excitation. *Br J Pharmacol,* 164, 1672-83.

Suarez, J., Rivera, P., Llorente, R., Romero-Zerbo, S. Y., Bermudez-Silva, F. J., de Fonseca, F. R. & Viveros, M. P. (2010) Early maternal deprivation induces changes on the expression of 2-AG biosynthesis and degradation enzymes in neonatal rat hippocampus. *Brain Res,* 1349, 162-73.

Sugiura, T., Kondo, S., Sukagawa, A., Nakane, S., Shinoda, A., Itoh, K., Yamashita, A. & Waku, K. (1995) 2-Arachidonoylglycerol: a possible endogenous cannabinoid receptor ligand in brain. *Biochem Biophys Res Commun,* 215, 89-97.

Sumislawski, J. J., Ramikie, T. S. & Patel, S. (2011) Reversible gating of endocannabinoid plasticity in the amygdala by chronic stress: a potential role for monoacylglycerol lipase inhibition in the prevention of stress-induced behavioral adaptation. *Neuropsychopharmacology,* 36, 2750-61.

Summerford, C. & Samulski, R. J. (1998) Membrane-associated heparan sulfate proteoglycan is a receptor for adeno-associated virus type 2 virions. *J Virol,* 72, 1438-45.

Summerford, C., Bartlett, J. S. & Samulski, R. J. (1999) AlphaVbeta5 integrin: a co-receptor for adeno-associated virus type 2 infection. *Nat Med,* 5, 78-82.

Szulc, J., Wiznerowicz, M., Sauvain, M. O., Trono, D. & Aebischer, P. (2006) A versatile tool for conditional gene expression and knockdown. *Nat Methods,* 3, 109-16.

Takahashi, K. A. & Castillo, P. E. (2006) The CB1 cannabinoid receptor mediates glutamatergic synaptic suppression in the hippocampus. *Neuroscience,* 139, 795-802.

Tang, W., Ehrlich, I., Wolff, S. B., Michalski, A. M., Wolfl, S., Hasan, M. T., Luthi, A. & Sprengel, R. (2009) Faithful expression of multiple proteins via 2A-peptide self-processing: a versatile and reliable method for manipulating brain circuits. *J Neurosci,* 29, 8621-9.

Tanimura, A., Yamazaki, M., Hashimotodani, Y., Uchigashima, M., Kawata, S., Abe, M., Kita, Y., Hashimoto, K., Shimizu, T., Watanabe, M., Sakimura, K. & Kano, M. (2010) The endocannabinoid 2-arachidonoylglycerol produced by diacylglycerol lipase alpha mediates retrograde suppression of synaptic transmission. *Neuron,* 65, 320-7.

Tighilet, B., Huntsman, M. M., Hashikawa, T., Murray, K. D., Isackson, P. J. & Jones, E. G. (1998) Cell-specific expression of type II calcium/calmodulin-dependent protein kinase isoforms and glutamate receptors in normal and visually deprived lateral geniculate nucleus of monkeys. *J Comp Neurol,* 390, 278-96.

Uchigashima, M., Yamazaki, M., Yamasaki, M., Tanimura, A., Sakimura, K., Kano, M. & Watanabe, M. (2011) Molecular and morphological configuration for 2-arachidonoylglycerol-mediated retrograde signaling at mossy cell-granule cell synapses in the dentate gyrus. *J Neurosci,* 31, 7700-14.

Urlinger, S., Baron, U., Thellmann, M., Hasan, M. T., Bujard, H. & Hillen, W. (2000) Exploring the sequence space for tetracycline-dependent transcriptional activators: novel mutations yield expanded range and sensitivity. *Proc Natl Acad Sci U S A,* 97, 7963-8.

van der Stelt, M., Veldhuis, W. B., Maccarrone, M., Bar, P. R., Nicolay, K., Veldink, G. A., Di Marzo, V. & Vliegenthart, J. F. (2002) Acute neuronal injury, excitotoxicity, and the endocannabinoid system. *Mol Neurobiol,* 26, 317-46.

Van Gaal, L., Pi-Sunyer, X., Despres, J. P., McCarthy, C. & Scheen, A. (2008) Efficacy and safety of rimonabant for improvement of multiple cardiometabolic risk factors in overweight/obese patients: pooled 1-year data from the Rimonabant in Obesity (RIO) program. *Diabetes Care,* 31 Suppl 2, S229-40.

Varela, J. A., Wang, J., Christianson, J. P., Maier, S. F. & Cooper, D. C. (2012) Control over stress, but not stress per se increases prefrontal cortical pyramidal neuron excitability. *J Neurosci,* 32, 12848-53.

Varma, N., Carlson, G. C., Ledent, C. & Alger, B. E. (2001) Metabotropic glutamate receptors drive the endocannabinoid system in hippocampus. *J Neurosci,* 21, RC188.

Varvel, S. A. & Lichtman, A. H. (2002) Evaluation of CB1 receptor knockout mice in the Morris water maze. *J Pharmacol Exp Ther,* 301, 915-24.

Varvel, S. A., Wise, L. E., Niyuhire, F., Cravatt, B. F. & Lichtman, A. H. (2007) Inhibition of fatty-acid amide hydrolase accelerates acquisition and extinction rates in a spatial memory task. *Neuropsychopharmacology,* 32, 1032-41.

Vilela, L. R., Medeiros, D. C., Rezende, G. H., de Oliveira, A. C., Moraes, M. F. & Moreira, F. A. (2013) Effects of cannabinoids and endocannabinoid hydrolysis inhibition on pentylenetetrazole-induced seizure and electroencephalographic activity in rats. *Epilepsy Res*.

Wallace, M. J., Martin, B. R. & DeLorenzo, R. J. (2002) Evidence for a physiological role of endocannabinoids in the modulation of seizure threshold and severity. *Eur J Pharmacol,* 452, 295-301.

Wallace, M. J., Blair, R. E., Falenski, K. W., Martin, B. R. & DeLorenzo, R. J. (2003) The endogenous cannabinoid system regulates seizure frequency and duration in a model of temporal lobe epilepsy. *J Pharmacol Exp Ther,* 307, 129-37.

Walther, W. & Stein, U. (2000) Viral vectors for gene transfer: a review of their use in the treatment of human diseases. *Drugs,* 60, 249-71.

Wang, J. J., Niu, D. B., Zhang, T., Wang, K., Xue, B. & Wang, X. M. (2005) A tetracycline-regulatable adeno-associated virus vector for double-gene transfer. *Neurosci Lett,* 378, 106-10.

Wang, M., Hill, M. N., Zhang, L., Gorzalka, B. B., Hillard, C. J. & Alger, B. E. (2012) Acute restraint stress enhances hippocampal endocannabinoid function via glucocorticoid receptor activation. *J Psychopharmacol,* 26, 56-70.

Warrens, A. N., Jones, M. D. & Lechler, R. I. (1997) Splicing by overlap extension by PCR using asymmetric amplification: an improved technique for the generation of hybrid proteins of immunological interest. *Gene,* 186, 29-35.

Weinberg, M. S., Samulski, R. J. & McCown, T. J. (2012) Adeno-associated virus (AAV) gene therapy for neurological disease. *Neuropharmacology*.

Wettschureck, N., van der Stelt, M., Tsubokawa, H., Krestel, H., Moers, A., Petrosino, S., Schutz, G., Di Marzo, V. & Offermanns, S. (2006) Forebrain-specific inactivation of Gq/G11 family G proteins results in age-dependent epilepsy and impaired endocannabinoid formation. *Mol Cell Biol,* 26, 5888-94.

Wilson, R. I. & Nicoll, R. A. (2001) Endogenous cannabinoids mediate retrograde signalling at hippocampal synapses. *Nature,* 410, 588-92.

Wise, L. E., Long, K. A., Abdullah, R. A., Long, J. Z., Cravatt, B. F. & Lichtman, A. H. (2012) Dual Fatty Acid Amide Hydrolase and Monoacylglycerol Lipase Blockade Produces THC-Like Morris Water Maze Deficits in Mice. *ACS Chem Neurosci,* 3, 369-78.

Wu, Z., Asokan, A. & Samulski, R. J. (2006a) Adeno-associated virus serotypes: vector toolkit for human gene therapy. *Mol Ther,* 14, 316-27.

Wu, Z., Miller, E., Agbandje-McKenna, M. & Samulski, R. J. (2006b) Alpha2,3 and alpha2,6 N-linked sialic acids facilitate efficient binding and transduction by adeno-associated virus types 1 and 6. *J Virol,* 80, 9093-103.

Wyeth, M. S., Zhang, N., Mody, I. & Houser, C. R. (2010) Selective reduction of cholecystokinin-positive basket cell innervation in a model of temporal lobe epilepsy. *J Neurosci,* 30, 8993-9006.

Yoshida, T., Fukaya, M., Uchigashima, M., Miura, E., Kamiya, H., Kano, M. & Watanabe, M. (2006) Localization of diacylglycerol lipase-alpha around postsynaptic spine suggests close proximity between production site of an endocannabinoid, 2-arachidonoyl-glycerol, and presynaptic cannabinoid CB1 receptor. *J Neurosci,* 26, 4740-51.

Yoshida, T., Uchigashima, M., Yamasaki, M., Katona, I., Yamazaki, M., Sakimura, K., Kano, M., Yoshioka, M. & Watanabe, M. (2011) Unique inhibitory synapse with particularly rich endocannabinoid signaling machinery on pyramidal neurons in basal amygdaloid nucleus. *Proc Natl Acad Sci U S A,* 108, 3059-64.

Zanettini, C., Panlilio, L. V., Alicki, M., Goldberg, S. R., Haller, J. & Yasar, S. (2011) Effects of endocannabinoid system modulation on cognitive and emotional behavior. *Front Behav Neurosci,* 5, 57.

Zhong, P., Pan, B., Gao, X. P., Blankman, J. L., Cravatt, B. F. & Liu, Q. S. (2011) Genetic deletion of monoacylglycerol lipase alters endocannabinoid-mediated retrograde synaptic depression in the cerebellum. *J Physiol,* 589, 4847-55.

Zhu, P., Aller, M. I., Baron, U., Cambridge, S., Bausen, M., Herb, J., Sawinski, J., Cetin, A., Osten, P., Nelson, M. L., Kugler, S., Seeburg, P. H., Sprengel, R. & Hasan, M. T. (2007) Silencing and un-silencing of tetracycline-controlled genes in neurons. *PLoS One,* 2, e533.

Appendix

Abbreviations

2A	peptide linker
2-AG	2-arachidonoyl glycerol
4-NPA	4-nitrophenyl acetate
AA	arachidonic acid
AAV	adeno-associated virus
AAV1/2	mosaic AAV composed of capsid proteins from AAV1 and AAV2
ABHD12	serine hydrolases α-β-hydrolase domain 12
ABHD6	serine hydrolases α-β-hydrolase domain 6
AC	adenylyl cyclase
ACSF	artificial cerebrospinal fluid
AEA	anandamide
ANOVA	analysis of variance
bGHpA	bovine growth hormone polyadenylation sequence
bp	base pair
BSA	bovine serum albumin
CA	cornu ammonis
CAG	cytomegalovirus immediate early enhancer/chicken β-actin hybrid promoter
cap	genes encoding viral capsid proteins
CB1	cannabinoid type 1
cDNA	complementary deoxyribonucleic acid
CMV	cytomegalovirus
CNS	central nervous system
COX-2	cyclooxygenase 2
Cpu	caudate putamen
Cre	recombinase from bacteriphage 1, **c**auses **re**combination between loxP sites
Ctx	cortex
DAGL	diacylglycerol lipase
DAPI	4',6-diamidino-2-phenylindole

DNA	deoxyribonucleic acid
dox	doxycycline
DSE	depolarization-induced suppression of excitation
DSI	depolarization-induced suppression of inhibition
eEPSC	evoked excitatory postsynaptic current
eIPSC	evoked inhibitory postsynaptic current
EMT	endocannabinoid membrane transporter
FAAH	fatty acid amide hydrolase
FJC	Fluoro-Jade C
fw	forward
GABA	γ-aminobutyric acid
GAPDH	glyceraldehyde 3-phosphate dehydrogenase
GC	granule cell layer of the dentate gyrus
GDP	guanosine diphosphate
GFAP	glial fibrillary acidic protein
GOI	gene of interest
GPR55	G protein-coupled receptor 55
GTP	guanosine triphosphate
HA	human influenza hemagglutinin epitope
HEK	human embryonic kidney 293
Hil	hilar region
HPA	hypothalamic-pituitary-adrenal
hrGFP	humanized renilla green fluorescent protein
HSPG	heparan sulfate proteoglycan
HU-210	CB1 receptor agonist, (6aR)-trans-3-(1,1-Dimethylheptyl)-6a,7,10,10a-tetrahydro-1-hydroxy-6,6-dimethyl-6H-dibenzo[b,d]pyran-9-methanol
i.p.	intraperitoneal
IgG	immunoglobulin G
IRES	internal ribosome entry site
ITR	inverted terminal repeat
KA	kainic acid
kb	kilobase pair
kD	kiloDalton
KRAB	krueppel-associated box
LMol	stratum lacunosum-molecularis

loxP	locus of crossover (x) in P1
LTP	long-term potentiation
Luc	stratum lucidum
LV	lateral ventricle
MAGL	monoacylglycerol lipase
MAPK	mitogen-activated protein kinase
mGluR	metabotropic glutamate receptor
Mol	stratum moleculare
mRNA	messenger ribonucleic acid
NAPE-PLD	N-acyl phosphatidylethanolamine phospholipase D
NArPE	N-arachidonoyl phosphatidylethanolamine
NAT	N-acyltransferase
NMDA	N-methyl-D-aspartate
OEA	oleoyl ethanolamide
OE-PCR	overlap extension polymerase chain reaction
Or	stratum oriens
ORF	open reading frame
pAAV	AAV plasmid
PBS	phosphate buffered saline
PCR	polymerase chain reaction
PEA	palmitoyl ethanolamide
PLC	phospholipase C
PPAR	peroxisome proliferator-activated receptor
Psp	tissue-specific promoter
Pyr	CA1/CA3 pyramidal cell layer
qPCR	quantitative polymerase chain reaction
Rad	stratum radiatum
rep	genes for viral replication
rev	reverse
RNA	ribonucleic acid
RT	room temperature
rtTA	reverse transcriptional activator
SDS-PAGE	sodium dodecyl sulfate polyacrylamide gel electrophoresis
SEM	standard error of mean
spA	short bovine growth hormone polyadenylation sequence

SR141716A	CB1 antagonist, "rimonabant", N-(Piperidin-1-yl)-5-(4-chlorophenyl)-1-(2,4-dichlorophenyl)-4-methyl-1H-pyrazole-3-carboxamide
Stop	transcriptional termination element flanked by loxP sites
SV40	simian virus 40
Syn	human synapsin promoter
tet	tetracycline
tetO	tet resistant operon
tetR	tet repressor
THC	Δ9-tetrahydrocannabinol
TRE	tetracycline responsive element
TRPV1	transient receptor potential cation channel subfamily V1
tTA	transcriptional activator
tTS	transcriptional silencer
VGluT1	vesicular glutamate transporter 1
WHO	World Health Organization
WPRE	woodchuck hepatitis virus post-transcriptional regulatory element
WPRE2	short form of the woodchuck hepatitis virus posttranscriptional regulatory element

Further abbreviations were used according to the international system of units. The one letter code of amino acids was used for protein sequences.

List of figures